School of Doctoral Studies in Biological Sciences

University of South Bohemia in České Budějovice

Faculty of Science

Chromera velia heme pathway localization

Ph.D. Thesis

Mgr. Jitka Richtová

Supervisor: Prof. Miroslav Oborník, Ph.D.

Biology Centre CAS v.v.i., Institute of Parasitology

University of South Bohemia in České Budějovice, Faculty of Science

České Budějovice 2021

This thesis should be cited as: Richtová J., 2021. *Chromera velia* heme pathway localization. Ph.D. Thesis Series, University of South Bohemia, Faculty of Science, School of Doctoral Studies in Biological Sciences, České Budějovice, Czech Republic.

Annotation

This thesis is focused on the localization of the heme pathway in *Chromera velia* – the closest known photosynthetic relative of apicomplexan parasites. The heme pathway belongs to essential processes in most living organisms. Organisms use enzymes of various evolutionary origins, reflecting their complex evolutionary history. The core of this study represents the combination of computational and experimental localization of the *C. velia* heme pathway. We showed that the localization of the heme pathway in the cell is driven by multiple factors, including the demand for pathway products, the need for tight regulation of the pathway, and the evolutionary origin of the enzymes.

Declaration:

I hereby declare that I am the author of this dissertation and that I have used only those sources and literature detailed in the list of references.

České Budějovice, 2021 ....

Jitka Richtová

Declaration [in Czech]

Prohlašuji, že svoji disertační práci jsem vypracoval samostatně pouze s použitím pramenů a literatury uvedených v seznamu citované literatury. Prohlašuji, že v souladu s § 47b zákona č. 111/1998 Sb. V platném znění souhlasím se zveřejněním své disertační práce, a to v nezkrácené podobě elektronickou cestou ve veřejně přístupné části databáze STAG provozované Jihočeskou univerzitou v Českých Budějovicích na jejích internetových stránkách, a to se zachováním mého autorského práva k odevzdanému textu této kvalifikační práce. Souhlasím dále s tím, aby toutéž elektronickou cestou byly v souladu s uvedeným ustanovením zákona č. 111/1998 Sb. zveřejněny posudky školitele a oponentů práce i záznam o průběhu a výsledku obhajoby kvalifikační práce. Rovněž souhlasím s porovnáním textu mé kvalifikační práce s databází kvalifikačních prací Theses.cz provozovanou Národním registrem vysokoškolských kvalifikačních prací a systémem na odhalování plagiátů.

České Budějovice, 2021   ....

                                                        Jitka Richtová

This thesis originated from a partnership of the Faculty of Science, University of South Bohemia, and Institute of Parasitology, Biology Centre CAS v.v.i., supporting doctoral studies in the Molecular biology and genetics study program.

List of papers and author's contribution:

- <u>Richtová J</u>., Sheiner L., Gruber A., Yang S., Striepen B., Kořený L., Oborník M. (2021) **Using diatom and apicomplexan model to study the heme pathway of *Chromera velia.*** *International Journal of Molecular Sciences* 22: 6495. DOI: 10.3390/ijms221264950
  Impact factor: 5.923 (2020)

Richtová J. did heterologous expression experiments in T. gondii and P. tricornutum and did cell imaging of P. tricornutum cells. Jitka took part in immunogold labeling and made its interpretation. Jitka prepared figures, schemes, and tables in the manuscript (except Figure 3). Jitka also wrote and edited the manuscript. J. R. contribution: 80%.

- Sharaf A., Füssy Z., Tomčala A., <u>Richtová J.</u>, Oborník M. (2019) **Isolation of plastids and mitochondria from *Chromera velia.*** *Planta* 250: 1731–1741. DOI: 10.1007/s00425-019-03259-3
  Impact factor: 4.116 (2021)

Richtová J. performed the C. velia cells staining, imaging under the confocal microscope and prepared pictures for publication. J. R. contribution: 15%.

- Füssy Z., Masařová P., <u>Kručinská J</u>., Esson H. J., Oborník M. (2017) **Budding of the alveolate alga *Vitrella brassicaformis* resembles sexual and asexual processes in apicomplexan parasites**. *Protist* 168: 80-91. DOI: 10.1016/j.protis.2016.12.001
  Impact factor: 2.566 (2020)

Richtová J. performed the C. velia imaging under the confocal microscope and edited the manuscript. J. R. contribution: 10%.

- Tomčala A., Kyselová V., Schneedorferová I., Opekarová I., Moos M., Urajová P., <u>Kručinská J.</u>, Oborník M. (2017) **Separation and identification of lipids in the photosynthetic cousins of Apicomplexa *Chromera velia* and *Vitrella brassicaformis***. *Journal of Separation Science* 40: 3402-3413. DOI: 10.1002/jssc.201700171
  Impact factor: 3.645 (2020)

Richtová J. performed the C. velia cells staining, imaging under the confocal microscope and prepared pictures for publication. J. R. contribution: 20%.

- Oborník M., <u>Kručinská J.</u>, Esson H. J. (2016) **Life cycles of chromerids resemble those of colpodellids and apicomplexan parasites.** *Perspectives in Phycology* 3: 21-27. DOI: 10.1127/pip/2016/0038

  Impact factor: nonavailable

Richtová J. designed an experimental part that led to revealing the process of zoospore formation. Jitka did all pictures, video, and time-lapse pictures from a microscope and drafted a concluding life cycle scheme. Jitka also edited the manuscript. J. R. contribution: 40%.

Miroslav Oborník, the supervisor of this Ph.D. thesis and co-author of all presented papers, approves the contribution of Jitka Richtová in these papers as described above.

………….…………………………….………

Prof. Miroslav Oborník, Ph.D.

TABLE OF CONTENTS

Chromera velia heme pathway localization

Jitka Richtová

Faculty of Science, University of South Bohemia; Institute of Parasitology, Biology center ASCR, České Budějovice, Czech Republic**.**

Abstract:

Chromera velia, an alveolate alga with complex, rhodophyte-derived plastid, is living proof of the photosynthetic history of apicomplexan parasites, which include severe pathogens such as *Plasmodium falciparum,* the causative agent of malaria. Therefore, *Chromera* is a perfect object to study the metabolic transition from phototrophy to parasitism. One of the most fundamental metabolic processes for living organisms is heme biosynthesis. The final product, heme, has a crucial function in many metabolic processes, such as electron and gas transfer. Intracellular localization of particular steps of heme biosynthesis differs among various organisms. This is partially caused by the organism's evolutionary history, the need for the tight regulation of the synthesis, and the demand for final products in the cell compartment. This thesis aimed to describe *C. velia* as an organism of interest in the perspective of its heme pathway localization.

1. Introduction (A way to the discovery of Chromera velia)

The phylum Apicomplexa contains causative agents of many human and livestock diseases. Among the most prominent members are *Plasmodium falciparum* and *Toxoplasma gondii*, inflicting malaria and toxoplasmosis, respectively. The related economic importance of this group evoked scientific focus, and apicomplexan parasites (Sporozoa; Apicomplexa; Cavalier-Smith, 2018) became a very intensively studied group of protists.

In 1975 Kilejian et al. described a circular 35kb long extrachromosomal DNA in *Plasmodium lophurae* (malarial parasite of ducks) (Kilejian, 1975). The original presumption supposed that this DNA would belong to parasite mitochondria (Kilejian, 1975; Williamson et al., 1985; Gardner et al., 1988); however, that changed soon after the linear 6kb molecule of DNA encoding classical mitochondrial genes was found (Suplick et al., 1988; Aldritt et al., 1989; Vaidya et al., 1989; Feagin, 1992). The extrachromosomal DNA circle, later described also in *T. gondii* (Borst et al., 1984), displayed procaryotic ancestry. Still, the genes were closer to plastids of plants and algae than expected Alphaproteobacteria (Gardner et al., 1991b, 1991a, 1993, 1994). Finally, the complete genome sequence uncovered the plastid-like nature of the 35kb DNA circle (Wilson et al., 1996). This finding, together with its localization to a multiple-membrane bound compartment (McFadden et al., 1996; Köhler et al., 1997), led to the conclusion that Sporozoa (Cavalier-Smith, 2018) possess a DNA bearing organelle likely with photosynthetic history (Gardner et al., 1991b) that was later termed "apicoplast" (from apicomplexan plastid, (Köhler et al., 1997)). Chasing the apicoplast among all sporozoans (apicomplexan parasites) failed only in some gregarines (Toso and Omoto 2007) and *Cryptosporidium* (Zhu et al., 2000). All remaining members of this group were found to possess this novel genome-containing organelle (Waller and McFadden, 2005; McFadden and Yeh, 2017). Analyses of all apicoplast genomes support their single-origin and a stable evolutionary state, likely before the diversification of Sporozoa. The number of apicoplast membranes was contentious initially (McFadden, 2011). The increasing number of high-quality pictures showed a variable number of apicoplast membranes that span from two to four within the same organelle. Membrane pockets and rolled loops of membranes forming inner membrane complexes were also described (Köhler et al., 2005; Hopkins et al., 1999; Lemgruber et al., 2013). The multi-membrane packaging of the organelle goes hand in hand with complex endosymbiosis.

Another question was the origin of the apicoplast in the green or red algae lineage. This problem was even more complicated because the traditional features used to define plastid lineages, such as pigments and photosynthesis-associated genes, are absent from the apicoplast (Waller and McFadden,

2005). The closest photosynthetic relatives to Sporozoa (Cavalier-Smith, 2018) at that time were considered dinoflagellates. However, their plastid genome consists solely of genes coding for photosynthesis-related proteins. These genes are highly divergent and uniquely arranged on DNA minicircles (Zhang et al., 1999; Barbrook and Howe, 2000; Howe et al., 2008). Therefore, plastid genomes of dinoflagellates are virtually incomparable with that of nonphotosynthetic sporozoan plastids (Janouškovec et al., 2010). The investigation of the origin of the apicoplast took more than a decade during which the scientific community once tended to the "red" origin (Williamson et al., 1994; McFadden and Waller, 1997; Blanchard and Hicks, 1999; Waller and McFadden, 2005) and other time to the "green" ancestry (Köhler et al., 1997; Dzierszinski et al., 1999; Funes et al., 2002). Soon after identifying the apicoplast, McFadden and Waller (1997) proposed that the photosynthetic ancestor of Sporozoa was similar to coral zooxanthellae, symbionts from the group of dinoflagellates. Therefore, various scientific groups searched for a living photosynthetic ancestor of the apicoplast containing parasites. The breakthrough came in 2008 when Robert Moore and his colleagues took samples of a stony coral *Plesiastrea versipora* (Faviidae) from Sydney Harbour (Australia). By a set of methods commonly used to isolate dinoflagellates of the genus S*ymbiodinium* (York Jr., 1986), they also get a unicellular brownish organism later called *Chromera velia* (Moore et al., 2008; Apicomonada, Apicomplexa; Cavalier-Smith, 2018)*.*

1.1.   Morphology and ultrastructure

The predominant form of *C. velia* in culture is a coccoid cell with a diameter of 5-7 µm (Moore et al., 2008), dividing by binary division to form autosporangia with 2-4 autospores (Oborník et al., 2011). The coccoid cell can undergo the transition to rounded zoosporangium with up to 15 µm in diameter, which later releases highly motile, oval-shaped zoospores having the maximum length and width of 7.3 and 4.8 µm, respectively. The hallmark feature of *C. velia*'s motile forms is the pair of flagella. Both are emerging from their own shallow pocket in the cell body. The anterior flagellum is approximate to the size of the cell body, whilst the posterior flagellum is 3-4 times longer (Weatherby et al., 2011). Autosporangia of *C. velia* can be enclosed by a veil-like wall that is remarkably thicker than standard coccoid cell wall, thus forming a resting cyst (Oborník et al., 2011; Oborník et al., 2016)

The *C. velia* cell wall consists mainly of cellulose (Tortorelli et al., in press). The cell wall is transparent to let most of the light reach the plastid. By extending its lobes through the whole cell, the plastid occupies most of the cell space. The content of *C. velia* cell varies in response to the current environment; therefore, different storage granules and vacuoles can be found in the cell. *Chromera* can accumulate a high amount of triacylglycerols in lipid droplets which it can use later as an energy source

(Tomčala et al., 2017; Tomčala et al., 2020). One of the growth-limiting factors in the ocean is nitrogen; therefore, microalgae use guanine crystals ($C_5H_5N_5O$) as a reservoir (Mojzeš et al., 2020). *C. velia* was found to possess a dynamic number of guanine crystals changing according to N content in the supplied medium (Gonepogu et al., unpublished data). The intracellular morphology of the *C. velia* flagellates is more or less the same as the coccoid cells, with all critical compartments including photosynthetic plastid. However, as their life span is relatively short (described later in "Life cycle"), they do not accumulate energy in various compartments as happens in coccoid cells during the *C. velia* cultivation (Tomčala et al., 2017, Gonepogu, unpublished data).

The nucleus of *C. velia* is easily recognizable by its typical eukaryotic morphology and scattered chromatin. The nucleus is usually centrally located and measures up to 1 μm (Oborník et al., 2011). Direct FISH with telomeric probes estimated the number of chromosomes in the *C. velia* to be four (Vazač et al., 2018). The endoplasmic reticulum and Golgi apparatus of *C. velia* look the same as in the majority of protists (Moore et al., 2008, Oborník et al., 2011). The *C. velia* plastid is surrounded by four membranes, and its thylakoids are organized in stacks of three (Moore et al., 2008; Oborník et al., 2011, Oborník and Lukeš 2015). Even though many micrographs of *C. velia* were taken so far, no pyrenoid or similar structure were observed within or nearby its plastid, contrary to the second known chromerid, *Vitrella brassicaformis* (Oborník et al., 2011, Quigg et al., 2012, Oborník and Lukeš 2015). Mitochondria are known to dynamically change their shape by dislocation, fusion, and fission (Clarisse et al., 2021). In *C. velia* coccoid cells, mitochondria are represented by several double-membraned vesicles of variable width and length and tubular cristae inside (Oborník et al., 2011; Sharaf et al., 2019a). Cortical alveoli are common ultrastructural features of Alveolata, which also give the group its name. These flattened vesicles are situated just beneath the cell wall, and in Sporozoa, they are vital for their motility during the host invasion process (Soldati et al., 2004; Gould et al., 2008). Alveoli are supported by a layer of microtubules that strengthen the cell wall (Morrissette and Sibley, 2002). Microtubules are also present in motile forms of *C. velia* at the vicinity of the micropyle, where they form a part of the pseudoconoid (Oborník et al., 2011; Portman et al., 2014). The micropyle is a small opening in the cell wall (Votýpka et al., 2017; Bartošová-Sojková et al., 2015), and the pseudoconoid is a form of open conoid, a conserved sporozoan element used to interact with host cell together with the assistance of other parts of the apical complex like micronemes and rhoptries (Kořený et al., 2021). The complex endomembrane system, occupying a similar position as the micronemes and rhoptries of Sporozoa, was described in *C. velia* (Portman et al., 2014). However, any traces of an apical complex have not been detected in the second described chromerid *V. brassicaformis* (Füssy et al., 2017). The not yet observed connection between pseudoconoid and anterior flagellum by unidentified fibers was described in *C. velia* flagellates (Portman et al., 2014). The exact function of the apical complex machinery in *C. velia* needs a further

detailed investigation. Microtubules are vital components of all known eukaryotic flagella, with no exception in chromerids. The "9+2" microtubule arrangement in the flagellum axoneme is one of the iconic structures in cell biology (Ginger et al., 2008). This pattern is also found in both flagella of *C. velia* motile stages (Oborník et al., 2011, Portman et al., 2014).
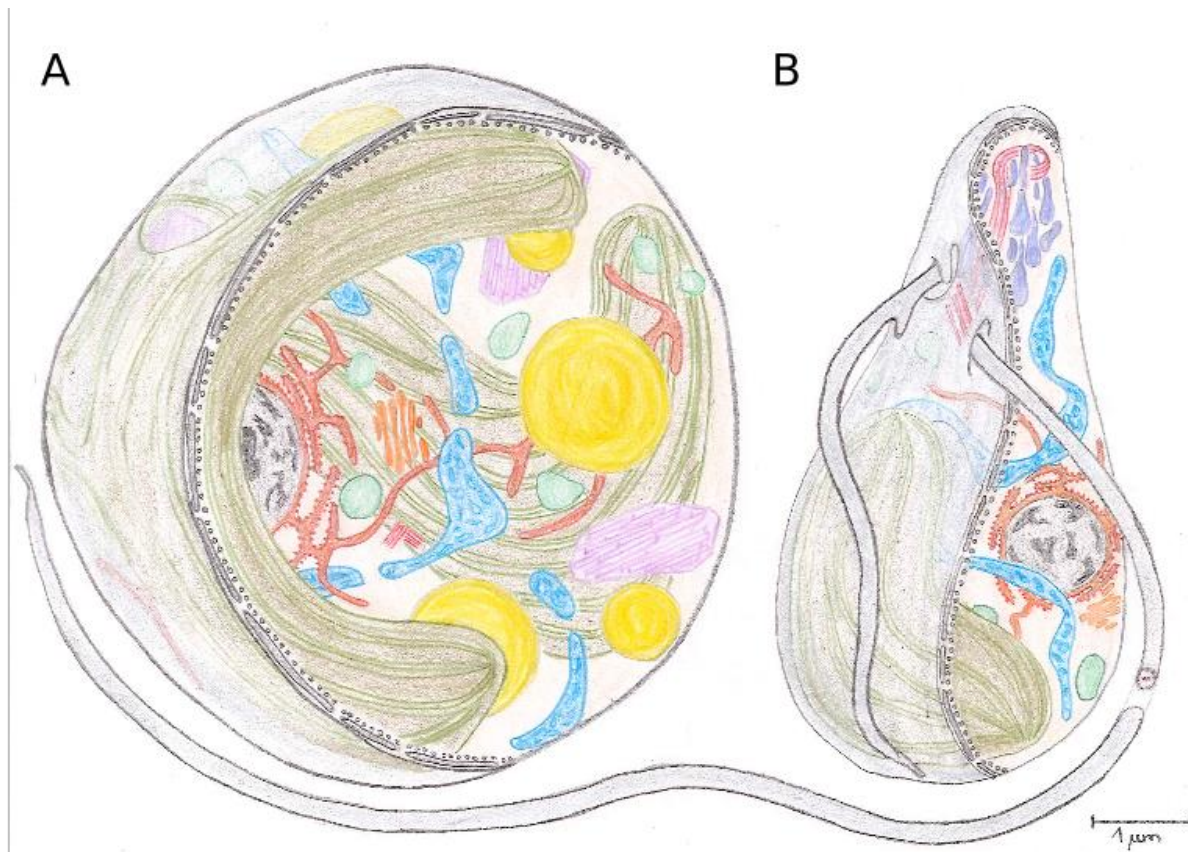

Figure 1: Drawing of *C. velia* coccoid (A) and zoospore (B) cells. A) Nucleus (black and grey), endoplasmic reticulum (brown), Golgi (orange), mitochondria (light blue), vacuoles with guanine crystals (violet), lipid bodies (yellow), unspecified vacuoles (light green), centrioles (red), cortical alveoli with an underlying microtubular corset (black). B) Nucleus (black and grey), endoplasmic reticulum (brown), Golgi (orange), mitochondria (light blue), unspecified vacuoles (light green), pseudoconoid microtubules (red), anterior endomembrane system (dark blue). This drawing is based on the following works: (Moore et al., 2008; Oborník et al., 2011; Weatherby et al., 2011; Portman et al., 2014; Oborník et al., 2016; Tomčala et al., 2017; Mojžeš et al., 2020; Gonepogu unpublished data).

In the original TEM description (Moore et al., 2008), a distinctive light grey oval-shaped compartment with centrally located fiber-shaped structures was denoted as the mitochondrion. However, this vesicle was later assigned as a novel structure called "chromerosome" with so far not understand function (Oborník et al., 2011). The chromerosome was shown as a structure with a dynamic development: it starts as a circular vesicle of the homogenously transparent lumen, the shape later elongates, and two distinctive poles connected through a set of fibers appear. At its advanced stage, the chromerosome

takes about half of the cell space, forming a bulbous part filled with several different vesicles and a prominent rod-like projection reaching the opposite side of the cell. The structure of this appearance resembles ejectisome of cryptomonads or even extrusomes and trichocysts of colpodellids and dinoflagellates, respectively (Oborník et al., 2011). As mentioned above, the function of the chromerosome is obscure. It would need consistent work to find what conditions lead *C. velia* to form such a large and complicated structure with an undoubtedly important function.

1.2. Evolutionary origin, phylogenetic position

When *C. velia* was introduced to the scientific community, the currently used eukaryotic tree of life consisted of 5-6 supergroups: Excavata, Archeaplastida (or Plantae), Unikonts (or separately: Opisthokonta and Amoebozoa), Chromalveolata, and Rhizaria (Baldauf, 2003; Simpson and Roger, 2004; Adl et al., 2005; Keeling et al., 2005) that were build up on molecular phylogenetic evidence combined with derived cell-biological features. However, it suffered from limited amounts of unicellular eukaryotes diversity (Patterson, 1999). In 2007, Burki et al. presented a phylogenetic study based on a large dataset combining over 29.000 amino acid positions with extensive taxa sampling (49 mainly unicellular species). They proposed a new supergroup by uniting Stramenophiles, Alveolata (already present within Chromalevolata), and Rhizaria, called "SAR." The SAR group become a home for *C. velia*.

The initial estimate of the evolutionary position of *C. velia* was shown in the description article (Moore et al., 2008). It was based on nuclear and plastid phylogenies using nuclear LSU and SSU rDNA, plastid LSU and SSU rDNA, and PsbA (photosystem II protein D1). Phylogenetic analyses of nuclear rDNAs reveal a close relationship between *C. velia,* colpodellids, and sporozoans. This relationship was also confirmed by plastid rDNA, where *C. velia* plastid branched at the root of the apicoplasts. Phylogenetic analyses based on plastid rDNA excluded sequences from peridinin-pigmented plastids of dinoflagellates because of their high divergency. The psbA gene set lacks all apicoplast bearing taxons as the psbA gene is not present in their genome. The resulting phylogenetic tree showed *C. velia* as a relative of peridinin dinoflagellate plastids. Dinoflagellates, so far known to hold a position of the closest photosynthetic relatives of sporozoans in the eukaryotic tree of life, were dethroned, and *Chromera* took place. This phylogenetic position was later strengthened by analyses of glyceraldehyde 3-phosphate dehydrogenase (GAPDH) amino acid sequences (plastid-targeted and cytosolic paralogues, Oborník et al., 2009). Janouškovec et al., 2010 analyzed complete plastid genome sequences and showed trees computed from a combined dataset of eight nuclear genes. Also, a new chromerid *Vitrella brassicaformis* (Oborník et al., 2012), hidden under the code CCMP 3155, appeared for the first time.

This extensive work affirms *C. velia* as a photosynthetic alveolate fulfilling the phylogenetic gap between sporozoans and dinoflagellates.
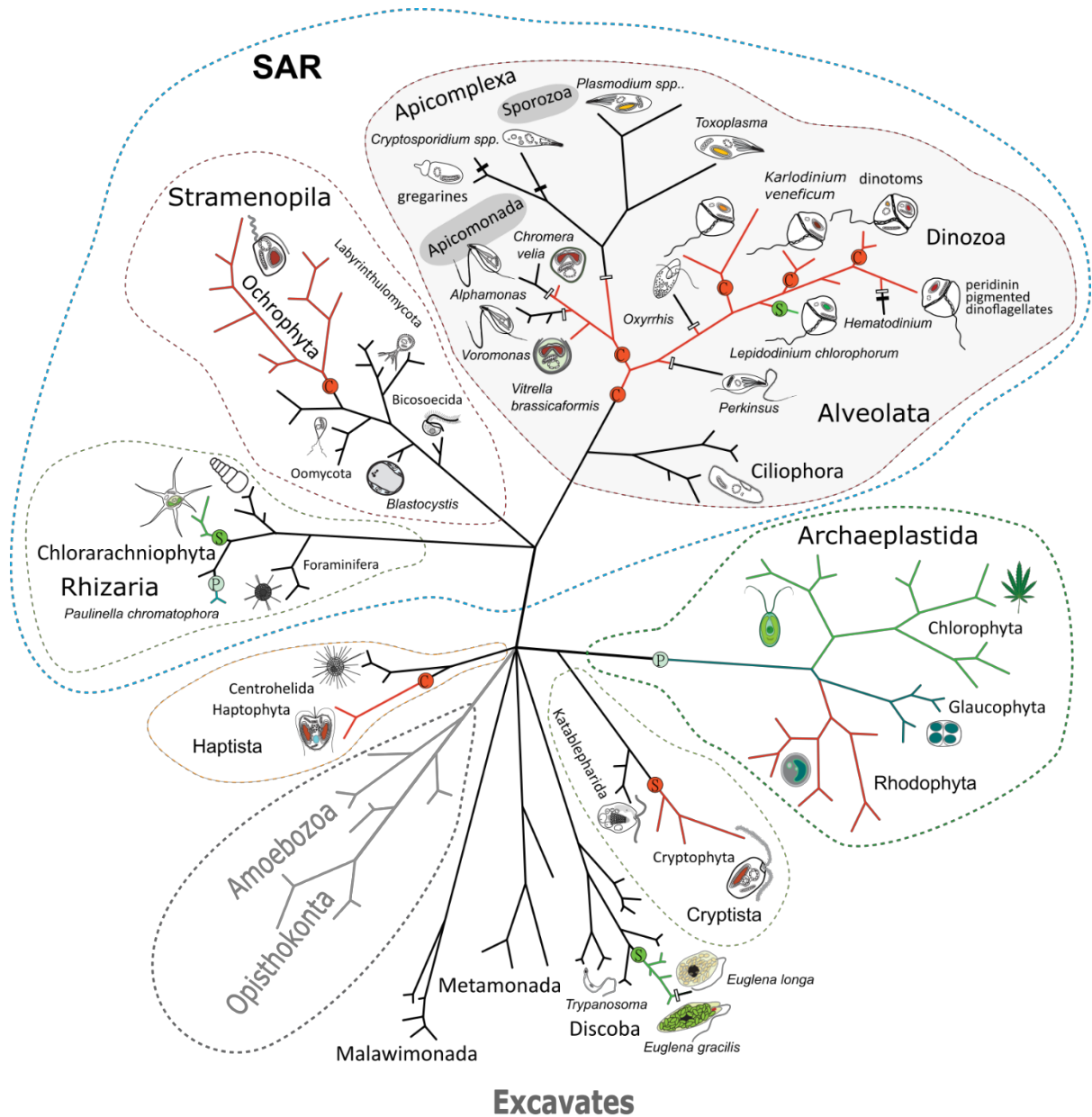
Figure 2: Diversity of eukaryotic phototrophs. Apicomonada and Sporozoa, where *C.* velia and *T. gondii,* respectively, are present, are highlighted by grey. The figure was adapted from the original in Oborník (2019), according to Cavalier-Smith (2018).

Phylogenetic trees were not the only evidence that firmly settles *C. velia* within the SAR group. Additional features link plastid of *Chromera* once with their photosynthetic and the other time with parasitic SAR relatives. Starting from the edge, the *Chromera* plastid is surrounded by four membranes suggesting that this organelle originates from a complex endosymbiosis (Moore et al., 2008). In contrast,

peridinin-pigmented plastids of dinoflagellates are bounded by three membranes (Cavalier-Smith, 2000). The apicoplast of *P. falciparum* possesses four membranes envelop (Lemgruber et al., 2013), the plastid of *T. gondii* was proposed to be bounded by altering two to four membranes (Köhler, 2005). *C. velia* thylakoid membranes, where the light-dependent reaction of photosynthesis occurs, are organized in stacks of three or more (Moore et al., 2008), similar to peridinin-pigmented dinoflagellates and stramenopiles (Schnepf, 1999, Bína et al., 2016). The pigments, which *C. velia* thylakoid uses to absorb the energy from the sun, are chlorophyll *a*, violaxanthin, a novel carotenoid (fucoxanthin isomer), and β, β carotene as a minor component (Moore et al., 2008). The absence of chlorophyll *c* is unexpected as this pigment is commonly found in almost all rhodophyte-derived plastids, except eustigmatophytes. This unusual pigmentation within the SAR group can be explained by the tertiary endosymbiotic origin of chromerid plastid (Füssy et al., 2018; Oborník 2020; Oborník and Lukeš, 2013). Most photosynthetic organisms use the codon UGG to encode tryptophan in the plastid-encoded proteins. However, *C. velia* uses UGA, usually used as a stop codon, to code for tryptophan. Such a stop codon reassignment has been reported in various mitochondria and nonphotosynthetic plastids of coccidians (Moore et al., 2008; Oborník and Lukeš, 2015; Su et al., 2019). All photosynthetic eukaryotes, except dinoflagellates, use plastid-encoded Rubisco I form to fix the atmospheric carbon to energy-rich molecules. In contrast, dinoflagellates use nucleus-encoded originally bacterial Rubisco form II, and so does the *Chromera* (Janouškovec et al., 2010). Another peculiarity known from dinoflagellates is polyuridylylation of transcripts 3' end. This form of processing was also shown in *C. velia* (Janouškovec et al., 2010). All red algal-derived plastids are united by the presence of the ribosomal superoperon, traces of which are also found in *Chromera* (Janouškovec et al., 2010).

In 2008, when *C. velia* was described, the tree of life mainly resulted from phylogenetics based on single or few gene analyses in combination with biological features. The utilization of next-generation sequencing techniques enabled the availability of complete genomes of different organisms (Behjati and Patricks, 2013). Moreover, genome amplification performed on a single cell revealed many unknown protists hidden in oceans (Sieracki et al., 2019). We are now facing a new phenomenon: for many organisms, the complete genome can be known, whilst the cell morphology can be entirely unknown (Burki et al., 2020). *Chromera velia* is, together with *V. brassicaformis* and colpodellids, part of the class Apicomonadea, a sister group of Sporozoa forming myzozoan infraphylum Apicomplexa (Cavalier-Smith, 2018). The importance of *C. velia*, or chromerids in general, lies in linking organisms with currently different trophic strategies and being thus a perfect tool to study related changes in cellular metabolism.

1.3. Environment and life cycle

Chromera velia was isolated by the method commonly used to isolate intracellular symbionts of corals. Therefore, it was presented as a "coral-associated" alga (Moore et al., 2008). Soon it was found as an organism that is fast-growing and easily maintained in a standard artificial seawater medium (f/2 or Guillard medium) known to keep various coastal marine phytoplankton, especially diatoms (Guillard et al., 1962). *C. velia* culture can be kept in laboratory conditions for almost an infinite time by supplying a new medium and diluting the culture. Standard cultivation conditions are 26°C, 12/12 light/dark regime, with the illumination during the light cycle of 100 µE m-2s-1.
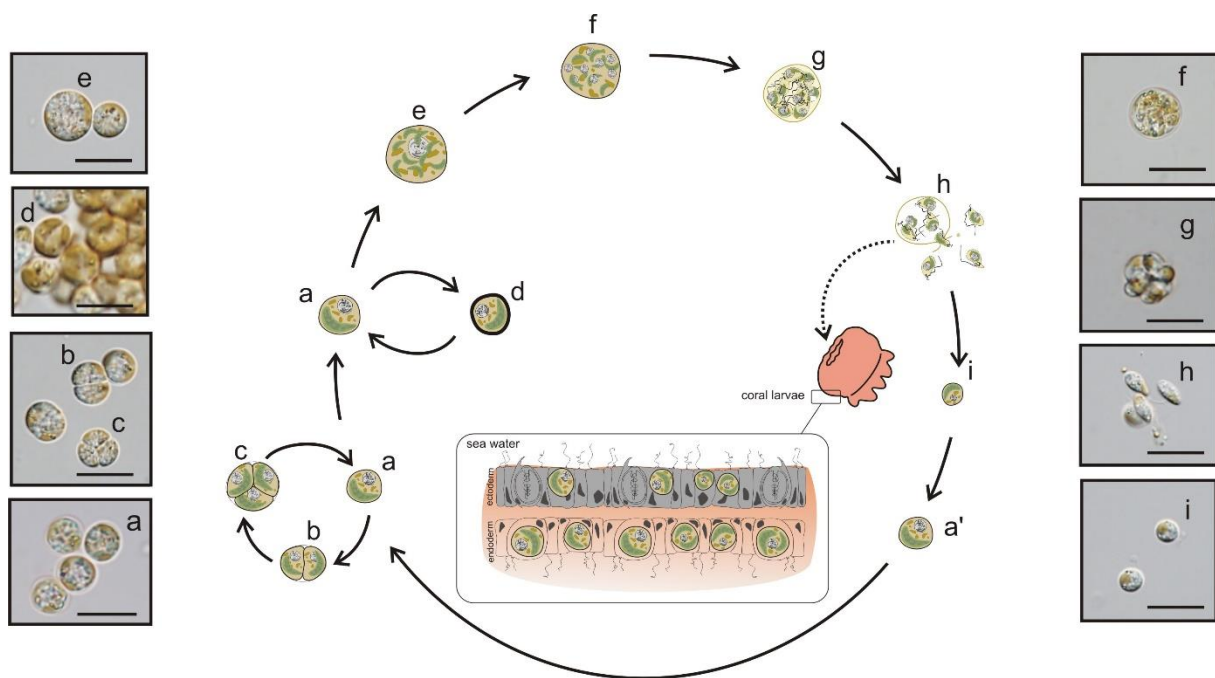
Figure 3: Life cycle of *Chromera velia*. Coccoid cell (a) can transform to autosporangium (b,c) or can form a cyst (d). In certain conditions (described in the text), the coccoid cell can develop into a zoosporangium (e-g) which later ruptures and releases an even number of highly motile zoospores (h). Zoospores can infect coral larvae or shed their flagella, encyst (i) and form a vegetative cell again (a'). The scale bar is 10 µm. Figure taken from Oborník et al., 2016.

To follow the entire life cycle of *C. velia* in culture, it is optional to start with an approximately one-month-old, wealthy culture (5500 cells/ml; or OD_{600}= 1,5) diluted to a fresh medium in a 1:100 ratio. Such a starting culture contains solely coccoid cells up to 10 µm in diameter (as mentioned before). Some of them can be in the process of binary division, forming 2-4 new coccoid cells (Oborník et al., 2016). The lag phase, during which cells adapt to a new environment and synthesize cellular components for basal metabolism (Forget et al., 2010), takes about three days. During the following log

phase, the number of cells in the culture doubles twice within approximately 24 hours (Richtová, unpublished data). During these days (the 4th day after inoculation), cells bigger than the standard coccoid cells reaching up to 15 μm in diameter are observed. These are zoosporangia, cells that can later produce 2-12 highly motile zoospores/flagellates (Oborník et al., 2016). TEM sections of *C. velia* zoosporangium resemble trophozoites of colpodellids. Similarly, an even number of zoospores are organized within vacuole in rosettes around a centrally located residual body that serves as the source of energy during the zoospore's development (Brugerolle, 2002, Muñiz-Hernández et al., 2011). The maturation of zoosporangia takes another two days; after that, *C. velia* flagellates moving fast in a zic-zac manner can be observed.
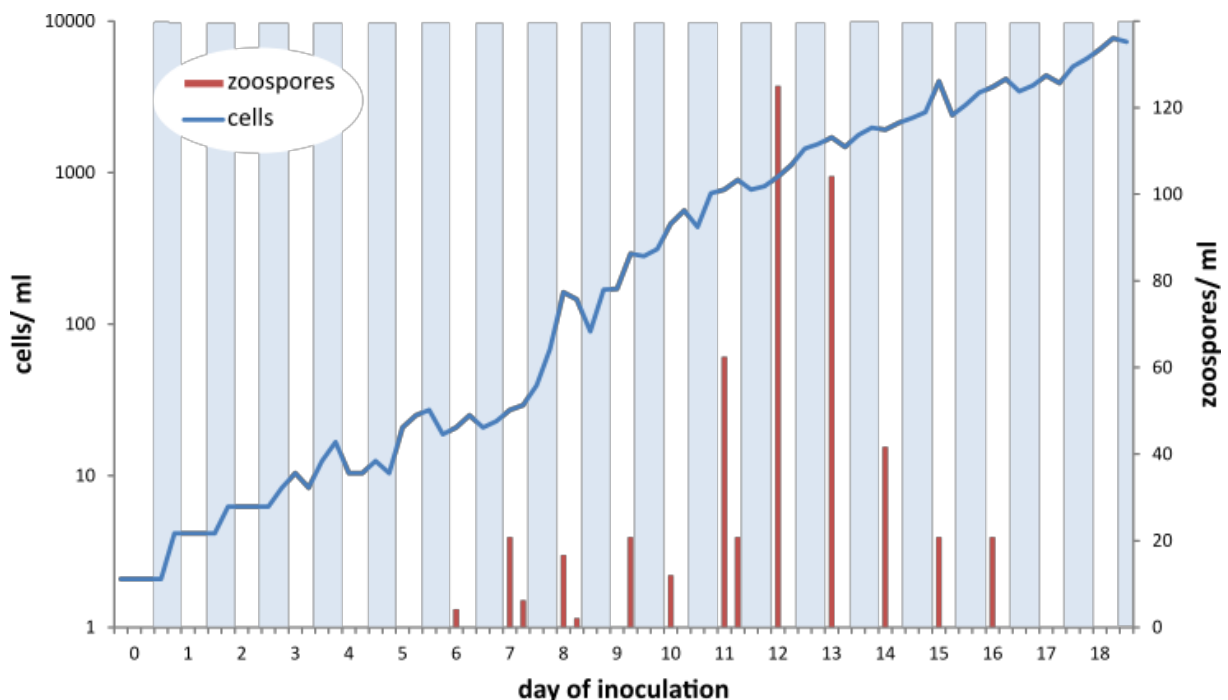
Figure 4: *C. velia* **zoosporogenesis during the cultivation**. Graph showing the appearance of zoospores in the culture of *C. velia* during the cultivation in a 12/12 dark/light regime. The dark period is denoted by a blue stripe (Richtová, unpublished data).

Zoosporogenesis is a light-dependent process usually observed on the 7th day of inoculation with the peak on the 11th day (Oborník et al., 2011). Once the zoospores are mature, zoosporangium ruptures and release them to medium, leaving the residual body and empty zoosporangium wall behind (link to the youtube video of *Chromera* excystation: https://youtu.be/yTr5nLmdCIE). The whole process is done within few seconds, depending on the size of the crack in the wall (Oborník et al., 2016). The highest number of zoospores can be found in the culture within 4-6 hours after the illumination, and their life

as fast bi-flagellated cells takes only about 10 minutes. Then the flagellate spins quickly around its axis, whilst probably drops both flagella away and transforms into a small coccoid (about 4 μm in diameter; Oborník et al., 2011; Oborník et al., 2016). After another two days (the 13th day of inoculation), the production of zoospores in the culture rapidly decreases to no zoospores observed at day 17 of inoculation (Oborník et al., 2011, Richtová unpublished data). No zoospores are observed in older cultures; even the number of cells within the culture is still increasing by binary division of present coccoid cells. Therefore, we suggest that *C. velia* zoosporogenesis is a light-dependent process that also relies on the culture density (Richtová, unpublished data; Oborník et al., 2011). The *C. velia* culture log phase slowly converts to the stationary phase approximately after a month of inoculation (Richtová, unpublished data). In such a culture, we can observe an increasing number of cells with highly developed plastid and thick cell walls (Oborník et al., 2016).
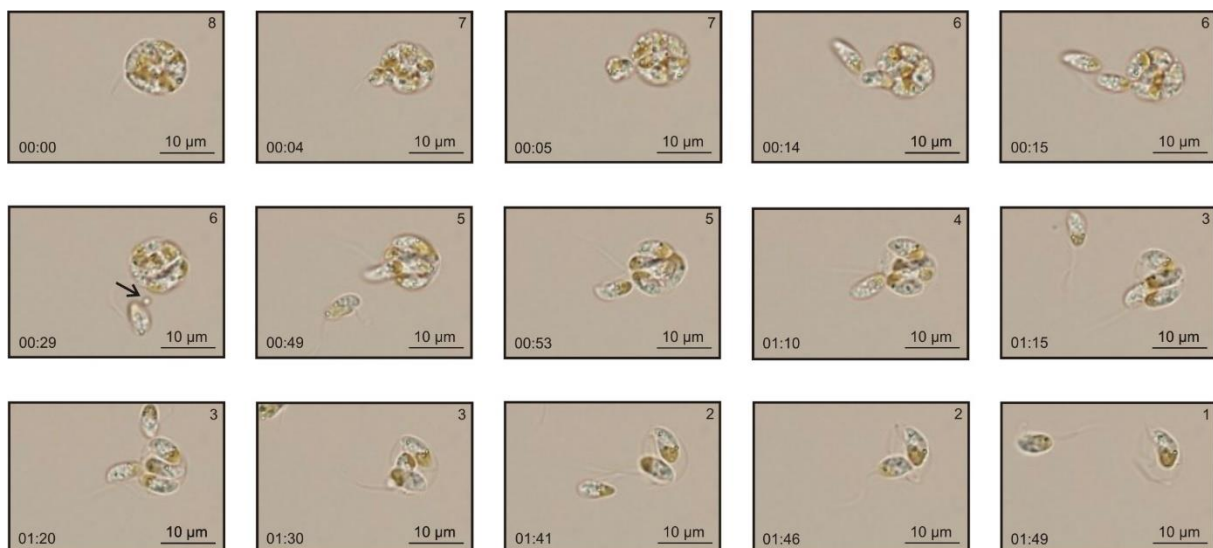
Figure 5: Timelaps showing the release of *C. velia* zoospores from zoosporangium. In this particular case, eight zoospores are released one by one through a narrow rupture in the zoosporangium cell wall. Within the process, also the residual body is let off the zoosporangium (6, arrow). Figure taken from Oborník et al., 2016.

As already mentioned before, *C. velia* was discovered as a coral-associated alga, which is easily kept solely in the culture, indicating that it can live independently as a phototroph thanks to its plastid. However, Cumbo and colleagues (2013) have identified *C. velia* cells inside the nubbins of *Montipora digitata* and also successfully and repeatedly infected the larvae of *Acropora digitifera*. Well studied coral symbiont, dinoflagellate *Symbiodinium*, is usually found within the coral larvae endoderm, which it typically infects via the larvae oral pore (Cumbo et al., 2013, Harii et al., 2009). *C. velia* was located not only in the endoderm but also in the ectoderm of coral larvae, suggesting it can also enter the larvae

through the ectoderm (Cumbo et al., 2013). I suppose that *C. velia* zoospores may use the machinery of the apical complex (mentioned above) to invade the coral larvae. The density of *C. velia* in coral larvae declined during the time (Cumbo et al., 2013), indicating that *Chromera* is a rather bothering roommate of coral larvae than a proper mutualist. It was later supported by data from coral host transcriptome analyzed at 4-, 12- and 48-hours post-infection by *C. velia*. The host response to *C. velia* resembled a reaction to pathogen rather than to a proper mutualist like *Symbiodinium*, showing that *Chromera* clearly brings no benefits to its host and is more probably a coral parasite or accidental bystander (Mohamed et al., 2018). The most recent theory of Oborník (2020) describes *Chromera* as a photoparasite, which means alga that takes advantage of both: nutrients from host cytoplasm and energy from its own photosystem (Oborník 2020).

1.4. Metabolism

It is believed that early heterotrophic organisms were swimming in a soup of nutrients. However, the evolution processes soon favored those who could synthesize molecules which sources had become limited (Fani, 2012). In the end, this selection pressure led to a complex but also highly ordered system of metabolic pathways in extant cells. A key feature that distinguishes all algae from other eukaryotes is the possession of plastids and their capability of photosynthesis (Beardall and Raven, 2012). The *C. velia* plastid is equipped with chlorophyll *a* and xanthophylls (violaxanthin and a novel isomer of isofucoxanthin). The green and orange color of these pigments, respectively (Delgado-Vargas et al., 2000), gives *C. velia* its brownish or gold tint. The light-dependent reaction of photosynthesis occurs inside the chloroplast, within the thylakoids, where the protein complexes enable the transport of electrons and protons across the membrane, thus generating the membrane potential. The membrane potential is later used to produce energy-rich molecules (ATP, NADPH) necessary in carbon assimilation reactions (Larkum et al., 2003).

C. velia photosynthesis was found to represent a simple, however exceptionally efficient model. The antennae of *C. velia* are organized similarly to antennae of diatoms, and they can quickly adapt to various light conditions by its reorganization. To capture as much light energy as possible during low-light conditions, *C. velia* distributes the antennae system to transmit the light energy to both photosystems (Quigg et al., 2012). Also, the amount of chlorophyll *a*, the primary light absorption pigment, increases in low-light conditions. During high-light conditions, *C. velia* exposes carotenoid pigments, mainly violaxanthin, providing fast photoprotection by non-photochemical quenching, a process that quickly dissipates absorbed light energy into heat (Kaňa et al., 2016; Kotabová et al., 2012; Kotabová et al., 2011). Like dinoflagellates, *C. velia* employs the bacterial RUBISCO type II, which was

found to be very efficient in carbon fixation and, together with algal carotenoid, contributes to a powerful photoacclimation mechanism (Quigg et al., 2012). Critical structures in photosynthetic apparatus are the large pigment-protein complexes, photosystem I, and photosystem II (Dudkina et al., 2015). Both structures have their ancestral forms in cyanobacterial predecessors, and their core structures are well established across all photosynthetic eukaryotes (Busch and Hippler, 2011). Sobotka and coworkers (2017) found that *C. velia* photosynthetic apparatus underwent notable structural changes by losing several canonical subunits, with two superoxide dismutases permanently attached to the photosystem I and three yet unknown subunits. It was also suggested that the whole photosynthetic apparatus of *C. velia* forms a supercomplex with rapid electron transfer that could further enhance the efficiency and adaptability of its photosynthesis (Sobotka et al., 2017).

A

| Peak	RT (min)	Maxima in eluant (nm)			%III/II	Identity	Molar ratio : Chl *a*	fg per cell
1	9.28	439	575	628	n/a	MgDVP-like	0.003	0.3
2	10.85	417	441	470	100	Unknown carotenoid 1	0.009	1.0
3	13.12		461		0	Unknown carotenoid 2	0.012	1.5
4	17.19	417	440	470	96	Violaxanthin	0.222	25.3
5	20.18	419	441	471	87	Unknown carotenoid 3	0.013	1.5
6	21.64		470.4		0	Unknown carotenoid 4	0.255	31.9
7	25.41	430		665	n/a	Chl *a* deriv	0.010	1.7
8	26.32	428		660	n/a	Chl *a* deriv	0.016	2.8
9	27.10	429		660	n/a	Chl *a*	1.000	169.4
10	27.54	428		660	n/a	Chl *a* epimer	0.012	2.1
11	29.29		454	479	28	β,β-carotene	0.088	9.0

B
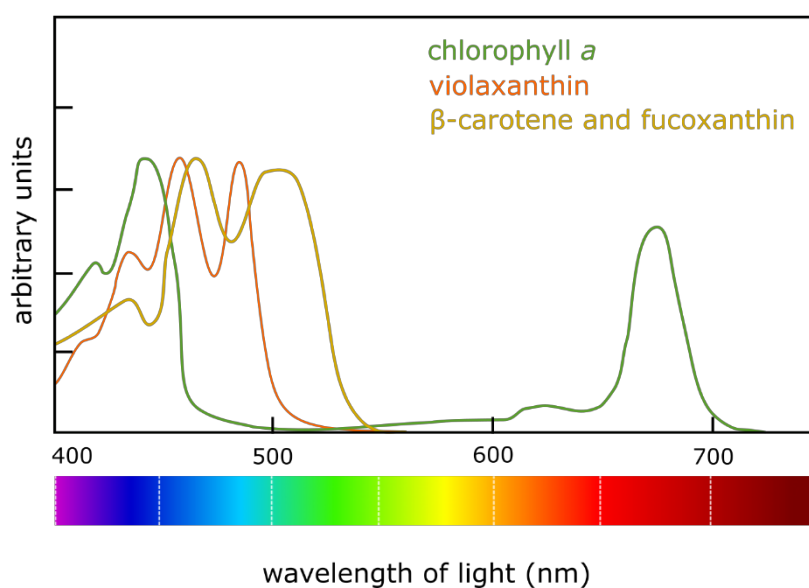
Figure 6: **Photosynthetic pigments of *C. velia*.** A) Table of pigments identified in *C. velia* (supplementary data from Moore et al., 2008). B) Absorption spectra of *C. velia* photosynthetic pigments. The figure is based on absorption spectra described in Croce et al., 2020; Kume et al., 2018; Snyder et al., 2004

Plastids also run important light-independent reactions. *In silico* analyses of proteins participating in the most important metabolic processes suggest that the plastid of *C. velia* efficiently cooperates with cytosol and mitochondrion to produce lipids, isoprenoids, and tetrapyrroles (the latter one will be discussed in detail in a separate chapter). However, in contrast to most other phototrophs, the vast majority of amino acids seem to be synthesized outside the plastid in the cytosol. *C. velia* also uniquely combines plastid ornithine and cytosolic arginine cycle for synthesis and decomposition of Arg (Füssy et al., 2019). The cytosolic localization of nitrogen metabolism is unorthodox among phototrophs (Dorrel et al., 2014). Füssy et al. (2019) suggest that the interplay between plastid, cytosol, and mitochondria on carbon and nitrogen allocation is pivotal for efficient *C. velia* metabolism that might play a role in its trophic versatility. Forty-eight genes coding for aminoacyl-tRNA synthetases were identified in *C. velia*, representing thus the complete set of 20 aminoacyl-tRNA synthetases needed to ligate tRNAs to amino acids. Their intracellular targeting was found to be independent of their evolutionary origin (Sharaf et al., 2019).

Canonical mitochondrion of eukaryotic protist is a two-membrane bounded organelle with lamellar cristae witch hallmark function is to supply molecular energy for various cell processes. However, this brief description can be applied only for mitochondria of protists living in aerobic and moderate environments. The more extreme the environment is, the more reduced mitochondria can be found (Müller et al., 2012). The textbook function of mitochondrion is oxidative phosphorylation; however, mitochondria of protists living in low-oxygen conditions have lost this function. Synthesis of Fe-S clusters, prosthetic groups of several essential proteins, was thought to be the excuse to keep such a rudimental mitochondrion (mitosome and hydrogenosome) in the cell (Hampl et al., 2019). However, Karnkowska and colleagues (2016) described that the oxymonad, now known as *Monocercomonoides exilis* (Treitli et al., 2018), synthesizes Fe-S clusters in the cytosol. They were also unable to find even a trace of mitochondrial proteins, which led them to conclude that *M. exilis* is the first eukaryotic cell without mitochondria (Karnakowska et al., 2016). Having no mitochondria is an example of extreme adaptation to a very specific environment, *e.g.,* the caecum of guinea pigs in the case of symbiotically living *M. exilis*. Parasitic lifestyle affects the composition of respiratory chain complexes responsible for core mitochondrial function (Müller et al., 2012). There are four respiratory chain complexes, which can form supercomplexes, ATP synthase, which makes dimers, and several free complexes within mitochondria. Their coexistence shapes the cristae and provides a mechanism to ensure efficient oxidation of all available substrates (Dudkina et al., 2015). Loss of complex III and IV is a pattern known to many eukaryotic anaerobes and the plant-pathogen *Phytomonas*. The ciliate *Nyctotherus* and the stramenopile *Blastocystis* lost even ATP synthase (complex V). The bloodstream stage of *Trypanosoma brucei* shuts down its respiratory chain, activates alternative oxidase and glycerol-3-phosphate

dehydrogenase, and generates protein gradient by switching the ATP synthase into the reverse (Tielens and van Hellemond, 2009). Respiratory chains of both chromerids (*C. velia* and *V. brassicaformis*) were thoroughly investigated by Flegontov et al. (2015). They found that *C. velia* respiratory chain works entirely without the complex I and III. The whole respiratory chain operates as two separate parts. In the first one, the complex II and alternative NADH dehydrogenase, glycerol 3-phosphate dehydrogenase, electron-transfer flavoprotein: ubiquinone oxidoreductase, and other enzymes generate electrons and channel them to ubiquinone, which passes them to alternative oxidase. The second respiratory sub-chain is constituted by complex IV and ATP synthase. The complex IV is the only one that pumps protons into the mitochondrial intermembrane space and thus creates a membrane potential. Contrary to *Chromera,* complex III was found in *Vitrella,* and also its respiratory chain is not split and functions continuously. Enzymes known to work in anaerobic protists and absent in almost all major parasitic sporozoan lineages were found in both chromerids, which points to their common ancestor's metabolic versatility. At least *Chromera* is capable of various living strategies (Flegontov et al., 2015). A similar electron transport system and oxidative phosphorylation were recently described in *Amoebophrya ceratii*, a dinoflagellate know to infect other dinoflagellates (John et al., 2019).

The transition metal composition in the marine environment differs substantially from the terrestrial one. Levels of iron are extremely low (0.02-1nM). However, as a critical compound of cell respiration and metabolism, it is a limiting factor for the growth of marine phytoplankton (Pollard et al., 2009, Turnerand Hunter, 2001). Therefore, cells must have evolved mechanisms of iron uptake from their surroundings (Sutak et al., 2010). The mechanism is best studied in *Saccharomyces cerevisiae*. Here the two different strategies of iron uptake were described. The reductive system, where ferric complexes are first dissociated outside the cell and then transported across the cell membrane via a high-affinity permease system (Ftr1) coupled to a copper-dependent oxidase (Fet3). And the non-reductive (copper-independent) strategy that uses siderophores to transport the iron ions inside the cell where the dissociation process occurs (Philpott, 2006). In diatoms, the membrane-bound phytotransferrin ISIP2A was found to mediate the iron uptake. This process is co-limited by the availability of carbonate (McQuaid et al., 2018). There is no evidence for the synthesis of siderophores by eukaryotic phytoplankton. However, diatoms are supposed to employ bacterial siderophores to intake organic iron in low free-iron conditions (Coale et al., 2019). Diatoms use ferritin to store and release iron in a controlled fashion (Marchetti et al., 2009). Also, *C. velia* growth was found to be positively influenced by the content of iron in the media. When exposed to iron-limited conditions, cells of *C. velia* shown decreased rates of respiration and photosynthesis; however, changes in the cell size or morphology were not observed. *C. velia* cells were found to keep the iron, yet no evidence for the ferritin proteins was found, and the way it stores iron remains unknown (Sutak et al., 2010). *C. velia* was found to

accumulates the Fe^{3+} at the cell wall, thus concentrating the ions near the transport sites for consecutive non-reductive but siderophore-independent uptake. The precise mechanism of how the ions are further transported inside the *C. velia* cells remains unknown. It is possible that a novel mechanism shared with apicomplexan or dinoflagellates (which mechanism of iron uptake is also yet not fully elucidated) can work there (Sutak et al., 2010).

There are two enzymes known to act in synthesizing fatty acids: FAS-I and FAS-II (fatty acid synthase type I and type II, respectively). FAS-I is a huge multi-modular enzyme working in the cytosol of heterotrophic organisms (Chirala and Wakil., 2004). FAS-II is referred to as a bacterial type, although it works in plants and primary algae as well. Contrary to FAS-I, FAS-II operates as a complex of separate enzymes located in the plastid (Ryall et al., 2003). Both FAS's repeatedly add two-carbon units to a carboxylic acid chain attached to an acyl carrier protein, thus generating fatty acids. Most apicomplexan parasites use the FAS-II system. However, coccidians were found to use both types of FAS's parallelly depending on the current life stage. The fatty acid synthesis minimalist is, for example, *Theileria parva* that lacks *de novo* synthesis and is also unable of elongation fatty acid chain and therefore takes all fatty acids from the host cell (Mazumdar and Striepen, 2007). The fatty acid biosynthesis in *C. velia* was thoroughly studied based on genomic and metabolic data. The *de novo* synthesis of short saturated fatty acids (C14:0-C18:0) is done by plastid localized FAS-II. The process of elongation and desaturation is suggested to be operated by FAS-I like multi-modular enzymes located in the cytosol and the endoplasmic reticulum (Tomčala et al., 2020).

Lipids are essential components of all organisms as building blocks of all cells (phospholipids), energy source (triacylglycerols) and plays a vital role in cell signaling (lipid rafts, Santos and Preta, 2018). The matrix of photosynthetic membranes is equipped with glycerolipids, which plays a crucial role in stabilizing protein complexes of the photosynthetic machinery (Boudiére et al., 2014). The most abundant are glycoglycerolipids, *i.e.,* monogalactosyldiacylglycerol (MGDG) and digalactosyldiacylglycerol (DGDG), which fraction in total lipid composition can reach up to 85 %. MGDG and DGDG were inherited from cyanobacteria, predecessors of all plastids, and are now shared with photosynthetic organisms. Even the nonphotosynthetic plastid of *Euglena* was found to retain the synthesis of galactolipids (Füssy et al., 2020). Also, plastid of sporozoans is no longer connected with photosynthetic processes galactolipid-like compounds were detected in their lysates (Botté et al., 2011; Boudiére et al., 2014; Oborník and Lukeš, 2013). The plant-like biosynthesis of galactolipids was found in *C. velia*, and the MGDG and DGDG synthase were found to be phylogenetically related to their counterparts in diatoms. The DGDG was shown to be located within the plastid membranes (Botté et al., 2011). Findings about glycoglycerolipids link *C. velia* with its photosynthetic relatives, and so do the studies on its sterols (cyclic lipid molecules with structural function in cell membranes). Analyses of *C.*

velia sterol composition and synthesis also suggest its ancient origin (Leblond et al., 2012). The TEM micrographs of *C. velia* revealed the presence of lipid droplets in their cytoplasm, which can be visualized by BODIPY staining (Oborník et al., 2011, Tomčala et al., 2017). Later it was shown that this novel alga could quickly accumulate an enormous amount of triacylglycerols. More than 250 intact lipid molecules and 14 species of fatty acid were detected in the chromerids lipidome. It was also suggested that *C. velia* replaced phospholipids with sulfo- and betaine lipids in response to the phosphorous deficient environment (Tomčala et al., 2017).

The overall metabolic profile of *C. velia* suggests its extraordinary adaptability, effectively working as a free-living phototroph capable of switching to photoparasitism when necessary or when environmental conditions are suitable. During the long-time cultivation, we found out that it is also an alga that can survive for an extremely long time without the light source, taking advantage of its valuable reserves from times of prosperity. *C. velia* can form a cyst that survives in high-salinity and low wateriness environment conditions that are often the result of culture forgotten in the cultivation box, however resembling the situation of coral exposed to dryness during low tide.

2. Tetrapyrrole biosynthesis

Tetrapyrroles are pointedly called "the pigments of life." Biochemists of the early '20s were fascinated by the red color of animal blood and the green color of leaves in all plants, yet no one knew the structure or chemistry of responsible pigments. It had to be a striking outcome when R. Willstätter studying chlorophyll and H. Fischer investigating heme, realized that these two materials, so different in appearance and function, are structurally related (Battersby, 2000). Nowadays, we know more than 30 biologically active chemical structures derived from the same biosynthetic primogenitor, uroporphyrinogen III (Moss, 1988). The tetrapyrrole biosynthetic pathway is extensively branched, leading to the hemes, chlorophylls, bilins, corrins (vitamin B12), siroheme, and coenzyme F430. The specific structure differences: the nature of their peripheral side chains, the oxidation state of the macrocycle itself, and the centrally chelated metal ion; give them properties that make tetrapyrroles essential for the life of the cell (Bryant et al., 2020).

2.1   The metal heart of tetrapyrroles

Chlorophylls are Mg^{2+} containing tetrapyrroles. Contrary to metal ions contained in other modified tetrapyrroles, the magnesium ion in chlorophyll is not redox-active. Its main role is to potentiate the

chemistry of tetrapyrrole ring during the process of energy transfer. Chlorophylls are intimately involved in primary steps of photosynthesis: light-harvesting the solar energy, energy transfer to reaction centers, and light energy conversion in the photochemistry process of splitting of water molecules or the production of strong reductants for carbon dioxide fixation and ATP generation (Katz et al., 1978; Bryant et al., 2020). Iron ion, which can exist in several oxidation states, gives heme its wide range of biological roles. In respiratory cytochromes, it serves as a one-electron carrier. Heme acts as a prosthetic group in various enzymes and serves as a signaling molecule controlling molecular and cellular processes. Heme also has a sensing role for diatomic gases like CO, NO, O_2 (Bryant et al., 2020, Mense and Zhang, 2006). Corrinoids are a diverse group of cofactors and coenzymes that harbor cobalt ion within a tetrapyrrole corin ring. The most popular is vitamin B12, or cobalamin, where the corrin ring is bound to a lower nucleotide, and either adenosyl or a methyl group constitutes an upper ligand. This vitamin is made only in certain Bacteria and Archaea; however, it is essential for DNA synthesis and cellular energy production even in mammals (Rowley and Kendall, 2019). The same enzyme that inserts cobalt for cobalamins is also responsible for inserting Ni^{2+} into the sirohydrochlorin that is consecutively stepwise converted to coenzyme F_{430}. Coenzyme F_{430} is a crucial unit of methyl-coenzyme M reductase, an enzyme of methanogenic Archaea responsible for generating about one billion tons of methane gas per annum. This enzyme is also involved in anaerobic methane oxidation mediated by bacterial/archaeal mats on the ocean floor (Moore et al., 2017). Siroheme is the simplest of the modified cyclic tetrapyrroles produced from uroporphyrinogen III even by a single multifunctional enzyme CysG in proteobacteria. Siroheme works as a cofactor of sulfite and nitrite reductases that, alongside with a 4Fe-4S cluster, operate the six-electron reduction of sulfite to sulfide or nitrite to ammonia. Siroheme, which is structurally isobacteriochlorin containing Fe^{2+}, is also a precursor of heme d_1. Heme d_1 is a cofactor of dissimilatory nitrite reductase cytochrome cd_1 needed for bacterial respiration by denitrification. Contrary to siroheme, heme d_1 displays a green color (Layer, 2020; Bryant et al., 2020; Pennington et al., 2020; Stroupe and Getzoff, 2009). The porphyrin ring of heme can be break down by a specific controlled reaction carried out by heme oxygenase and producing free iron, carbon monoxide, and biliverdin IXα – the first precursor of open tetrapyrroles called bilins. In mammals, biliverdin IXα is reduced to bilirubin, which is, apart from others, responsible for the yellow color in bruises. Oxygenic photosynthetic organisms use different ferredoxin-dependent bilin reductases, reducing diverse parts of biliverdin and producing bilins with different spectral properties. For example, phycocyanobilin is the prosthetic group in proteins of light-harvesting antennae in cyanobacteria, which gives them their typical blueish color (Beale, 2008; Rockwell et al., 2014; Bryant et al., 2020).

2.2　The tree-like tetrapyrrole synthesis

The tetrapyrrole pathway leading to all the above-mentioned groups of tetrapyrroles can be divided into three segments. The first part considers the synthesis of 5-aminolevulinic acid (ALA), the foundation stone of the whole pathway. The second part includes the biosynthesis of the first closed macrocycle, the above-mentioned uroporphyrinogen III. All following intermediate molecules of the biosynthesis are photosensitizers potentially generating single oxygen (Tanaka and Tanaka, 2007), and their biosynthesis forms the third part of the tetrapyrrole pathway. The pathway could be terminated by the last "empty" macrocycle – protoporphyrin IX. However, it is a bit complicated because metal ion insertion already happened in the branch leading to siroheme, heme b, and d, coenzyme F_{430}, and corrinoids. There is also a release of the central iron ligand when bilins are produced (described above).

There was a simple rule dividing organisms based on the way ALA is synthesized into two groups. The first group consisting predominantly of photosynthetic organisms and most bacteria, including cyanobacteria and archaea. These organisms synthesize ALA in three consecutive steps from glutamate (Glu) via the so-called C5 pathway (Tanaka and Tanaka, 2007). Using the energy from ATP hydrolysis, glutamate is activated by Glu-tRNA synthetase (GLUTS) to yield Glu-tRNA^{Glu}. Glu-tRNA^{Glu} is subsequently reduced by Glu-tRNA reductase (GLUTR) to Glu 1-semialdehyde in an NADPH-dependent manner. The ALA synthesis is finished by Glu 1-semialdehyde aminomutase (GLUAM), catalyzing the transamination with the help of pyridoxal phosphate (vitamin B6) as an enzyme cofactor (Bryant et al., 2020; Tanaka et al., 2011). The second group is formed mainly by nonphotosynthetic eukaryotes and some Alphaproteobacteria, which use a C4 pathway firstly proposed by David Shemin and coworkers (1946; also called a Shemin pathway). The C4 pathway comprises single-step condensation of succinyl-CoA with glycine mediated by 5-aminolevulinic acid synthase (ALAS). Glycine binds to the ALAS monomer via the same cofactor (pyridoxal phosphate) used in the C5 pathway by Glu 1-semialdehyde aminomutase. After the proton abstraction, the succinyl-CoA is attached to ALAS, and a transient intermediate (2-amino-3-ketoadipate) is generated. Finally, the loss of CO_2 and CoA leads to the release of the ALA (Bryant et al., 2020). Before the chromerid tetrapyrrole pathway was inspected, it was thought that the Shemin pathway is domain solely of heterotrophic, nonphotosynthetic organisms. However, *C. velia* was described as a first known exception - the photosynthetic organism using the C4 pathway for tetrapyrrole synthesis (Kořený et al., 2011).

The second part of the pathway, from ALA to uroporphyrinogen III, is believed to be conserved among all organisms that are synthesizing tetrapyrroles (Bryant et al., 2020; Cihlář et al., 2019; Tanaka and Tanaka, 2007). ALA dehydratase (ALAD, also named porphobilinogen synthetase, PBGS) is a homo-octameric enzyme (in bacteria) with zinc ions that condense two molecules of ALA to give a pyrrole

porphobilinogen. As the name suggests, four pyrroles are needed to utilize the first, yet still linear, tetrapyrrole hydroxymethylbilane. The polymerization of pyrroles is proceeded by porphobilinogen deaminase (PBGD, also named hydroxymethylbilane synthase, HMBS), a soluble monomer working without any dissociable prosthetic group or metal ion. PBGD contains a covalently linked dipyrromethane cofactor involved in the highly ordered binding of the reaction intermediates. During the process, the enzyme deaminates each porphobilinogen and incorporates it sequentially into a linear structure (Tanaka et al., 2011). Cyclization of the linearly-structured hydroxymethylbilane to the macrocycle of uroporphyrinogen III is done by uroporphyrinogen III synthase (UROS). UROS is a monomeric enzyme that inverts the orientation of hydroxymethylbilane pyrrole ring D. It is a critical process because it was found that hydroxymethylbilane spontaneously cyclizes to form the nonphysiological product, uroporphyrinogen I, abnormal porphyrin without the pyrrole ring D flip. The uroporphyrinogen I cannot be processed further, which leads to the accumulation of photosensitizing porphyrins that in humans causes the cutaneous lesions associated metabolic disorder known as congenital erythropoietic porphyria (Tanaka et al., 2011; Ortiz de Montellano and Paul, 2008; Sassa and Kappas, 2000).

The third part of the synthesis starts when the first tetrapyrrole macrocycle is successfully made and where the pathway branches for the first time. One branch usually methylates the uroporphyrinogen III and leads to siroheme, cobalamin, and coenzyme F430 biogenesis, whilst the other branch uses decarboxylation and leads intermediate towards protoporphyrinogen IX, a common precursor of heme and chlorophyll biosynthesis (Tanaka et al., 2011). For the purposes of this thesis, I will describe the synthesis through the so-called protoporphyrin branch. However, it should be noted that heme can also be produced by the corrin branch, either by the coproporphyrin route or by the siroheme route with Coproporphyrin III, or didecarboxysiroheme as intermediates, respectively (Bryant et al., 2020). The protoporphyrin branch starts with the action of uroporphyrinogen decarboxylase (UROD). UROD decarboxylates each uroporphyrinogen III pyrrole ring, beginning with the residue on the ring D and proceeding in a clockwise direction with the final loss of four molecules of CO2 and release coproporphyrinogen III. The enzyme is a homodimer and needs no exogenous cofactor; it is suggested to be one of the most catalytically proficient enzymes from nature (Tanaka et al., 2011; Bryant et al., 2020). The coproporphyrinogen III then proceeds to oxidative decarboxylation of the two propionate side chains attached to rings A and B, which is done by coproporphyrinogen III oxidase (CPOX). Two more molecules of CO_2 and another intermediate in the row, protoporphyrinogen IX, are released. The precise enzyme mechanism is not known yet; however, it was found that under anoxygenic conditions, organisms switch to oxygen-independent and phylogenetically unrelated versions of the enzyme (Bryant et al., 2020, Oborník and Green, 2005; Tanaka and Tanaka, 2007). Protoporphyrinogen IX is a non-

fluorescent intermediate. After the six-electron oxidation and the introduction of three new double bonds, catalyzed by protoporphyrinogen IX oxidase (PPOX), protoporphyrinogen IX is converted to fluorescent protoporphyrin IX, the last tetrapyrrole without the central metal ion, however already of the typical red color of porphyrins (Tanaka et al., 2011; Bryant et al., 2020). Same as with CPOX, there are oxygen-dependent and oxygen-independent versions of the PPOX. The best-studied is the oxygen-dependent form that was found to be a homodimer (Dailey et al., 2017). The terminal step of the protoporphyrin branch is the insertion of metal ion into the protoporphyrin IX. In this step, the empty tetrapyrrole ring is either filled with magnesium or iron ion by Mg-chelatase (MGCH) or ferrochelatase (FECH), respectively. Although the reaction done by previously mentioned enzymes differs mainly in the inserted ion, their structure is entirely different (Tanaka et al., 2007). FECH is a monomeric enzyme that does not require a cofactor or external energy source, like ATP. Cyanobacteria and higher plants are known to possess two FECH variants, one that is ubiquitously expressed throughout the plant tissues and the other one expressed only in photosynthetic ones. The latter one was found to possess a conserved chlorophyll-binding motif that is indispensable for the enzyme activity and plays a regulatory role (Sobotka et al., 2011, Tanaka et al., 2011). Contrary to FECH, MGCH requires ATP and the participation of all three subunits of the heterotrimeric enzyme (Shepherd et al., 2013).
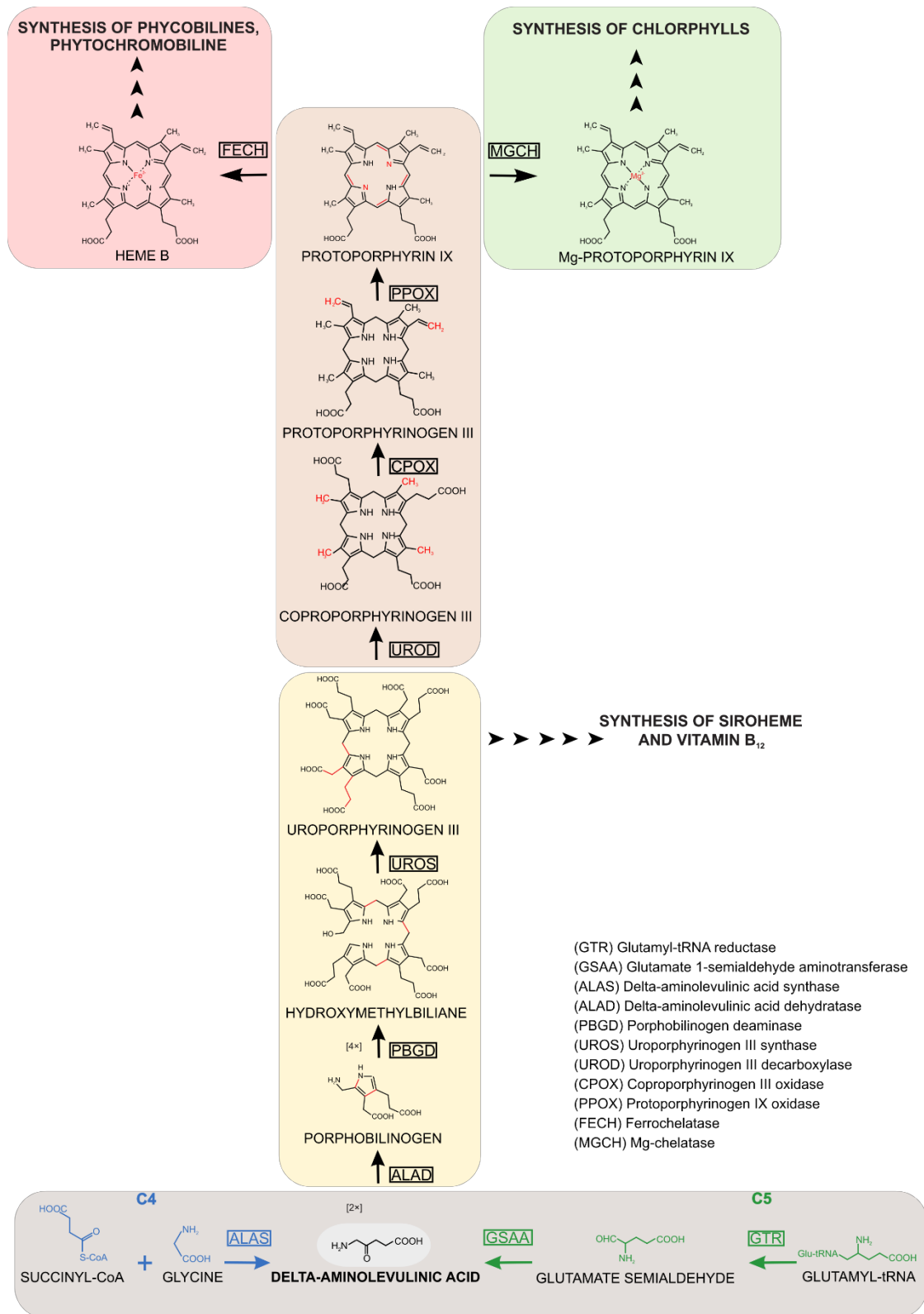
Figure 7: The tetrapyrrole biosynthesis. The synthesis can be divided into several parts. First, aminolevulinic acid is made either by C5 or by the C4 pathway (grey box). Next, the first enclosed macrocycle, uroporphyrinogen III, is synthesized (yellow box). Uroporphyrinogen III is subsequently transformed to protoporphyrin IX (brown box), the last porphyrin without central ligand (orange box). Iron or magnesium ions are added by ferrochelatase or Mg-chelatase, respectively (red and green box).

2.3 Regulation

The importance and indispensability of tetrapyrrole pathway products were already mentioned several times. The common precursor of the pathway, 5-aminolevulinic acid, points to an overly sensitive system, which allows simple regulation. The tight regulation is crucial because the pathway intermediates are highly reactive photosensitizers that, when light-activated, react with molecular oxygen producing reactive oxygen species like superoxide anion (O^{2-}), hydrogen peroxide (H_2O_2), and hydroxyl radical ($HO\bullet$). These molecules are formed by the partial reduction of oxygen and induce series of biological reactions that ultimately lead to cell death (Ray et al., 2012; Kou et al., 2017). A specific disorder for each step of the tetrapyrrole synthesis was described in humans, making at least eight types of different porphyria (Shepherd et al., 2013). However, porphyrin photosensitizers were found to be helpful in photodynamic therapy and are now widely used in treating various medical issues, including tumors (Wachowska et al., 2011; Kou et al., 2017). The whole problem of regulating tetrapyrroles biosynthesis far exceeds the theme of this thesis; therefore, only the porphyrin branch regulation will be described here.

For many years, the knowledge concerning tetrapyrrole regulation was limited to a single interaction between heme and ALA synthesizing enzyme (ALAS for C4 pathway, or GLUTR for C5 pathway). Although the regulation by the heme feedback inhibition of ALA formation is accepted as the major site of regulation, it is now known that the whole tetrapyrrole synthesis is controlled by a multi-level system working during different steps of the pathway. This complex regulatory mechanism not only protects the cell against the unwanted formation of reactive oxygen species, but it also fine-tunes the metabolic flow with the varying needs of tetrapyrroles under different developmental and environment conditions (Kobayashi and Masuda, 2016; Shepherd et al., 2013).

Analyses of mutants with the altered formation of different synthesis steps suggested that enzymes catalyzing steps between uroporphyrinogen III and protoporphyrin IX are in plants maintained at a higher level to prevent accumulation of potentially dangerous intermediates (Tanaka and Tanaka, 2007, Kobayashi and Masuda, 2016). It was also shown that mutants deficient in FECH show the formation of necrotic lesions caused by the accumulation of intermediates. However, MGCH mutants did not show such lesions nor display increased levels of intermediates, which advise that heme regulates both – heme synthesis itself and chlorophyll synthesis. Besides the heme feedback inhibition of ALA synthesis, another feedback inhibition between protoporphyrinogen IX and ALAD was described in *Escherichia coli* (Zhang et al., 2015). Higher plants were found to encode GLUTR by two genes. One (*HemA1*) is expressed primarily in photosynthetic tissues, its expression is induced by light, and it is subjected to a feedback control not only by heme but also by chlorophyll. Expression of other *HemA* genes is not affected by

light and occurs ubiquitously throughout plant tissues (Tanaka and Tanaka, 2007). The ATP/ADP ratio works contrarily at the branchpoint of protoporphyrin IX; the presence of ATP activates MGCH, whereas it inhibits the FECH activity (Cornah et al., 2002). It was found in maize chloroplasts that ATP/ADP ratio is increased in the light, suggesting channeling of protoporphyrin IX to chlorophyll branch during the day. Another common influencer is a GUN4 which binds to both the protoporphyrin IX and Mg-protoporphyrin IX, possibly controlling the substrate flow into chlorophyll or heme branch (Tanaka and Tanaka, 2007).

In photosynthetic organisms, the tetrapyrrole pathway also compromises the synthesis of chlorophyll. It is clear that during the light phase of the day, the tetrapyrrole pathway prioritizes the chlorophyll synthesis to saturate the need for photosystem complexes. Based on the expression profiles in response to light and the circadian clock, Matsumoto and coworkers (2004) classified tetrapyrrole biosynthetic genes of *Arabidopsis thaliana* into four clusters. The central regulation role is suggested for the c1 cluster of genes repressed in the dark but rapidly induced by light, like the previously mentioned *HEMA1* coding for GLUTR. The next cluster, c2, contains mainly genes coding the middle part of the heme/chlorophyll pathway. These genes expression is induced by light; however, it is not controlled by circadian clocks (Matsumoto et al., 2004). The expression of these genes is likely coordinated with mechanisms mentioned earlier (Kobayashi et al., 2016). Many genes involved in heme synthesis form a c3 cluster of genes neither induced by light nor controlled by the circadian rhythm system. The last c4 cluster is formed only by two genes: protochlorophyllide oxidoreductase A and B (PORA and PORB), whose transcripts accumulate in the dark and rapidly decrease with illumination. It should be noted that various conditions, except light and the circadian clock, form a complex regulation of genes involved in the pathway (Kobayashi et al., 2016). Also, posttranslational regulatory proteins strongly affect the tetrapyrrole biosynthesis pathway. The mRNA level of the "fluorescent in blue light" protein (FLU) protein was found to be increased by light, and the FLU itself is suggested to downregulate the GLUTR by interaction with its coding gene *HEMA1*. GLUTR is further posttranslationally regulated by GLUTR binding protein (GPB), which interacts with the enzyme itself and inhibits its degradation; thus, GBP allows for ongoing ALA synthesis. GBP activity is almost unaffected by light and circadian rhythms (Kobayashi et al., 2016).

Already in 1971, based on biochemical and physiological experiments, Shlyk proposed the existence of a chlorophyll biosynthesis center. A massive complex of enzymes involved in chlorophyll synthesis that would channel intermediates from one enzyme directly to the other, thus enhancing the enzyme effectivity and minimizing the potential hazard of free intermediates (Tanaka and Tanaka, 2007; Shlyk, 1971). During the time existence of metabolon, complexes were proposed for various pathways, including the TCA cycle (Robinson and Srere, 1985), the urea cycle (Cheung et al., 1989), fatty acid

metabolism (Srere and Sumegi, 1994), glycolysis (Campanella et al., 2005) and corrinoid synthesis (Deery et al., 2012). Forming such metabolons provides several advantages for the synthesis. Metabolon creates a kind of micro-environment with suitable pH, hydrophobicity, the concentration of reactants and products, and even the cofactors. They also protect the cell from contact with reactive or unstable intermediates and mediate interaction with regulation factors. These complexes also affect the proximity of involved proteins with other proteins and their positioning within or between organelles (Piel et al., 2019). The first evidence that CPOX, PPOX, and FECH from a mammalian heme pathway coexist in protein membrane-associated complex was already done in 1978 by Grandchamp and coworkers. Nowadays, much more is known about the heme metabolon, even all works were done on mammalian heme synthesis. Nevertheless, it shows the high organization of more than 20 components, including enzymes for the heme synthesis (ALAS, CPOX, PPOX, FECH), proteins involved in iron-sulfur cluster homeostasis, and necessary mitochondrial transporters (Piel et al., 2019; Medlock et al., 2015).

2.4 Localization in various organisms

Eukaryotic cells are subdivided into membrane-bound compartments, and different metabolic pathways occur within them or are shared among them. Over 70% of superpathways from UniProt and KEGG pathway databases were found to have multiple localization (Zhao and Qu., 2010). Compartmentalization of the metabolic pathway results from the interplay of several factors: enzymes evolutionary origin, demand for the product, substrate availability, and pathway regulation mechanisms (Richtová et al., 2021). Localization of the tetrapyrrole pathway differs across the eukaryotic tree of life, from a simple localization of the complete pathway within a chloroplast of, e.g., plant, through biosynthesis shared between mitochondria and cytosol of, e.g., animals to heme pathway that is dispersed through mitochondria, cytoplasm and apicoplast (remnant plastid) of intracellular apicomplexan parasites (Cihlář et al., 2016). Cases of coexistence of two independent tetrapyrrole pathways, each localized in different compartments, were also described (Kořený and Oborník, 2011; Cihlář et al., 2016).

The succinyl-CoA is a product of the mitochondrially located TCA cycle (Kořený et al., 2011). ALAS enzyme of C4 tetrapyrrole synthesis utilizes the succinyl-CoA and glycine for the production of ALA. Therefore, localization of the ALAS within mitochondria is reasonable and can be found in all primary eukaryotic heterotrophs (Opisthokonta, Amoeobzoa, early branching Stramenopila, Alveolata, Rhizaria, and members of the group previously described as "Excavata"). After the ALA formation, the tetrapyrrole synthesis continues with four steps in the cytosol (Ajioka et al., 2006). This transition is believed to protect mitochondria from the potential production of reactive oxygen species (Vavilin and

Vermaas., 2002; Cihlář et al., 2019). Yeasts, rhizarians, and ciliates keep the CPOX mediated production of coproporphyrinogen in the cytosol; however, animals and fungi have this step already located back in mitochondria. The very last two steps of heme biosynthesis (PPOX and FECH) proceed in mitochondria in all primary heterotrophs, which relates to the pathway regulation and the existence of heme metabolon complex (Cihlář et al., 2019; Piel et al., 2019). Mechanisms transporting the ALA from mitochondria to cytosol and coproporphyrinogen III from cytosol to mitochondria are yet unknown (Swenson et al., 2020). Enzymes of the primary heterotrophs heme pathway are of eukaryotic origin with an exception for ALAS and UROS that were found to be of Alphaproteobacterial (mitochondrial) origin (Oborník and Green, 2005; Kořený and Oborník, 2011).

The tetrapyrrole pathway of primary eukaryotic phototrophs is strongly influenced by the massive need for chlorophyll in photosystems (Mochizuki et al., 2010). The entire pathway, including the C5 beginning, is located within plastids, thus ensuring a fast supply of tetrapyrroles to photosynthesis and related processes. Several pathway enzymes exist in more than one version, reflecting the endosymbiotic origin of the plastid (Kořený and Oborník, 2011). The endosymbiosis joined up two pathways – one from primary heterotroph and the other (C5 based biosynthesis) from cyanobacteria. During the evolution, the primary phototrophs favored mainly genes of cyanobacterial origin, however keeping some of mitochondrial (Alphaproteobacterial) or eukaryotic (final host nucleus) origin (Cihlář et al., 2016; Cihlář et al., 2019). As heme is also needed for cytochromes of respiratory chains in mitochondria, it was suggested that the last two or three steps of the synthesis are localized parallelly in chloroplast and mitochondria of primary phototrophs. Related enzymes are often present in two evolutionary distinctive copies, suggesting that one can work in plastid and the other one in the mitochondrion (Kořený and Oborník, 2011; Kořený et al., 2011, Cihlář et al., 2016; Cihlář et al., 2019). As mentioned earlier, the expression of one of the genes is often induced by light (Matsumoto et al., 2004).

The eukaryotic tree of life has many lineages originated by multiple endosymbiotic events (Keeling et al., 2015). Therefore, we can find here groups of complex algae with red or green plastid, or even sporozoans with the remnant transparent complex plastid. Euglenids are algae with relatively recent secondary plastids derived from green alga (Rogers et al., 2007). They are suggested to represent the example of evolutionary intermediate in a metabolic transformation of a primary heterotroph to a photoautotroph through secondary endosymbiosis (Kořený et al., 2011). Euglenids possess two independently working tetrapyrrole pathways. One is derived from the eukaryotic host, uses C4 synthesis of ALA, and is localized partially in the mitochondria and cytosol. The second is inherited from the algal symbiont, synthesizes ALA by the C5 pathway, and is completely localized in the plastid. An analogous situation, with the two tetrapyrrole pathways working separately in one cell, was described in the chlorarachniophyte *Bigelowiella natans* (Cihlář et al., 2016). Cihlář and coworkers (2019) assume

that freshwater thecamoeba *Paulinella chromatophora* also runs two tetrapyrrole biosynthesis. One originated from the eukaryotic host and located in mitochondria and cytosol, and the second one running in the photosynthetic cyanelle. Dinotoms are a group of dinoflagellates that contain two evolutionary distinct plastids, each resulting from a different endosymbiosis. Both plastids, original peridinin plastid and younger plastid of the diatom origin, possess the C5 tetrapyrrole pathway (Hehenberger et al., 2014; Cihlář et al., 2019).

Sporozoans possess a unique form of heme synthesis. The origin of involved enzymes reflects the complex history of these parasites, including the photosynthetic period. The best-studied heme pathway is in *T. gondii* and *P. falciparum*. Both synthesize ALA by C4 pathway, as do primary heterotrophs. ALA is then exported to apicoplast, where the following four steps are localized. The sixth step, protoporphyrinogen IX synthesis mediated by CPOX, is localized in the cytosol, and the last two steps proceeded by PPOX and FECH are again in mitochondria (Bergmann et al., 2020; Ke et al., 2014; Kořený et al., 2013). Dispersion of the heme pathway among three different cellular compartments requires specific transporters working within apicoplast and mitochondrial membrane to allow the trafficking of intermediates between them. These parasite-specific transporters would be a promising drug target; however, they have not yet been identified (Kloehn et al., 2020).

Another curious localization of the heme pathway is working in *C. velia*. Even being an efficient phototroph, *C. velia* starts its tetrapyrrole biosynthesis identically as the above-mentioned related sporozoans, with ALAS in its mitochondrion. The remaining enzymes of the pathway are suggested to be localized within the plastid. It should be noted that similar to ALAS; also PBGD and second pseudoparalog of FECH is of Alphaproteobacterial (mitochondrial) origin (Oborník and Green, 2005 Kořený et al., 2011; Oborník, 2021, Richtová et al., 2021). However, contrary to ALAS, they are supposed to be localized within the *C. velia* plastid. Such unprecedented separation of the pathway's beginning and end would require complex regulation mechanisms (Richtová et al., 2021).

3. Protein targeting

The development of cellular compartmentalizations was undoubtedly one of the most intriguing events in evolution. It significantly enhanced the metabolic efficiency of the cell. On the other hand, compartmentalization of the cell also brings the need to sort all proteins specifically. All nucleus-encoded proteins are synthesized on ribosomes in the cytosol; however, many of their products are delivered elsewhere. Almost half of the proteins of the average cell are transported into or across a

membrane, which necessarily employs complete machinery of transport and translocon systems (Schatz and Dobberstein, 1996; Chen et al., 2019).

3.1   Organellar targeting

Theory proposing that all proteins contain the information for sorting and translocation encoded in their nascent chain was first published by Blobel and Sabatiny in 1971 (honored with Nobel prize in 1991). Nowadays, we distinguished several types of so-called targeting signals. These leads proteins to the mitochondria, chloroplast, peroxisome, and nucleus, or lead to the endoplasmic reticulum (ER) with further sorting via the secretory system (Owji et al., 2018; Kunze and Berger, 2015). Membrane-targeted proteins usually contain one or several signals at their N-terminus. Proteins that do not have an N-terminal signal complete their translation in the cytosol, and their future depends on whether they possess any other targeting signal further down the peptide chain (Kunze and Berger, 2015). N-terminal signal peptides (SP) directs the protein to ER, which serves as a hub for further protein sorting (Belucci et al., 2018). Even though many ER signal peptides were described, no significant aminoacids sequence conservation within the targeting signals was found. Artificial signal sequences and peptides were successfully targeted to the ER, further demonstrating that overall properties, rather than the specific sequence form a functional targeting signal (Chen et al., 2019).

Protein SPs typically consist of 25-30 amino acid residues. The general SPs are structured in three main sections: 1) the positively charged N-region, 2) the hydrophobic core H-region, 3) the cleavage site C-region (von Heijne and Abrahmsen, 1989). The N- region is characterized by the presence of basic residues. The precise order of the residues was found to be more important than the mere presence of positive residues, forming a higher positive charge in the C-region (Green et al., 1989; Owji et al., 2018). The N-region is responsible for interaction with the signal recognition particle, and its positive charge also determines the protein orientation favoring or preventing translocation (Nilsson et al., 2015). The H-region consists of 7-15 residues. Its hydrophobicity determines the orientation of the SP towards the cell membrane, if SP cleavage occurs, which type of the secretory pathway is followed (SRP or Sec, discussed later) and if further protein processing occurs (von Heijne and Abrahmsen, 1989; Owji et al., 2018). H-regions contain a species-specific motif that is not interchangeable even when the hydrophobicity is maintained at the same level (Duffy et al., 2010). Possession of Gly, Pro, Ser in the middle of the H- region serves as a helix-breaker forming a hairpin-like structure. This structure facilitates entering the membrane and subsequent cleavage by signal peptidase (Owji et al., 2018). The C-region consists of 3-7 neutral or polar amino acids that form an extended β-conformation, providing the signal peptidase's binding site. The positions -1 and -3 prior to the cleavage site are critical for the

function of the C-region. This sequence, known as the AXA motif (von Heijne et al., 1984), provides the interaction between SP and signal peptidase (Owji et al., 2018).

So far, five major protein import pathways were found to direct proteins to mitochondria. The type of targeting signal distinguishes them. The classical one used by the majority (60%) of mitochondrial matrix proteins is based on cleavable presequences (called mitochondrial transit peptides) and directs the precursor protein through specific mitochondrial translocons into the matrix. The other four protein import pathway don't possess a cleavable presequence; however, they have different kinds of internal targeting signals (reviewed in Wiedemann and Pfanner, 2017). The mitochondrial transit peptide forms an amphiphilic α-helix is typically rich in arginine and leads a protein to the mitochondrial matrix. Proteins with the destination in the mitochondrial intermembrane space often contain a sorting signal following the mitochondrial transit peptide. This signal resembles the bacterial ER signal peptide (Chen et al., 2019).

Plastids are, similar to mitochondria, semiautonomous organelles that can synthesize organelle-encoded proteins by their own translation machinery. However, most of the genes were relocated to the nucleus by a process called endosymbiotic gene transfer (Martin and Herrmann, 1998; Jiroutová et al., 2010). These genes possess an N-terminal chloroplast transit peptide that specifically drives a pre-protein through the translocon complexes of the outer and inner plastid membrane. This recognition site was first discovered in the nucleus-encoded subunit of the *Chlamydomonas reinhardtii* Rubisco (Dobberstein et al., 1977). Chloroplast transit peptides are variable in their length (from 20 to 100 aa) and possess no condensed blocks of sequence conservation (Jarvis et al., 2008). Their common characteristics are the overall positive charge (gained mainly by the hydroxylated residues, particularly serine), generally reduced acidic residues and conserved secondary structure. An amphiphilic α-helix structure appears to be crucial for the interaction with the outer chloroplast membrane. However, this structure is not observed in aqueous solutions and is proposed to be activated upon contact with the chloroplast galactolipid-containing membrane (Jarvis et al., 2008; Patron and Waller, 2007). The linear structure of the transit peptide in an aqueous solution is important for interaction with cytosolic chaperones. Exception of the general absence of the sequence conservation is the high level of Ala at the first position after Met in plants and "green" plastid and highly conserved Phe at the same, or +1, position in the "red" lineage plastids, e.g., glaucophytes, rhodophytes (Patron and Waller., 2007). Proteins targeted to thylakoids possess a secondary thylakoid signal that follows the transit peptide (Chen et al., 2019).

Most proteins are specifically targeted to either chloroplast or mitochondria; however, cases of dually targeted proteins have also been described (Duchene et al., 2005; Peeters and Small., 2001). Dual

targeting can be achieved by ambiguous transit peptides that can interact with both semiautonomous organelles (Sharma et al., 2018, Carrie and Small., 2013). Such transit peptides could be based on similarities of mitochondrial and chloroplast transit peptides as the above-mentioned overall positive charge and presence of α-helix (Patron and Waller., 2007).

Proteins synthesized in the cytoplasm can also be targeted to the nucleus or peroxisomes. Nuclear targeting is mediated by specialized structures called nuclear pores and depends on the presence of specific C-terminally located "nuclear localization signals" (NLS). A shared characteristic between studied NLS is the high abundance of basic amino acids (Freitas and Cunha, 2009). Contrary to the above-mentioned targeting mechanisms, the peroxisomal proteins can be transported into the organelle in a fully folded stage. Peroxisomal targeting signals exist in two forms, PTS1 and PTS2. The more common PTS1 consists of conserved C-terminally located tripeptide, whereas PTS2 is a nonapeptide localized at the N-terminus of the protein (Platta and Erdmann, 2007; Kunze and Berger, 2015).

 Proteins targeted to plastids that originated by a complex endosymbiosis need to cross one or two additional membranes compared to proteins targeted to primary plastids. For this purpose, pre-proteins are equipped with a bipartite targeting sequence (BTS) that is composed of a classical ER-like signal peptide (SP) followed by a transit peptide-like sequence (TP; Felsner et al., 2010). It was found that the cleavage site between SP and TP of diatoms possess a conserved sequence motif "ASA-FAP" (Gruber et al., 2015; Kilian and Kroth, 2005; Gruber et al., 2007). TPs of secondary plastids pretty much resemble those of primary plastids. They are depleted in acidic residues, therefore, have a positive charge (Felsner et al., 2010). They have an N-terminally located α-helix structure formed only in the lipidic environment (Ralph et al., 2004; Patron and Waller, 2007; Boucher and Yeh, 2019). It was demonstrated that the N-terminus of the TP is a critical part of the process of targeting. The first position of the transit peptide (after the cleavage of SP) is conserved to Phe, Tyr, Trp, and Leu in diatoms other groups of algae with complex plastids of red algal origin (Gould et al., 2006; Kilian and Kroth, 2005; Felsner et al., 2010; Ralph et al., 2004). Most plastid-targeted proteins from *C. velia* were found to possess the Phe at +1 position of TP (Füssy et al., 2019); however, exceptions can be found (Richtová et al., 2021; Füssy et al., 2019). The Phe motif is absent from green-derived secondary plastids, which led to the proposal that the Phe in position +1 of TP is conserved for all rhodophyte-derived complex plastids (Patron and Waller., 2007; Durnford and Gray, 2006).

3.2   Protein transport to complex plastid

Transport of nuclear-encoded proteins to the stroma of secondary plastids represents one of the most complex protein transport machinery among unicellular eukaryotes. The process of transport begins immediately after ribosomes synthesize the first amino acids. The outermost membrane of complex plastids is thought to have originated from a phagotrophic membrane that encapsulated the symbiont during the engulfment. In cryptophytes, stramenopiles, and haptophytes, the outermost membrane fused with the host ER and became chloroplast ER (cER). The surface of cER is covered with 80S ribosomes. The ER membrane of apicomplexan parasites remained separate from the outermost phagosomal membrane, with no associated ribosomal particles (Bolte et al., 2009; Stork et al., 2013; Lemgruber et al., 2013). The hydrophobic core of SP is cotranslationally recognized by the signal recognition particles (SRP). Recently two homologs of bacterial proteins associated with SRP function (namely FFh and FtsY) were described in Alveida, Heterolobosea, Hemimastigophora, and *Goniomonas*. The presence of these proteins in such unrelated eukaryotes, together with their monophyly, predicted mitochondrial localization and affinity of the Ffh group to Alphaproteobacteria, suggests their origin as far as from the last eukaryotic common ancestor (Pyrih et al., 2021). The whole complex of the ribosome and nascent protein chain with SRP is targeted to SRP receptors of ER/cER where the nascent chain is stepwise translocated by the Sec61 translocon (Nilsson et al., 2015). During the translocation process, the SP is cleaved of by signal peptidase complex, and the TP is exposed to chaperons in the ER/cER lumen. The chaperon Hsp70 (heat shock protein) was found to be essential for the process of apicoplast import (Tonkin et al., 2008; Foth et al., 2003). Homologue of this ER chaperone was also found in *C. velia* (Janouškovec et al., 2010). Plastid targeted pre-proteins within the cER lumen are in close contact with the following translocon machinery. However, in sporozoans, such pre-proteins must traverse the cytoplasm in vesicles budding from the ER. Further details regarding the transport of vesicles to the outermost membrane of the apicoplast are not known yet. SNARE-mediated delivery of the protein cargo was proposed, although more detailed studies are needed (Hempel et al., 2014; Sheiner et al., 2015; Boucher et al., 2019).

The TP directs the pre-protein through the remaining membranes of the complex plastid. The second outermost membrane, also called the periplastidial membrane, is supposed to be a derivate of symbiont cytoplasmic membrane (Maier et al., 2015). To traverse this membrane, organisms came with an intriguing solution – an adaptation of symbiont derived, pre-existing machinery. The function of the ER-associated degradation (ERAD) complex has changed, from quality control of misfolded proteins to recognition and translocation of plastid-targeted protein cargo in the former endosymbiont

Via the standard ERAD system (which is still retained in the host cell), proteins are transported from the ER lumen to cytosol, where they are degraded by the ubiquitin-proteasome system (Hempel et al., 2014; Boucher and Yeh, 2019; Agrawal et al., 2009). Several organisms with complex plastids were found to possess two independent versions of ERAD encoded in the nucleus. ERAD-L components for the host protein control system and the second set of homologous versions coming from the symbiont. Further analyses of the symbiont-derived ERAD detected BTSs at the N-terminus and showed their targeting to the periplastidial membrane or the apicoplast (Hempel et al., 2014; Hempel et al., 2009; Sommer et al., 2007). The former symbiont's ERAD system, which now acts as protein translocon of the periplastidial membrane, was called SELMA, referring to symbiont-specific ERAD-like machinery (Hempel et al., 2009). The central components of SELMA are the membrane Derline like proteins, particularly Der1, which form the translocation channel. Der1 is also suggested to recognize the critical +1 positioned Phe, or Tyr of the transit peptide (Hempel et al., 2009; Sommer et al., 2007). Der1 was so far found in all investigated complex plastids with the red-algal origin, including *C. velia* (Petersen et al., 2014). The SELMA system is thought to be derived from one and the same symbiont's ERAD machinery (Gould et al., 2015; Hempel et al., 2014), supporting a common origin of complex plastids of the red lineage. The SELMA core protein Der1 was not found in *Bigelowiella natans*, chlorarachniophyte with complex plastid derived from a green algal endosymbiont. How green-algal-derived plastids imports protein across the periplastidial membrane is not yet described (Hirakawa et al., 2012, Boucher and Yeh, 2019).

The pre-protein is further extracted from the Der pore in the SELMA complex by AAA-ATPase cdc48 and its cofactors (Sheiner et al., 2013; Boucher and Yeh, 2019). Two more membranes are in the way of stromal targeted pre-protein. These membranes are homologs of the primary plastid envelope (Hempel et al., 2014; Mallo et al., 2018). In primary plastids, the transport of pre-protein into the stroma is mediated via translocons of the outer and the inner membrane, TOC, and TIC, respectively. Both translocons are formed by a complex set of proteins, where Toc75 and Tic20 or Tic22 are accepted as a marker of the presence of the TOC and TIC complexes, respectively (Maier et al., 2015; Boucher and Yeh, 2019). The homolog of Toc75 was firstly identified *in silico* in chlorarachniophytes (Gilson et al., 2006; Hirakawa et al., 2012). Then protein of the Omp85 family with properties like Toc75 was described in *Phaeodactylum tricornutum*. The protein was shown to localize within the third outermost membrane (Bullman et al., 2010, Wunder et al., 2007). In sporozoans, the Toc75 was located in the corresponding apicoplast membrane and was shown to be essential for parasite growth and import (Sheiner et al., 2015). No homolog of Toc75 was found in *C. velia* so far. Similarly, the Tic22 homolog located in the apicoplast was described in *Toxoplasma gondii* and *Plasmodium falciparum,* where it was shown to be indispensable for the parasite survival. Tic22 enables the plastid pre-proteins to reach the stroma (Glaser et al., 2012; Mallo et al., 2018). Homologs of Tic20 and Tic110 were found in *C. velia* (Petersen

et al., 2014). When the plastid stromal protein reaches its destination, the TP is cleaved off by stromal processing peptidase (SPP), and proteins are folded to their mature conformation (Hempel et al., 2014; Tonkin et al., 2008).
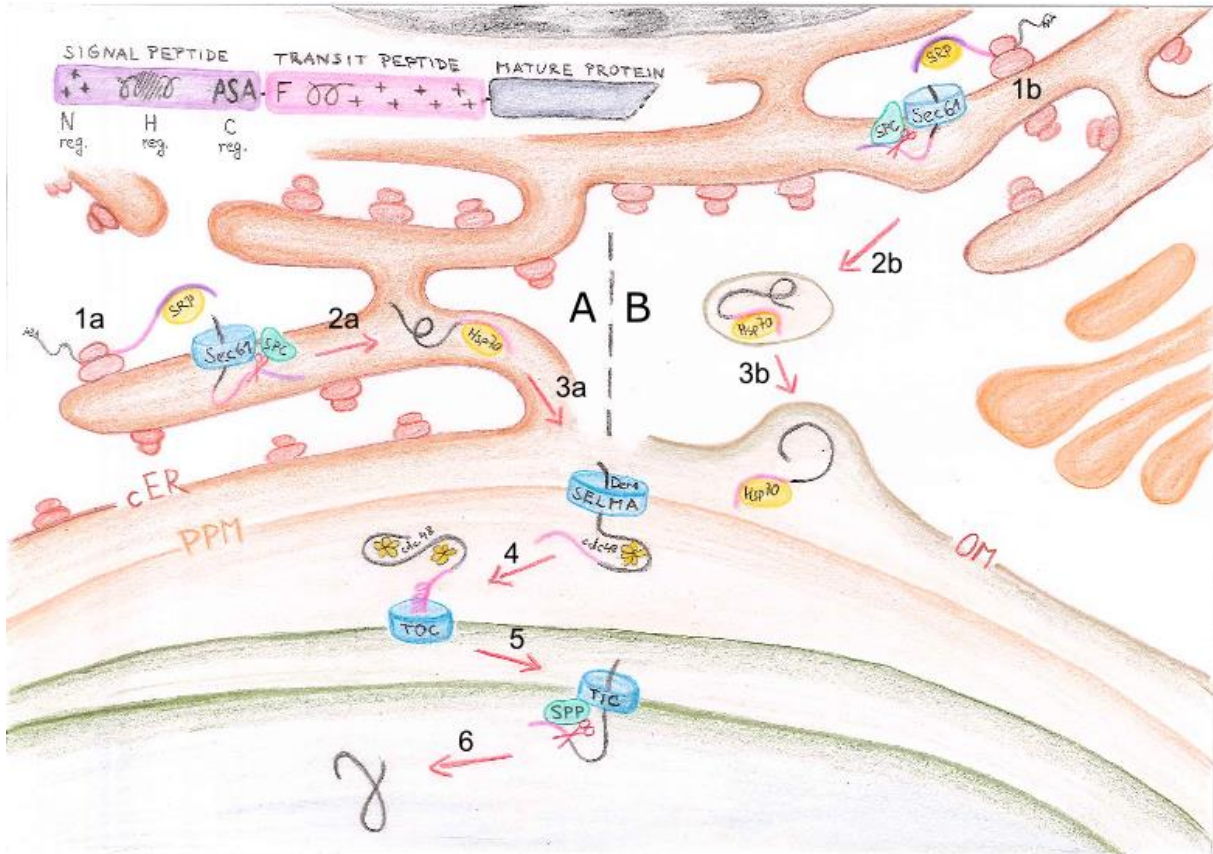

Figure 8: Scheme of protein targeting to complex plastid of the red lineage. The protein targeted to complex plastid is equipped with a bipartite targeting sequence consisting of signal and transit peptides (upper-left corner of the figure). The pre-protein is synthesized on the ribosome (1a, 1b) and co-translationally binds to the signal recognition particle (SRP), which directs the pre-protein through the Sec61 translocon of the endoplasmic reticulum (ER). The endoplasmic reticulum is in cryptophytes, haptophytes, and ochrophytes continuous with the outermost membrane of complex plastid (chloroplast ER, cER; side "A" of the figure). However, in sporozoans, apicomonads, and dinozoans, the ER membrane is not connected to the outermost membrane (OM) of the complex plastid (side "B" of the figure). Inside the ER or cER lumen, the signal peptide is cleaved by signal peptidase complex (SPC), and chaperon Hsp70 binds to pre-protein transit peptide (2a, 2b). The pre-protein and chaperon complex continues directly to the SELMA complex through the cER lumen or reaches the outermost plastid membrane via the ER-mediated vesicle transport (3a, 3b). The Der1 translocon of SELMA recognizes the transit peptide and channels the transition through the periplastidal membrane (PPM). The pre-protein is extracted from the SELMA by AAA-ATPase cdc48 and its cofactors (4). Homologs of primary plastid TOC and TIC translocons mediate the transport through the two innermost membranes of the plastid (5). Inside the plastid stroma, the transit peptide is cleaved off by stromal processing peptidase (SPP), and the mature protein is released (6). The

figure is based on the following works: Tonkin et al., 2008; Hempel et al., 2009; Bolte et al., 2009; Hirakawa et al., 2012; Sheiner et al., 2013; Stork et al., 2013; Gould et al., 2015; Boucher et al., 2019.

3.3   Targeting predictions

When Blobel and Sabatiny in 1971 proposed their signal hypothesis, the nature of the signal peptide was the scientist's focus. As described previously (3.1 Organellar targeting), the N-terminal targeting sequence is almost free of conserved sequence blocks. However, some common characteristics were described and allow recognition of the signal peptide. A quadruplet of at least three hydrophobic residues marked the hydrophobic core (H-region). Amino acids with small, neutral residues were found to be strongly overrepresented at the -1 and -3 positions in relation to the cleavage site, whereas positions +1, -1, and -4 were found to have no apparent preferences (Nielsen et al., 2019; von Heijne 1983). The first prediction method was therefore based on finding the beginning of the H-region, followed by defining a window for processing between +12 and +20 aa position for which the "processing probability" was calculated. The highest score denoted the cleavage site (von Heijne, 1983). Gunnter von Heijne also introduced the (-3, -1) rule that is still valid (Nielsen et al., 2019). Bioinformatics was in its childhood at that time, meaning that each prediction involved many statistical and machine learning technologies (Nielsen et al., 2019).

In 1992 Nakai and Kanehisa collected the empirical knowledge of sequence-function relationships and transformed them into a collection of if-then rules that could be computationally adapted to analyze sequence data. They came with a set of rules that can predict the various organellar location of proteins from unknown sequences. Since that time, the pool of empirical knowledge became significantly larger, and the prediction tools now routinely work with neural network methods that Nakai signed as desirable in 1992. The breakthrough came in 2000 when Emanuelsson et al. introduced the TargetP. TargetP extended the power of previously reported SignalP (identifying SPs; Nielssen et al., 1997) and ChloroP (identifying chloroplast TPs; Emanuelsson et al., 1999). TargetP can discriminate between proteins targeted to the chloroplast, mitochondria, secretory pathway, or "other" localization with up to a 90% success rate. TargetP is also predicting cleavage sites, however, with only a 40% success rate in the case of chloroplast pre-sequences (Emanuelsson et al., 2000).

Prediction servers are characterized by two factors (i) the input data, (ii) the construction of prediction rules. The input data can either constitute the complete amino acid sequence or some features derived from the sequence, e.g., α-helix or β-sheet structures, hydrophobicity. Prediction rules range from manually set collections to entirely automatic pattern techniques (Emanuelsson, 2002). The less complex the signal of interest is, the less data is needed to set the prediction rules. However, it also

enhances the probability of false-positive signals from sequences that contain such signal-like motif by chance. A typical example is peroxisome targeting prediction, where C-terminal PTS1 signals are detected in twice as many non-peroxisomal proteins as true peroxisome located proteins (Emanuelsson et al., 2002). An important aspect is also the group of proteins or the organisms on which the prediction tool is trained (e.g., plant proteins, bacteria; Emanuelsson et al., 2002). There are many prediction tools available today. To name a few of them: Predotar (trained for plant sequences to distinguish between chloroplast and mitochondria-targeted proteins; Small et al., 2004), MitoProt (predicts mitochondrial localization based on calculating several physiochemical parameters; Claros, 1995), TMHMM (general predictor of α-helical transmembrane regions, Krogh et al., 2001), and ApicoAP (suited to identify apicoplast targeted proteins; Cilingir et al., 2012). A potential user should carefully choose among them to find the most suitable one and avoid misleading research results (Richtová et al., 2021).

Predictions of intracellular locations for proteins from organisms with secondary plastid have to deal with their complex targeting sequence (BTS). Before specific algorithms for secondary endosymbiotic organisms were introduced, the combination of SignalP and TargetP was the best solution (Kořený et al., 2011; Cihlář et al., 2016). The latest version of the online tool (SignalP 5.0) uses a deep neural network approach to predict SP in all domains of life (Almagro Armenteros et al., 2019). SignalP 5.0 was found to have higher overall performance in the organisms for which it was developed than previous versions. When signal peptides were examined in diatoms, the latest version of SignalP was found to be less sensitive (Gruber et al., 2020). TargetP exists in two versions: one for plant proteins (recognizing cTP, SP, and mTP) and one for other eukaryotic proteins (trained to recognize SP and mTP; Emanuelsson, 2002). When TargetP is used to directly analyze the whole sequence of proteins that potentially contain a BTS, the "non-plant" version of TargetP should be used. Otherwise, TargetP would search for cTP known from primary plastids and green algae, thus a type of sequence not present in diatoms (Gruber et al., 2020). Prediction tools customized for nuclear-encoded plastid proteins in algae with secondary plastids of the red lineage are available since 2008 (HECTAR; Gschloessl et al., 2008) and 2015 (ASAFind; Gruber et al., 2015). ASAFind is based on output from SignalP or even the latest version of TargetP (2.0) and the recognition of conserved "ASAFAP" motifs. Its efficiency was tested on a large dataset of published protein localization data for the diatom *P. tricornutum*. ASAFind was found to work with both high specificity and high sensitivity (Gruber et al., 2015). Recently a modified version (ASAFind+) has been developed, which provides predictions specifically optimized for the two chromerids, *C. velia* and *V. brassicaformis* (Füssy et al., 2019).

3.4   Experimental localizations

Even though a great variety of powerful prediction tools exists, experimental protein localizations remain the gold standard in characterizing unknown proteins. There is quite a lot of advanced experimental techniques in the currently used model organisms. Ross Dalbey and coworkers (2002) divided vital techniques to study protein export into the following four categories.

Techniques that investigate the fate of the proteins within the cell. For example, protease experiments with cell extract containing intact ER vesicles enabled the discovery that mutant Sec61α accumulates secretory proteins like carboxypeptidase and pre-pro-alpha factor in the cytosol. In such experiments, proteins translocated to ER are protease-resistant, whereas cytoplasmic proteins will be processed by added protease (Deshaies and Schekman, 1987). Another approach comprises studies of protein translocation across the ER based on protease-accessibility to proteins modified in the ER lumen. Very laborious is also the analysis of protein in isolated intact cell compartments (Dalbey et al., 2002). Recently a work describing the isolation of *C. velia* plastids and mitochondria was published (Sharaf et al., 2019).

Genetics plays a significant role in the discovery of proteins components involved in translocation machinery. These techniques work with the characterization of mutants that arose in the culture with specific conditions. For example, several Sec mutants with blocked secretion pathways were characterized by looking for a cell with increased density of cell content in culture cultivated in temperature non-permissive (37°C) conditions (Novick et al., 1980).

In vitro techniques characterize purified proteins and reconstitute transport events in a test tube. These techniques can determine the need for energy and chaperons for translocation and whether translocation can occur posttranslationally. Such a method can work with artificially synthesized [^{35}S]-labeled pre-protein that is during or after the synthesis added to the environment with ER vesicles. If the protein was translocated to ER lumen, it would be protected from subsequently added protease. The influence of various modifications on translocation and protein processing can be followed by detecting radioactive amino acids. The eukaryotic SRP was identified using ER microsomal systems (Walter and Blobel, 1980, Dalbey et al., 2002). *In vitro* techniques are also methods of choice to identify the minimum components necessary for the membrane translocation (Dalbey et al., 2002).

Cell biology techniques allow following the protein within a cell using electron and fluorescence light microscopy (Dalbey et al., 2002). Electron microscopy techniques enable the investigation of the cell in such detail where the individual membranes of apicoplasts are distinguishable (Lembgruber et al., 2013). This, combined with secondary antibodies with attached small (typically 50 or 100 Å in diameter)

gold particles, gives a powerful tool to study the protein localization within the cell (Faulk et al., 1971). With the progress in imaging techniques in 3D electron microscopy, immunogold labeling literally gains a new perspective (Flechsler et al., 2019). Contrary to electron microscopy, fluorescence microscopy gives the power of imaging the proteins in living cells. Here, reporter proteins such as "green fluorescent protein (GFP) provide a great tool to study protein localization. GFP emits visible green light when excited with blue light. When a fusion construct of a protein of interest with GFP attached to it is made and successfully introduced to a living cell, the location of the expressed transgene can be easily detected by fluorescence microscopy. Variations of GFP that differ in their fluorescent characteristics (excitation and emission wavelengths) allow to follow signals from various proteins of interest in one cell (Day and Davidson, 2009). The immunofluorescence techniques comprise the use of antibodies labeled, for example, by fluorescein rhodamine or horseradish peroxidase (Dalbey et al., 2002). Cell trackers are commercially available fluorescent chemical tools that enable imaging of specific cell compartments, i.e., ER-tracker, MitoTracker, LysoTracker, to name a few (Halabi et al., 2020). The combination of cell trackers with protein unhidden by fusion fluorescent protein or antibody enables compartment colocalization. The fluorescence confocal microscopy increased this to the next level by allowing high-resolution images and the optical sectioning to allow 3D reconstruction (Elliot, 2019).

4. Conclusions

The discovery of *Chromera velia* filled the gap between secondary photosynthetic algae and parasitic Apicomplexa. Its finding opens possibilities to understand what changes an organism must undergo when it changes a trophic strategy. Or, from another perspective, what prerequisites an organism must have to be able of such a trophic transition. *C. velia* morphology unveiled shared features between this novel photosynthetic alga and its apicomplexan relatives, which supported its phylogenetic position and vice versa (Moore et al., 2008; Oborník et al., 2011; Janouškovec et al., 2009). Keeping the alga in culture shows its high adaptability to the various environmental condition or capability to invade another organism (Oborník and Lukeš, 2013; Cumbo et al., 2013). Also, the complex life cycle of *C. velia* was described in detail (Oborník et al., 2016). Such versatility can be enabled only with an effective metabolism. The photosynthetic and respiratory apparatuses of *C. velia* were found to be significantly reduced, however, with a rapid electron transfer (Sobotka et al., 2017; Flegontov et al., 2015). Overall metabolism of *C. velia* represents a set of peculiarities working together to serve the organism (Sutak et al., 2010; Füssy et al., Tomčala et al., 2017; Tomčala et al., 2020). The heme biosynthesis is very well conserved and shared among organisms which is a consequence of the production of essential compounds for various cell processes. This thesis aimed to experimentally investigate the localization of this critical pathway in *C. velia*. This thesis follows up with previous work unveiling *C. velia* heme biosynthesis uniquity and suggesting its localization from *in silico* analyses (Kořený et al., 2011). Combination of recent prediction servers with modern experimental techniques supported previous results of ALA synthesis in the mitochondrion of this photosynthetic organism. Moreover, we shed more light on the protein targeting to plastids of complex origin by using two trophically different yet distantly relative organisms (*Phaeodactylum tricornutum* and *Toxoplasma gondii*). Organisms with complex plastids of red algal origin have shared features in targeting nuclear-encoded proteins to the complex plastid (Bouchner and Yeh, 2019). However, we showed that protein targeting in particular organisms is a precise mechanism combining multiple details. We also suggested that the final localization of the heme pathway in *Chromera velia* is an interplay of the enzyme origin, the demand for the final product of a pathway, and the need for strict regulation of the synthesis (Richtová et al., 2021).

REFERENCES:

Adl, S. M., Simpson, A. G. B., Farmer, M. A., Andersen, R. A., Anderson, O. R., Barta, J. R., Bowser, S. S., Brugerolle, G. U. Y., Fensome, R. A., Fredericq, S., James, T. Y., Karpov, S., Kugrens, P., Krug, J., Lane, C. E., Lewis, L. A., Lodge, J., Lynn, D. H., Mann, D. G., McCourt, R. M., Mendoza, L., Moestrup, Ø., Mozley-Standridge, S. E., Nerad, T. A., Shearer, C. A., Smirnov, A. V., Spiegel, F. W., and Taylor, M. F. J. R. (2005). The new higher level classification of eukaryotes with emphasis on the taxonomy of protists. *Journal of Eukaryotic Microbiology* 52, 399–451. doi: 10.1111/j.1550-7408.2005.00053.x.

Agrawal, S., van Dooren, G. G., Beatty, W. L., and Striepen, B. (2009). Genetic evidence that an endosymbiont-derived endoplasmic reticulum-associated protein degradation (ERAD) system functions in import of apicoplast proteins. *Journal of Biological Chemistry* 284, 33683–33691. doi: 10.1074/jbc.M109.044024.

Ajioka, R. S., Phillips, J. D., and Kushner, J. P. (2006). Biosynthesis of heme in mammals. *Biochimica et Biophysica Acta (BBA) - Molecular Cell Research* 1763, 723–736. doi: 10.1016/j.bbamcr.2006.05.005.

Aldritt, S. M., Joseph, J. T., and Wirth, D. F. (1989). Sequence identification of cytochrome b in *Plasmodium gallinaceum*. *Molecular and cellular biology* 9, 3614–3620. doi: 10.1128/mcb.9.9.3614.

Almagro Armenteros, J. J., Tsirigos, K. D., Sønderby, C. K., Petersen, T. N., Winther, O., Brunak, S., von Heijne, G., and Nielsen, H. (2019). SignalP 5.0 improves signal peptide predictions using deep neural networks. *Nature Biotechnology* 37, 420-423. doi: 10.1038/s41587-019-0036-z.

Baldauf, S. L. (2003). The Deep Roots of Eukaryotes. *Science* 300, 1703, 1703-1706. doi: 10.1126/science.1085544.

Barbrook, A. C., and Howe, C. J. (2000). Minicircular plastid DNA in the dinoflagellate *Amphidinium operculatum*. *Molecular and General Genetics* 263, 152-158. doi: 10.1007/s004380050042.

Bartošová-Sojková, P., Oppenheim, R. D., Soldati-Favre, D., and Lukeš, J. (2015). Epicellular Apicomplexans: Parasites "On the Way In." *PLoS Pathogens* 11, e1005080. doi: 10.1371/journal.ppat.1005080.

Battersby, A. R. (2000). Tetrapyrroles: the pigments of life. *Natural Product Reports* 17, 507–526. doi: 10.1039/ B002635M.

Beale, S. I. (2008). Photosynthetic pigments: perplexing persistent prevalence of 'superfluous' pigment production. *Current Biology* 18, R342–R343. doi: 10.1016/j.cub.2008.02.064.

Beardall, J., and Raven, J. (2012). "Algal Metabolism," in eLS, (Ed.), 1-8. doi: 10.1002/9780470015902.a0000321.pub2.

Behjati, S., and Tarpey, P. S. (2013). What is next generation sequencing? *Archives of disease in childhood - Education practice edition* 98, 236–238. doi: 10.1136/archdischild-2013-304340.

Bellucci, M., de Marchis, F., and Pompa, A. (2018). The endoplasmic reticulum is a hub to sort proteins toward unconventional traffic pathways and endosymbiotic organelles. *Journal of Experimental Botany* 69, 7–20. doi: 10.1093/jxb/erx286.

Bergmann, A., Floyd, K., Key, M., Dameron, C., Rees, K. C., Thornton, L. B., Whitehead, D. C., Hamza, I., and Dou, Z. (2020). *Toxoplasma gondii* requires its plant-like heme biosynthesis pathway for infection. *PLOS Pathogens* 16, e1008499. doi: 10.1371/journal.ppat.1008499.

Bína, D., Herbstová, M., Gardian, Z., Vácha, F., and Litvín, R. (2016). Novel structural aspect of the diatom thylakoid membrane: Lateral segregation of photosystem I under red-enhanced illumination. *Scientific Reports* 6, 25583. doi: 10.1038/srep25583.

Blanchard, J. L., and Hicks, J. S. (1999). The Non-Photosynthetic Plastid in Malarial Parasites and Other Apicomplexans is Derived from Outside the Green Plastid Lineage. *Journal of Eukaryotic Microbiology* 46, 367–375. doi: 10.1111/j.1550-7408.1999.tb04615.x.

Blobel, G., and Sabatini, D. D. (1971). "Ribosome-membrane interaction in eukaryotic cells," in *Biomembranes: Volume 2*, ed. L. A. Manson (Boston, MA: Springer US), 193–195. doi: 10.1007/978-1-4684-3330-2_16.

Bolte, K., Bullman, L., Hempel, F., Bozarth, A., Zauner, S., and Maier, U. G. (2009). Protein Targeting into Secondary Plastids1. *Journal of Eukaryotic Microbiology* 56, 9–15. doi: 10.1111/j.1550-7408.2008.00370.x.

Borst, P., Overdulve, J. P., Weijers, P. J., Fase-Fowler, F., and van den Berg, M. (1984). DNA circles with cruciforms from *Isospora (Toxoplasma) gondii*. *Biochimica et Biophysica Acta (BBA) - Gene Structure and Expression* 781, 100–111. doi: 10.1016/0167-4781(84)90128-3.

Botté, C. Y., Yamaryo-Botté, Y., Janouškovec, J., Rupasinghe, T., Keeling, P. J., Crellin, P., Coppel, R. L., Maréchal, E., McConville, M. J., and McFadden, G. I. (2011). Identification of plant-like galactolipids in *Chromera velia*, a photosynthetic relative of malaria parasites. *Journal of Biological Chemistry* 286, 29893–29903. doi: 10.1074/jbc.M111.254979.

Boucher, M. J., and Yeh, E. (2019). Plastid–endomembrane connections in apicomplexan parasites. *PLoS Pathogens* 15, e1007661. doi: 10.1371/journal.ppat.1007661.

Boudière, L., Michaud, M., Petroutsos, D., Rébeillé, F., Falconet, D., Bastien, O., Roy, S., Finazzi, G., Rolland, N., Jouhet, J., Block, M. A., and Maréchal, E. (2014). Glycerolipids in photosynthesis: Composition, synthesis and trafficking. *Biochimica et Biophysica Acta (BBA) - Bioenergetics* 1837, 470–480. doi: 10.1016/j.bbabio.2013.09.007.

Brugerolle, G. (2002). *Colpodella vorax*: ultrastructure, predation, life-cycle, mitosis, and phylogenetic relationships. *European Journal of Protistology* 38, 113–125. doi: 10.1078/0932-4739-00864.

Bryant, D. A., Hunter, C. N., and Warren, M. J. (2020). Biosynthesis of the modified tetrapyrroles-the pigments of life. *The Journal of biological chemistry* 295, 6888–6925. doi: 10.1074/jbc.REV120.006194.

Bullmann, L., Haarmann, R., Mirus, O., Bredemeier, R., Hempel, F., Maier, U. G., and Schleiff, E. (2010). Filling the gap, evolutionarily conserved Omp85 in plastids of chromalveolates. *Journal of Biological Chemistry* 285, 6848–6856. doi: 10.1074/jbc.M109.074807.

Burki, F., Roger, A. J., Brown, M. W., and Simpson, A. G. B. (2020). The new tree of eukaryotes. *Trends in Ecology and Evolution* 35, 43–55. doi: 10.1016/j.tree.2019.08.008.

Burki, F., Shalchian-Tabrizi, K., Minge, M., Skjaeveland, A., Nikolaev, S. I., Jakobsen, K. S., and Pawlowski, J. (2007). Phylogenomics reshuffles the eukaryotic supergroups. *PloS one* 2, e790–e790. doi: 10.1371/journal.pone.0000790.

Busch, A., and Hippler, M. (2011). The structure and function of eukaryotic photosystem I. *Biochimica et Biophysica Acta (BBA) - Bioenergetics* 1807, 864–877. doi: 10.1016/j.bbabio.2010.09.009.

Campanella, M. E., Chu, H., and Low, P. S. (2005). Assembly and regulation of a glycolytic enzyme complex on the human erythrocyte membrane. *Proceedings of the National Academy of Sciences of the United States of America* 102, 2402–2407. doi: 10.1073/pnas.0409741102.

Carrie, C., and Small, I. (2013). A reevaluation of dual-targeting of proteins to mitochondria and chloroplasts. *Biochimica et Biophysica Acta (BBA) - Molecular Cell Research* 1833, 253–259. doi: 10.1016/j.bbamcr.2012.05.029.

Cavalier-Smith, T. (2000). Membrane heredity and early chloroplast evolution. *Trends in Plant Science* 5, 174–182. doi: 10.1016/S1360-1385(00)01598-3.

Cavalier-Smith, T. (2018). Kingdom Chromista and its eight phyla: a new synthesis emphasising periplastid protein targeting, cytoskeletal and periplastid evolution, and ancient divergences. *Protoplasma* 255, 297–357. doi: 10.1007/s00709-017-1147-3.

Chen, Y., Shanmugam, S. K., and Dalbey, R. E. (2019). The principles of protein targeting and transport across cell membranes. *The protein journal* 38, 236–248. doi: 10.1007/s10930-019-09847-2.

Cheung, C. W., Cohen, N. S., and Raijman, L. (1989). Channeling of urea cycle intermediates in situ in permeabilized hepatocytes. *The Journal of biological chemistry* 264, 4038–4044. doi: 10.1016/S0021-9258(19)84958-X.

Chirala, S. S., and Wakil, S. J. (2004). Structure and function of animal fatty acid synthase. in Lipids, 39(11):1045-1053. doi: 10.1007/s11745-004-1329-9.

Cihlář, J., Füssy, Z., Horák, A., and Oborník, M. (2016). Evolution of the tetrapyrrole biosynthetic pathway in secondary algae: Conservation, redundancy and replacement. *PLoS ONE* 11, e0166338. doi: 10.1371/journal.pone.0166338.

Cihlář, J., Füssy, Z., and Oborník, M. (2019). "Evolution of tetrapyrrole pathway in eukaryotic phototrophs," in *Advances in Botanical Research* (Academic Press Inc.), 273–309. doi: 10.1016/bs.abr.2018.12.003.

Cilingir, G., Broschat, S. L., and Lau, A. O. T. (2012). ApicoAP: The first computational model for identifying apicoplast-targeted proteins in multiple species of apicomplexa. *PLoS ONE* 7, 7(5):e36598. doi: 10.1371/journal.pone.0036598.

Clarisse, U., Decelle, J., Jouneau, P.H., Flori, S., Gallet, B., Keck, J.B., Dal Bo, D., Moriscot, C., Seydoux, C., Chevalier, F., Schieber, N., Templin, R., Allorent, G., Courtois, F., Curien, G., Schwab, Y., Schoehn, G., Zeeman, S., Falconet, D., and Finazzi, G. (2021). Morphological bases of phytoplankton energy management and physiological responses unveiled by 3D subcellular imaging. *Nature Communications* 12 (1), 1049. doi: 10.1038/s41467-021-21314-0.

Claros, M. G. (1995). Mitoprot, a macintosh application for studying mitochondrial proteins. *Bioinformatics* 11 (4), 441-447. doi: 10.1093/bioinformatics/11.4.441.

Coale, T.H., Moosburner, M., Horák, A., Oborník, M, Barbeau, K.A., and Allen, A.E. (2019). Reduction-dependent siderophore assimilation in a model pennate diatom. *Proc. Natl. Acad. Sci. U. S. A.* 116 (47), 23609-23617 doi:10.1073/pnas.1907234116.

Cornah, J. E., Roper, J. M., Pal Singh, D., and Smith, A. G. (2002). Measurement of ferrochelatase activity using a novel assay suggests that plastids are the major site of haem biosynthesis in both photosynthetic and non-photosynthetic cells of pea (*Pisum sativum L.*). *The Biochemical journal* 362, 423–432. doi: 10.1042/0264-6021:3620423.

Croce, R., and van Amerongen, H. (2020). Light harvesting in oxygenic photosynthesis: Structural biology meets spectroscopy. *Science* 369 (6506), eaay2058. doi: 10.1126/science.aay2058.

Cumbo, V. R., Baird, A. H., Moore, R. B., Negri, A. P., Neilan, B. A., Salih, A., van Oppen, M. J. H., Wang, Y., and Marquis, C. P. (2013). *Chromera velia* is endosymbiotic in larvae of the reef corals *Acropora digitifera* and *A. tenuis*. *Protist* 164 (2), 237-244. doi: 10.1016/j.protis.2012.08.003.

Dailey, H. A., Dailey, T. A., Gerdes, S., Jahn, D., Jahn, M., O'Brian, M. R., and Warren, M. J. (2017). Prokaryotic heme biosynthesis: multiple pathways to a common essential product. *Microbiology and molecular biology reviews : MMBR* 81, e00048-16. doi: 10.1128/MMBR.00048-16.

Dalbey, R. E., Chen, M., and Wiedmann, M. (2002). "2 - Methods in Protein Targeting, Translocation and Transport," in, eds. R. E. Dalbey and G. B. T.-P. T. von Heijne Transport, and Translocation (London: Academic Press), 5–34. doi: 10.1016/B978-012200731-6.50004-5.

Day, R. N., and Davidson, M. W. (2009). The fluorescent protein palette: tools for cellular imaging. *Chemical Society reviews* 38, 2887–2921. doi: 10.1039/b901966a.

Deery, E., Schroeder, S., Lawrence, A. D., Taylor, S. L., Seyedarabi, A., Waterman, J., Wilson, K. S., Brown D., Geeves, M. A., Howard, M. J., Pickersgill, R. W., and Warren, M. J. (2012). An enzyme-trap approach allows isolation of intermediates in cobalamin biosynthesis. *Nature chemical biology* 8, 933–940. doi: 10.1038/nchembio.1086.

Delgado-Vargas, F., Jiménez, A. R., and Paredes-López, O. (2000). Natural pigments: carotenoids, anthocyanins, and betalains--characteristics, biosynthesis, processing, and stability. *Critical reviews in food science and nutrition* 40, 173–289. doi: 10.1080/10408690091189257.

Deshaies, R. J., and Schekman, R. (1987). A yeast mutant defective at an early stage in import of secretory protein precursors into the endoplasmic reticulum. *Journal of Cell Biology* 105 (2), 633-645. doi: 10.1083/jcb.105.2.633.

Dobberstein, B., Blobel, G., and Chua, N. H. (1977). In vitro synthesis and processing of a putative precursor for the small subunit of ribulose-1,5-bisphosphate carboxylase of *Chlamydomonas reinhardtii*. *Proceedings of the National Academy of Sciences of the United States of America* 74, 1082–1085. doi: 10.1073/pnas.74.3.1082.

Dorrell, R. G., Drew, J., Nisbet, R. E. R., and Howe, C. J. (2014). Evolution of chloroplast transcript processing in *Plasmodium* and its chromerid algal relatives. *PLOS Genetics* 10 (1), e1004008. doi: 10.1371/journal.pgen.1004008.

Duchêne, A.-M., Giritch, A., Hoffmann, B., Cognat, V., Lancelin, D., Peeters, N. M., Zaepfe,l M., Maréchal-Drouard, L., and Small, I. D. (2005). Dual targeting is the rule for organellar aminoacyl-tRNA synthetases in *Arabidopsis thaliana*. *Proceedings of the National Academy of Sciences of the United States of America* 102 (45), 16484-16489. doi: 10.1073/pnas.0504682102.

Dudkina, N. V, Folea, I. M., and Boekema, E. J. (2015). Towards structural and functional characterization of photosynthetic and mitochondrial supercomplexes. *Micron* 72, 39–51. doi: 10.1016/j.micron.2015.03.002.

Duffy, J., Patham, B., and Mensa-Wilmot, K. (2010). Discovery of functional motifs in h-regions of trypanosome signal sequences. *Biochemical Journal* 426, 135–145. doi: 10.1042/BJ20091277.

Durnford, D. G., and Gray, M. W. (2006). Analysis of *Euglena gracilis* plastid-targeted proteins reveals different classes of transit sequences. *Eukaryotic cell* 5, 2079–2091. doi: 10.1128/EC.00222-06.

Dzierszinski, F., Popescu, O., Toursel, C., Slomianny, C., Yahiaoui, B., and Tomavo, S. (1999). The protozoan parasite *Toxoplasma gondii* expresses two functional plant- like glycolytic enzymes. Implications for evolutionary origin of apicomplexans. *Journal of Biological Chemistry* 274 (35), 24888-24895. doi: 10.1074/jbc.274.35.24888.

Elliott, A. D. (2020). Confocal Microscopy: Principles and Modern Practices. *Current Protocols in Cytometry* 92 (1) e68. doi: 10.1002/cpcy.68.

Emanuelsson, O. (2002). Predicting protein subcellular localization from amino acid sequence information. *Briefings in bioinformatics* 3 (4) 361-376. doi: 10.1093/bib/3.4.361.

Emanuelsson, O., Nielsen, H., Brunak, S., and von Heijne, G. (2000). Predicting subcellular localization of proteins based on their N-terminal amino acid sequence. *Journal of molecular biology* 300, 1005–1016. doi: 10.1006/jmbi.2000.3903.

Emanuelsson, O., Nielsen, H., and Heijne, G. von (1999). ChloroP, a neural network-based method for predicting chloroplast transit peptides and their cleavage sites. *Protein Science* 8 (5), 978-984. doi: 10.1110/ps.8.5.978.

Fani, R. (2012). The origin and evolution of metabolic pathways: why and how did primordial cells construct metabolic routes? *Evolution: Education and Outreach* 5, 367–381. doi: 10.1007/s12052-012-0439-5.

Faulk, W. P., and Taylor, G. M. (1971). An immunocolloid method for the electron microscope. *Immunochemistry* 8. 8(11):1081-1083. doi: 10.1016/0019-2791(71)90496-4.

Feagin, J. E. (1992). The 6-kb element of *Plasmodium falciparum* encodes mitochondrial cytochrome genes. *Molecular and Biochemical Parasitology* 52, 145–148. doi: 10.1016/0166-6851(92)90046-M.

Felsner, G., Sommer, M. S., and Maier, U. G. (2010). The physical and functional borders of transit peptide-like sequences in secondary endosymbionts. *BMC Plant Biology* 10, 223-undefined. doi: 10.1186/1471-2229-10-223.

Flechsler, J., Heimerl, T., Pickl, C., Rachel, R., Stierhof, Y. D., and Klingl, A. (2020). 2D and 3D immunogold localization on (epoxy) ultrathin sections with and without osmium tetroxide. *Microscopy Research and Technique* 83 (6), 691-705. doi: 10.1002/jemt.23459.

Flegontov, P., Michálek, J., Janouškovec, J., Lai, D. H., Jirků, M., Hajdušková, E., Tomčala, A., Otto, T., Keeling, P. J., Pain, A., Oborník, M., and Lukeš, J. (2015). Divergent mitochondrial respiratory chains in phototrophic relatives of apicomplexan parasites. *Molecular Biology and Evolution* 32 (5) 1115-1131. doi: 10.1093/molbev/msv021.

Forget, N., Belzile, C., Rioux, P., and Nozais, C. (2010). Teaching the microbial growth curve concept using microalgal cultures and flow cytometry. *Journal of biological education* 44, 185–189. doi: 10.1080/00219266.2010.9656220.

Foth, B. J., Ralph, S. A., Tonkin, C. J., Struck, N. S., Fraunholz, M., Roos, D. S., Cowman, A. F., and McFadden, G. I. (2003). Dissecting apicoplast targeting in the malaria parasite *Plasmodium falciparum*. *Science* 299 (5607), 705-708. doi: 10.1126/science.1078599.

Freitas, N., and Cunha, C. (2009). Mechanisms and signals for the nuclear import of proteins. *Current genomics* 10, 550–557. doi: 10.2174/138920209789503941.

Funes, S., Davidson, E., Reyes-Prieto, A., Magallón, S., Herion, P., King, M. P., and González-Halphen, D. (2002). A Green Algal Apicoplast Ancestor. *Science* 298 (5601), 2155. doi: 10.1126/science.1076003.

Füssy, Z., Záhonová, K., Tomčala, A., Krajčovič, J., Yurchenko, V., Oborník, M., and Eliáš, M. (2020). The cryptic plastid of *Euglena longa* defines a new type of nonphotosynthetic plastid organelle. *mSphere* 5, e00675-20. doi:10.1128/msphere.00675-20.

Füssy, Z., Faitová, T., and Oborník, M. (2019). Subcellular compartments interplay for carbon and nitrogen allocation in *Chromera velia* and *Vitrella brassicaformis*. *Genome Biology and Evolution* 11 (7), 1765-1779. doi: 10.1093/gbe/evz123.

Füssy, Z., Masařová, P., Kručinská, J., Esson, H. J., and Oborník, M. (2017). Budding of the alveolate *alga Vitrella brassicaformis* resembles sexual and asexual processes in apicomplexan parasites. *Protist* 168, 80–91. doi: 10.1016/j.protis.2016.12.001.

Füssy, Z., and Oborník, M. (2018). "Complex endosymbioses I: From primary to complex plastids, multiple independent events," in *Methods in Molecular Biology* (Humana Press Inc.), 17–35. doi: 10.1007/978-1-4939-8654-5_2.

Gardner, M. J., Bates, P. A., Ling, I. T., Moore, D. J., McCready, S., Gunasekera, M. B. R., Wilson, R. J. M., and Williamson, D. H. (1988). Mitochondrial DNA of the human malarial parasite *Plasmodium falciparum*. *Molecular and Biochemical Parasitology* 31, 11–17. doi: 10.1016/0166-6851(88)90140-5.

Gardner, M. J., Feagin, J. E., Moore, D. J., Rangachari, K., Williamson, D. H., and Wilson, R. J. (1993). Sequence and organization of large subunit rRNA genes from the extrachromosomal 35 kb circular DNA of the malaria parasite *Plasmodium falciparum*. *Nucleic acids research* 21, 1067–1071. doi: 10.1093/nar/21.5.1067.

Gardner, M. J., Feagin, J. E., Moore, D. J., Spencer, D. F., W.Gray, M., Williamson, D. H., and Wilson, R. J. (1991a). Organisation and expression of small subunit ribosomal RNA genes encoded by a 35-kilobase circular DNA in *Plasmodium falciparum*. *Molecular and Biochemical Parasitology* 48, 77–88. doi: 10.1016/0166-6851(91)90166-4.

Gardner, M. J., Goldman, N., Barnett, P., Moore, P. W., Rangachari, K., Strath, M., Whyte, A., Williamson, D. H., and Wilson, R. J. (1994). Phylogenetic analysis of the rpoB gene from the plastid-like DNA of *Plasmodium falciparum*. *Molecular and Biochemical Parasitology* 66, 221–231. doi: 10.1016/0166-6851(94)90149-X.

Gardner, M. J., Williamson, D. H., and Wilson, R. J. M. (1991b). A circular DNA in malaria parasites encodes an RNA polymerase like that of prokaryotes and chloroplasts. *Molecular and Biochemical Parasitology* 44, 115–123. doi: 10.1016/0166-6851(91)90227-W.

Gilson, P. R., Su, V., Slamovits, C. H., Reith, M. E., Keeling, P. J., and McFadden, G. I. (2006). Complete nucleotide sequence of the chlorarachniophyte nucleomorph: Nature's smallest nucleus. *Proceedings of the National Academy of Sciences* 103, 9566 – 9571. doi: 10.1073/pnas.0600707103.

Ginger, M. L., Portman, N., and McKean, P. G. (2008). Swimming with protists: perception, motility and flagellum assembly. *Nature Reviews Microbiology* 6, 838–850. doi: 10.1038/nrmicro2009.

Glaser, S., van Dooren, G. G., Agrawal, S., Brooks, C. F., McFadden, G. I., Striepen, B., and Higgins, M. K. (2012). Tic22 is an essential chaperone required for protein import into the apicoplast. *Journal of Biological Chemistry* 287, 39505–39512. doi: 10.1074/jbc.M112.405100.

Gould, S. B., Maier, U. G., and Martin, W. F. (2015). Protein import and the origin of red complex plastids. *Current Biology* 25 (12), R515-R521. doi: 10.1016/j.cub.2015.04.033.

Gould, S. B., Sommer, M. S., Hadfi, K., Zauner, S., Kroth, P. G., and Maier, U. G. (2006). Protein targeting into the complex plastid of cryptophytes. *Journal of Molecular Evolution* 62, 674–681. doi: 10.1007/s00239-005-0099-y.

Gould, S. B., Tham, W. H., Cowman, A. F., McFadden, G. I., and Waller, R. F. (2008). Alveolins, a new family of cortical proteins that define the protist infrakingdom Alveolata. *Molecular Biology and Evolution* 25 (6), 1219-1230. doi: 10.1093/molbev/msn070.

Green, R., Kramer, R. A., and Shields, D. (1989). Misplacement of the amino-terminal positive charge in the prepro-α-factor signal peptide disrupts membrane translocation in vivo. *Journal of Biological Chemistry* 264, 2963–2968. doi: 10.1016/S0021-9258(19)81706-4.

Gruber, A., McKay, C., Kroth, P. G., Armbrust, E. V., and Mock, T. (2020). Comparison of different versions of SignalP and TargetP for diatom plastid protein predictions with ASAFind. *Matters* 81, 519–528. doi: not available.

Gruber, A., Rocap, G., Kroth, P. G., Armbrust, E. V., and Mock, T. (2015). Plastid proteome prediction for diatoms and other algae with secondary plastids of the red lineage. *Plant Journal* 81, 519–528. doi: 10.1111/tpj.12734.

Gruber, A., Vugrinec, S., Hempel, F., Gould, S. B., Maier, U. G., and Kroth, P. G. (2007). Protein targeting into complex diatom plastids: Functional characterisation of a specific targeting motif. *Plant Molecular Biology* 64, 519–530. doi: 10.1007/s11103-007-9171-x.

Gschloessl, B., Guermeur, Y., and Cock, J. M. (2008). HECTAR: A method to predict subcellular targeting in heterokonts. *BMC Bioinformatics* 9, 393. doi: 10.1186/1471-2105-9-393.

Guillard, R. R. L., and Ryther, J. H. (1962). Studies of marine planktonic diatoms: I. *Cyclotella nana* Haustedt, and *Detonula confervacea (cleve)* Gran. *Canadian Journal of Microbiology* 8, 229–239. doi: 10.1139/m62-029.

Halabi, E. A., Arasa, J., Püntener, S., Collado-Diaz, V., Halin, C., and Rivera-Fuentes, P. (2020). Dual-activatable cell tracker for controlled and prolonged single-cell labeling. *ACS Chemical Biology* 15 (6), 1613-1620. doi: 10.1021/acschembio.0c00208.

Hampl, V. (2019). "Organisms without mitochondria, how it may happen? Hydrogenosomes and mitosomes: mitochondria of anaerobic eukaryotes," in, ed. J. Tachezy (Cham: Springer International Publishing), 309–318. doi: 10.1007/978-3-030-17941-0_13.

Hanson, M. R., and Köhler, R. H. (2001). GFP imaging: methodology and application to investigate cellular compartmentation in plants. *Journal of Experimental Botany* 52, 529-539. doi: 10.1093/jexbot/52.356.529.

Harii, S., Yasuda, N., Rodriguez-Lanetty, M., Irie, T., and Hidaka, M. (2009). Onset of symbiosis and distribution patterns of symbiotic dinoflagellates in the larvae of scleractinian corals. *Marine Biology* 156, 1203–1212. doi: 10.1007/s00227-009-1162-9.

Hehenberger, E., Imanian, B., Burki, F., and Keeling, P.J. (2014). Evidence for the retention of two evolutionary distinct plastids in dinoflagellates with diatom endosymbionts. *Genome Biology and Evolution* 6 (9), 2321-34. doi:10.1093/gbe/evu182.

Hempel, F., Bolte, K., Klingl, A., Zauner, S., and Maier, U. G. (2014). "Protein transport into plastids of secondarily evolved organisms," in *Plastid Biology*, 291–303. doi: 10.1007/978-1-4939-1136-3_11.

Hempel, F., Bullmann, L., Lau, J., Zauner, S., and Maier, U. G. (2009). ERAD-derived preprotein transport across the second outermost plastid membrane of diatoms. *Molecular Biology and Evolution* 26, 1781–1790. doi: 10.1093/molbev/msp079.

Hirakawa, Y., Burki, F., and Keeling, P. J. (2012). Genome-based reconstruction of the protein import machinery in the secondary plastid of a chlorarachniophyte alga. *Eukaryotic Cell* 11, 324–333. doi: 10.1128/EC.05264-11.

Hopkins, J., Fowler, R., Krishna, S., Wilson, I., Mitchell, G., and Bannister, L. (1999). The plastid in *Plasmodium falciparum* asexual blood stages: a three-dimensional ultrastructural analysis. *Protist* 150, 283–295. doi: 10.1016/S1434-4610(99)70030-1.

Howe, C. J., Nisbet, R. E. R., and Barbrook, A. C. (2008). The remarkable chloroplast genome of dinoflagellates. *Journal of Experimental Botany* 59 (5),1035-1045 doi: 10.1093/jxb/erm292.

Janouškovec, J., Horák, A., Oborník, M., Lukeš, J., and Keeling, P. J. (2010). A common red algal origin of the apicomplexan, dinoflagellate, and heterokont plastids. *Proceedings of the National Academy of Sciences of the United States of America* 107 (24), 10949-10954. doi: 10.1073/pnas.1003335107.

Jarvis, P. (2008). Targeting of nucleus-encoded proteins to chloroplasts in plants. *New Phytologist* 179, 257–285. doi: 10.1111/j.1469-8137.2008.02452.x.

Jiroutová, K., Kořený, L., Bowler, C., and Oborník, M. (2010). A gene in the process of endosymbiotic transfer. *PloS one* 5, e13234–e13234. doi: 10.1371/journal.pone.0013234.

John, U., Lu, Y., Wohlrab, S., Groth, M., Janouškovec, J., Kohli, G. S., Mark, F. C., Bickmeyer, U., Farhat, S., Felder, M., Frickenhaus, S., Guillou, L., Keeling, P. J.,Moustafa, A., Porcel, B., Valentin, K., and Glöckner, G. (2019). An aerobic eukaryotic parasite with functional mitochondria that likely lacks a mitochondrial genome. *Science Advances* 5 (4), eaav1110. doi: 10.1126/sciadv.aav1110.

Kaňa, R., Kotabová, E., Kopečná, J., Trsková, E., Belgio, E., Sobotka, R., and Ruban, A.V. (2016). Violaxanthin inhibits nonphotochemical quenching in light-harvesting antenna of *Chromera velia*. *FEBS Letters* 590 (8), 1076-8105. doi: 10.1002/1873-3468.12130.

Karnkowska, A., Vacek, V., Zubáčová, Z., Treitli, S. C., Petrželková, R., Eme, L., Novák, L. Žárský, V., Barlow, L. D., Herman, E. K., Soukal, P., Hroudová, M., Doležal, P., Stairs, C. W., Roger, A., Eliáš, M., Dacks, J. B., Vlček, Č., and Hampl, V. (2016). A Eukaryote without a Mitochondrial Organelle. *Current Biology* 26, 1274–1284. doi: 10.1016/j.cub.2016.03.053.

Katz, J. J., Norris, J. R., Shipman, L. L., Thurnauer, M. C., and Wasielewski, M. R. (1978). Chlorophyll function in the photosynthetic reaction center. *Annual Review of Biophysics and Bioengineering* 7, 393–434. doi: 10.1146/annurev.bb.07.060178.002141.

Ke, H., Sigala, P. A., Miura, K., Morrisey, J. M., Mather, M. W., Crowley, J. R., Henderson, J.P., Goldberg, D. E., Long, C. A., and Vaidya, A. B. (2014). The heme biosynthesis pathway is essential for *Plasmodium falciparum* development in mosquito stage but not in blood stages. *Journal of Biological Chemistry* 289, 34827–34837. doi: 10.1074/jbc.M114.615831.

Keeling, P. J., Burger, G., Durnford, D. G., Lang, B. F., Lee, R. W., Pearlman, R. E., Roger, A. J., and Gray, M. W. (2005). The tree of eukaryotes. *Trends in Ecology & Evolution* 20, 670–676. doi: 10.1016/j.tree.2005.09.005.

Keeling, P. J., McCutcheon, J. P., and Doolittle, W. F. (2015). Symbiosis becoming permanent: Survival of the luckiest. *Proceedings of the National Academy of Sciences* 112, 10101–10103. doi: 10.1073/pnas.1513346112.

Kilejian, A. (1975). Circular mitochondrial DNA from the avian malarial parasite *Plasmodium lophurae*. *Biochimica et Biophysica Acta (BBA) - Nucleic Acids and Protein Synthesis* 390, 276–284. doi: 10.1016/0005-2787(75)90348-2.

Kilian, O., and Kroth, P. G. (2005). Identification and characterization of a new conserved motif within the presequence of proteins targeted into complex diatom plastids. *Plant Journal* 41, 175–183. doi: 10.1111/j.1365-313X.2004.02294.x.

Kloehn, J., Harding, C. R., and Soldati-Favre, D. (2020). Supply and demand—heme synthesis, salvage and utilization by Apicomplexa. *FEBS Journal* 88 (2), 382-404. doi: 10.1111/febs.15445.

Kobayashi, K., and Masuda, T. (2016). Transcriptional regulation of tetrapyrrole biosynthesis in *Arabidopsis thaliana*. *Frontiers in Plant Science* 7, 1811-undefined. doi: 10.3389/fpls.2016.01811.

Köhler, S. (2005). Multi-membrane-bound structures of Apicomplexa: I. the architecture of the *Toxoplasma gondii* apicoplast. *Parasitology Research* 96, 258–272. doi: 10.1007/s00436-005-1338-2.

Köhler, S., Delwiche, C. F., Denny, P. W., Tilney, L. G., Webster, P., Wilson, R. J. M., Palmer, J. D., and Roos, D. S. (1997). A plastid of probable green algal origin in apicomplexan parasites. *Science* 275 (5305), 1485-1489. doi: 10.1126/science.275.5305.1485.

Kořený, L., and Oborník, M. (2011). Sequence evidence for the presence of two tetrapyrrole pathways in *Euglena gracilis*. *Genome biology and evolution* 3, 359–364. doi: 10.1093/gbe/evr029.

Kořený, L., Oborník, M., and Lukeš, J. (2013). Make it, take it, or leave it: Heme metabolism of parasites. *PLoS Pathogens* 9, e1003088-undefined. doi: 10.1371/journal.ppat.1003088.

Kořený, L., Sobotk, R., Janouškovec, J., Keeling, P. J., and Oborník, M. (2011). Tetrapyrrole synthesis of photosynthetic chromerids is likely homologous to the unusual pathway of apicomplexan parasites. *Plant Cell* 23, 3454–3462. doi: 10.1105/tpc.111.089102.

Kořený, L., Zeeshan, M., Barylyuk, K., Tromer, E. C., van Hooff, J. J. E., Brady, D., Ke, H., Chelaghma, S., Ferguson, D. J. P., Eme, L., Tewari, R., and Waller, R. F. (2021). Molecular characterization of the conoid complex in Toxoplasma reveals its conservation in all apicomplexans, including *Plasmodium* species. *PLOS Biology* 19, e3001081. doi: 10.1371/journal.pbio.3001081.

Kotabová, E., Jarešová, J., Kaňa, R., Sobotka, R., Bína, D., and Prášil, O. (2014). Novel type of red-shifted chlorophyll *a* antenna complex from *Chromera velia*. I. Physiological relevance and functional connection to photosystems. *Biochimica et Biophysica Acta (BBA) - Bioenergetics* 1837, 734–743. doi: 10.1016/j.bbabio.2014.01.012.

Kotabová, E., Kaňa, R., Jarešová, J., and Prášil, O. (2011). Non-photochemical fluorescence quenching in *Chromera velia* is enabled by fast violaxanthin de-epoxidation. *FEBS Letters* 585 (12), 1941-1945. doi: 10.1016/j.febslet.2011.05.015.

Kou, J., Dou, D., and Yang, L. (2017). Porphyrin photosensitizers in photodynamic therapy and its applications. *Oncotarget* 8, 81591–81603. doi: 10.18632/oncotarget.20189.

Krogh, A., Larsson, B., von Heijne, G., and Sonnhammer, E. L. L. (2001). Predicting transmembrane protein topology with a hidden Markov model: Application to complete genomes. *Journal of Molecular Biology* 305 (3), 567-580. doi: 10.1006/jmbi.2000.4315.

Kume, A., Akitsu, T., and Nasahara, K. N. (2018). Why is chlorophyll b only used in light-harvesting systems? *Journal of Plant Research* 131, 961-972. doi: 10.1007/s10265-018-1052-7.

Kunze, M., and Berger, J. (2015). The similarity between N-terminal targeting signals for protein import into different organelles and its evolutionary relevance. *Frontiers in Physiology* 6, 259. doi: 10.3389/fphys.2015.00259.

Larkum, A. W. D., Douglas, S. E., and Raven, J. A. (2003). *Photosynthesis in Algae*. Advances i., ed. GOVINDJEE Springer, Dordrecht. doi: 10.1007/978-94-007-1038-2.

Layer, G. (2021). Heme biosynthesis in prokaryotes. *Biochimica et Biophysica Acta (BBA) - Molecular Cell Research* 1868, 118861. doi: 10.1016/j.bbamcr.2020.118861.

Leblond, J. D., Dodson, J., Khadka, M., Holder, S., and Seipelt, R. L. (2012). Sterol composition and biosynthetic genes of the recently discovered photosynthetic alveolate, *Chromera velia* (Chromerida), a close relative of Apicomplexans. *Journal of Eukaryotic Microbiology* 59, 191–197. doi: 10.1111/j.1550-7408.2012.00611.x.

Lemgruber, L., Kudryashev, M., Dekiwadia, C., Riglar, D. T., Baum, J., Stahlberg, H., Ralph, S. A., and Frischknecht, F. (2013). Cryo-electron tomography reveals four-membrane architecture of the *Plasmodium* apicoplast. *Malaria Journal* 12, 25. doi: 10.1186/1475-2875-12-25.

Maier, U. G., Zauner, S., and Hempel, F. (2015). Protein import into complex plastids: Cellular organization of higher complexity. *European Journal of Cell Biology* 94, 340–348. doi: 10.1016/j.ejcb.2015.05.008.

Mallo, N., Fellows, J., Johnson, C., and Sheiner, L. (2018). Protein import into the endosymbiotic organelles of apicomplexan parasites. *Genes* 9 (3), 567-580. doi: 10.3390/genes9080412.

Marchetti, A., Parker, M. S., Moccia, L. P., Lin, E. O., Arrieta, A. L., Ribalet, F., Murphy, M. E. P., Maldonado, M. T., and Armbrust, E. V. (2009). Ferritin is used for iron storage in bloom-forming marine pennate diatoms. *Nature* 457, 467–470. doi: 10.1038/nature07539.

Martin, W., and Herrmann, R.G. (1998). Gene transfer from organelles to the nucleus: How much, what happens, and why? *Plant Physiology* 118 (1), 9-17. doi:10.1104/pp.118.1.9.

Matsumoto, F., Obayashi, T., Sasaki-Sekimoto, Y., Ohta, H., Takamiya, K. I., and Masuda, T. (2004). Gene expression profiling of the tetrapyrrole metabolic pathway in *Arabidopsis* with a mini-array system. *Plant Physiology* 135 (4), 2379-2391. doi: 10.1104/pp.104.042408.

Mazumdar, J., and Striepen, B. (2007). Make it or take it: Fatty acid metabolism of apicomplexan parasites. *Eukaryotic Cell* 6 (10), 1727-1735. doi: 10.1128/EC.00255-07.

McFadden, G. I. (2011). The apicoplast. *Protoplasma* 248 (4), 641-650. doi: 10.1007/s00709-010-0250-5.

McFadden, G. I., Reith, M. E., Munholland, J., and Lang-Unnasch, N. (1996). Plastid in human parasites. *Nature* 381 (6582), 482. doi: 10.1038/381482a0.

McFadden, G. I., and Waller, R. F. (1997). Plastids in parasites of humans. *BioEssays* 19, 1033–1040. doi: 10.1002/bies.950191114.

McFadden, G. I., and Yeh, E. (2017). The apicoplast: now you see it, now you don't. *International Journal for Parasitology* 47, 137–144. doi: 10.1016/j.ijpara.2016.08.005.

McQuaid, J.B., Kustka, A.B., Oborník, M., Horák, A., McCrow, J.P., Karas, B.J., Zheng, H., Kindeberg, T., Andersson, A.J., Barbeau, K.A., and Allen, A. E. (2018). Carbonate-sensitive phytotransferrin controls high-affinity iron uptake in diatoms. *Nature* 555 (7697), 534-537. doi:10.1038/nature25982.

Medlock, A. E., Shiferaw, M. T., Marcero, J. R., Vashisht, A. A., Wohlschlegel, J. A., Phillips, J. D., and Dailey, H. A. (2015). Identification of the mitochondrial heme metabolism complex. *PloS one* 10, e0135896. doi: 10.1371/journal.pone.0135896.

Mense, S. M., and Zhang, L. (2006). Heme: a versatile signaling molecule controlling the activities of diverse regulators ranging from transcription factors to MAP kinases. *Cell Research* 16, 681–692. doi: 10.1038/sj.cr.7310086.

Mochizuki, N., Tanaka, R., Grimm, B., Masuda, T., Moulin, M., Smith, A. G., Tanaka, A., and Terry, M. J. (2010). The cell biology of tetrapyrroles: A life and death struggle. *Trends in Plant Science* 15, 488–498. doi: 10.1016/j.tplants.2010.05.012.

Mojzeš, P., Gao, L., Ismagulova, T., Pilátová, J., Moudříková, Š., Gorelova, O., Solovchenko, A., Nedbal, L., and Salih, A. (2020). Guanine, a high-capacity and rapid-turnover nitrogen reserve in microalgal cells. *Proceedings of the National Academy of Sciences* 117, 32722–32730. doi: 10.1073/pnas.2005460117.

Moore, R. B., Oborník, M., Janouškovec, J., Chrudimský, T., Vancová, M., Green, D. H., Wright, S. W., Davies, N. W., Bolch, C. J. S., Heimann, K., Šlapeta, J., Hoegh-Guldberg, O., Logsdon, J. M., and Carter, D. A. (2008). A photosynthetic alveolate closely related to apicomplexan parasites. *Nature* 452, 959–963. doi: 10.1038/nature06871.

Moore, S. J., Sowa, S. T., Schuchardt, C., Deery, E., Lawrence, A. D., Ramos, J. V., Billig, S., Birkemeyer, C., Chivers, P. T., Howard, M. J., Rigby, S. E. J., Layer, G., and Warren, M. J. (2017). Elucidation of the biosynthesis of the methane catalyst coenzyme F(430). *Nature* 543, 78–82. doi: 10.1038/nature21427.

Morrissette, N. S., and Sibley, L. D. (2002). Cytoskeleton of Apicomplexan Parasites. *Microbiology and Molecular Biology Reviews* 66 (1), 21-38. doi: 10.1128/mmbr.66.1.21-38.2002.

Moss, G. P. (1988). Nomenclature of tetrapyrroles. *European Journal of Biochemistry* 178, 277–328. doi: 10.1111/j.1432-1033.1988.tb14453.x.

Müller, M., Mentel, M., van Hellemond, J. J., Henze, K., Woehle, C., Gould, S. B., Yu, R., van der Giezen, M., Tielens, A. G. M., and Martin, W. F. (2012). Biochemistry and Evolution of Anaerobic Energy Metabolism in Eukaryotes. *Microbiology and Molecular Biology Reviews* 76 (2), 444-495. doi: 10.1128/mmbr.05024-11.

Muñiz-Hernández, S., González del Carmen, M., Mondragón, M., Mercier, C., Cesbron, M. F., Mondragón-González, S. L., González, S., and Mondragón, R. (2011). Contribution of the residual body in the spatial organization of *Toxoplasma gondii* tachyzoites within the parasitophorous vacuole. *Journal of Biomedicine and Biotechnology* 2011, 473983. doi: 10.1155/2011/473983.

Nakai, K., and Kanehisa, M. (1992). A knowledge base for predicting protein localization sites in eukaryotic cells. *Genomics* 14, 897–911. doi: 10.1016/S0888-7543(05)80111-9.

Nielsen, H., Engelbrecht, J., Brunak, S., and von Heijne, G. (1997). Identification of prokaryotic and eukaryotic signal peptides and prediction of their cleavage sites. *Protein Engineering* 10 (1), 1-6. doi: 10.1093/protein/10.1.1.

Nielsen, H., Tsirigos, K. D., Brunak, S., and von Heijne, G. (2019). A bief history of protein sorting prediction. *Protein Journal* 38, 200–216. doi: 10.1007/s10930-019-09838-3.

Nilsson, I., Lara, P., Hessa, T., Johnson, A. E., von Heijne, G., and Karamyshev, A. L. (2015). The code for directing proteins for translocation across ER membrane: SRP cotranslationally recognizes specific features of a signal sequence. *Journal of Molecular Biology* 427, 1191–1201. doi: 10.1016/j.jmb.2014.06.014.

Novick, P., Field, C., and Schekman, R. (1980). Identification of 23 complementation groups required for post-translational events in the yeast secretory pathway. *Cell* 21 (1) 205-215. doi: 10.1016/0092-8674(80)90128-2.

Oborník, M. (2019). Endosymbiotic evolution of algae, secondary heterotrophy and parasitism. *Biomolecules* 9, 266-undefined. doi: 10.3390/biom9070266.

Oborník, M. (2020). Photoparasitism as an intermediate state in the evolution of apicomplexan parasites. *Trends in Parasitology* 36 (9), 727-734. doi: 10.1016/j.pt.2020.06.002.

Oborník, M. (2021). Enigmatic evolutionary history of porphobilinogen deaminase in eukaryotic phototrophs. *Biology (Basel)*10 (5), 386. doi:10.3390/biology10050386.

Oborník, M., and Green, B. R. (2005). Mosaic origin of the heme biosynthesis pathway in photosynthetic eukaryotes. *Molecular Biology and Evolution* 22, 2343–2353. doi: 10.1093/molbev/msi230.

Oborník, M., Janouškovec, J., Chrudimský, T., and Lukeš, J. (2009). Evolution of the apicoplast and its hosts: From heterotrophy to autotrophy and back again. *International Journal for Parasitology* 39 (1), 1-12. doi: 10.1016/j.ijpara.2008.07.010.

Oborník, M., Kručinská, J., and Esson, H. (2016). Life cycles of chromerids resemble those of colpodellids and apicomplexan parasites. *Perspectives in Phycology* 3, 21–27. doi: 10.1127/pip/2016/0038.

Oborník, M., and Lukeš, J. (2013). "Cell biology of chromerids: Autotrophic relatives to apicomplexan parasites," in *International Review of Cell and Molecular Biology*, 333–369. doi: 10.1016/B978-0-12-407694-5.00008-0.

Oborník, M., and Lukeš, J. (2015). The organellar genomes of *Chromera* and *Vitrella*, the phototrophic relatives of apicomplexan parasites. *Annual Review of Microbiology* 69, 129–144. doi: 10.1146/annurev-micro-091014-104449.

Oborník, M., Modrý, D., Lukeš, M., Černotíková-Stříbrná, E., Cihlář, J., Tesařová, M., Kotabová, E., Vancová, M., Prášil, O., and Lukeš, J. (2012). Morphology, ultrastructure and life cycle of *Vitrella brassicaformis* n. sp., n. gen., a novel Chromerid from the Great barrier reef. *Protist* 163, 306–323. doi: 10.1016/j.protis.2011.09.001.

Oborník, M., Vancová, M., Lai, D. H., Janouškovec, J., Keeling, P. J., and Lukeš, J. (2011). Morphology and ultrastructure of multiple life cycle stages of the photosynthetic relative of apicomplexa, *Chromera velia*. *Protist* 162 (1), 115-130. doi: 10.1016/j.protis.2010.02.004.

Ortiz de Montellano, P. R. (2008). Hemes in biology. *Wiley Encyclopedia of Chemical Biology*, 1–10. doi: 10.1002/9780470048672.wecb221.

Owji, H., Nezafat, N., Negahdaripour, M., Hajiebrahimi, A., and Ghasemi, Y. (2018). A comprehensive review of signal peptides: Structure, roles, and applications. *European Journal of Cell Biology* 97, 422–441. doi: 10.1016/j.ejcb.2018.06.003.

Patron, N. J., and Waller, R. F. (2007). Transit peptide diversity and divergence: A global analysis of plastid targeting signals. *BioEssays* 29, 1048–1058. doi: 10.1002/bies.20638.

Patterson, D. J. (1999). The Diversity of Eukaryotes. *The American Naturalist* 154, S96–S124. doi: 10.1086/303287.

Peeters, N., and Small, I. (2001). Dual targeting to mitochondria and chloroplasts. *Biochimica et Biophysica Acta (BBA) - Molecular Cell Research* 1541, 54–63. doi: 10.1016/S0167-4889(01)00146-X.

Pennington, J. M., Kemp, M., McGarry, L., Chen, Y., and Stroupe, M. E. (2020). Siroheme synthase orients substrates for dehydrogenase and chelatase activities in a common active site. *Nature Communications* 11, 864. doi: 10.1038/s41467-020-14722-1.

Petersen, J., Ludewig-Klingner, A.-K., Michael, V., Bunk, B., Jarek, M., Baurain, D., and Brinkmann H. (2014). *Chromera velia*, endosymbioses and the rhodoplex hypothesis—plastid Eevolution in Cryptophytes, Alveolates, Stramenopiles, and Haptophytes (CASH Lineages). *Genome biology and evolution* 6 (3), 666-684. doi: 10.1093/gbe/evu043.

Philpott, C. C. (2006). Iron uptake in fungi: A system for every source. *Biochimica et Biophysica Acta (BBA) - Molecular Cell Research* 1763, 636–645. doi: 10.1016/j.bbamcr.2006.05.008.

Piel, R. B., Dailey, H. A., and Medlock, A. E. (2019). The mitochondrial heme metabolon: Insights into the complex(ity) of heme synthesis and distribution. *Molecular Genetics and Metabolism* 128, 198–203. doi: 10.1016/j.ymgme.2019.01.006.

Platta, H. W., and Erdmann, R. (2007). The peroxisomal protein import machinery. *FEBS Letters* 581, 2811–2819. doi: 10.1016/j.febslet.2007.04.001.

Pollard, R. T., Salter, I., Sanders, R. J., Lucas, M. I., Moore, C. M., Mills, R. A., Statham, P. J., Allen, J. T., Baker, A. R., Bakker, D. C. E., Charette, M. A., Fielding, S., Fones, G. R., French, M., Hickman, A. E., Holland, R. J., Hughes, J. A., Jickells, T. D., Lampitt, R. S., Morris, P. J., Nédélec, F. H., Nielsdóttir, M., Planquette, H., Popova, E. E., Poulton, A. J., Read, J. F., Seeyave, S., Smith, T., Stinchcombe, M., Taylor, S., Thomalla, S., Venables, H. J.,Williamson, R., and Zubkov, M. V. (2009). Southern Ocean deep-water carbon export enhanced by natural iron fertilization. *Nature* 457, 577–580. doi: 10.1038/nature07716.

Portman, N., Foster, C., Walker, G., and Šlapeta, J. (2014). Evidence of intraflagellar transport and apical complex formation in a free-living relative of the apicomplexa. *Eukaryotic cell* 13, 10–20. doi: 10.1128/EC.00155-13.

Pyrih, J., Pánek, T., Durante, I.M., Rašková, V., Cimrhanzlová, K., Kriegová, E., Tsaousis, A.D., Eliáš, M., and Lukeš, J. (2021). Vestiges of the bacterial signal recognition particle-based protein targeting in mitochondria. *Molecular Biology and Evolution* 38 (8), 3170-3187, doi:10.1093/molbev/msab090.

Quigg, A., Kotabová, E., Jarešová, J., Kaňa, R., Šetlík, J., Šedivá, B., Komárek, O., and Prášil, O. (2012). Photosynthesis in *Chromera velia* represents a simple system with high efficiency. *PLOS ONE* 7, e47036. Available at: 10.1371/journal.pone.0047036.

Ralph, S. A., Foth, B. J., Hall, N., and McFadden, G. I. (2004). Evolutionary pressures on apicoplast transit peptides. *Molecular Biology and Evolution* 21, 2183–2194. doi: 10.1093/molbev/msh233.

Ray, P. D., Huang, B.-W., and Tsuji, Y. (2012). Reactive oxygen species (ROS) homeostasis and redox regulation in cellular signaling. *Cellular signalling* 24, 981–990. doi: 10.1016/j.cellsig.2012.01.008.

Richtová, J., Sheiner, L., Gruber, A., Yang, S.-M., Kořený, L., Striepen, B., and Oborník, M. (2021). Using diatom and apicomplexan models to study the heme pathway of *Chromera velia*. *International Journal of Molecular Sciences* 22 (12), 6495. doi: 10.3390/ijms22126495.

Robinson, J. B. J., and Srere, P. A. (1985). Organization of Krebs tricarboxylic acid cycle enzymes in mitochondria. *The Journal of biological chemistry* 260, 10800–10805. doi: 10.1016/0006-2944(85)90023-7.

Rockwell, N., Lagarias, J. C., and Bhattacharya, D. (2014). Primary endosymbiosis and the evolution of light and oxygen sensing in photosynthetic eukaryotes. *Frontiers in Ecology and Evolution* 2, 66. doi: 10.3389/fevo.2014.00066.

Rogers, M. B., Gilson, P. R., Su, V., McFadden, G. I., and Keeling, P. J. (2007). The complete chloroplast genome of the chlorarachniophyte *Bigelowiella natans*: Evidence for independent origins of chlorarachniophyte and euglenid secondary endosymbionts. *Molecular Biology and Evolution* 24 (1), 54-62. doi: 10.1093/molbev/msl129.

Rowley, C. A., and Kendall, M. M. (2019). To B12 or not to B12: Five questions on the role of cobalamin in host-microbial interactions. *PLoS pathogens* 15, e1007479–e1007479. doi: 10.1371/journal.ppat.1007479.

Ryall, K., Harper, J. T., and Keeling, P. J. (2003). Plastid-derived Type II fatty acid biosynthetic enzymes in chromists. *Gene* 313 (1-2), 139-148. doi: 10.1016/S0378-1119(03)00671-1.

Santos, A. L., and Preta, G. (2018). Lipids in the cell: organization regulates function. *Cellular and Molecular Life Sciences* 75, 1909–1927. doi: 10.1007/s00018-018-2765-4.

Sassa, S., and Kappas, A. (2000). Molecular aspects of the inherited porphyrias. *Journal of Internal Medicine* 247, 169–178. doi: 10.1046/j.1365-2796.2000.00618.x.

Schatz, G., and Dobberstein, B. (1996). Common principles of protein translocation across membranes. *Science* 271, 1519. doi: 10.1126/science.271.5255.1519.

Schnepf, E., and ElbräChter, M. (1999). Dinophyte chloroplasts and phylogeny - A review. *Grana* 38, 81–97. doi: 10.1080/00173139908559217.

Sharaf, A., Füssy, Z., Tomčala, A., Richtová, J., and Oborník, M. (2019a). Isolation of plastids and mitochondria from *Chromera velia*. *Planta* 250 (5), 1731-1741. doi: 10.1007/s00425-019-03259-3.

Sharaf, A., Gruber, A., Jiroutová, K., and Oborník, M. (2019b). Characterization of aminoacyl-tRNA synthetases in chromerids. *Genes* 10 (8), 582. doi: 10.3390/genes10080582.

Sharma, M., Bennewitz, B., and Klösgen, R. B. (2018). Dual or not dual? Comparative analysis of fluorescence microscopy-based approaches to study organelle targeting specificity of nuclear-encoded plant proteins. *Frontiers in Plant Science* 9, 1350. doi: 10.3389/fpls.2018.01350.

Sheiner, L., Fellows, J. D., Ovciarikova, J., Brooks, C. F., Agrawal, S., Holmes, Z. C., Bietz, I.,Flinner, N., Heiny, S., Mirus, O., Przyborski, J. M., and Striepen, B. (2015). *Toxoplasma gondii* Toc75 Functions in import of stromal but not peripheral apicoplast proteins. *Traffic* 16, 1254–1269. doi: 10.1111/tra.12333.

Sheiner, L., and Striepen, B. (2013). Protein sorting in complex plastids. *Biochimica et Biophysica Acta - Molecular Cell Research* 1833, 352–359. doi: 10.1016/j.bbamcr.2012.05.030.

Shepherd, M., Medlock, A. E., and Dailey, H. A. (2013). "Porphyrin Metabolism," in *Encyclopedia of Biological Chemistry: Second Edition*, 544–549. doi: 10.1016/B978-0-12-378630-2.00052-9.

Shlyk, A. A. (1971). Biosynthesis of chlorophyll b. *Annual review of plant physiology* 22, 169–184. doi: 10.1146/annurev.pp.22.060171.001125.

Sieracki, M. E., Poulton, N. J., Jaillon, O., Wincker, P., de Vargas, C., Rubinat-Ripoll, L., Stepanauskas, R., Logares, R., and Massana, R. (2019). Single cell genomics yields a wide diversity of small planktonic protists across major ocean ecosystems. *Scientific Reports* 9 (1), 6025. doi: 10.1038/s41598-019-42487-1.

Simpson, A. G. B., and Roger, A. J. (2004). The real 'kingdoms' of eukaryotes. *Current Biology* 14, R693–R696. doi: 10.1016/j.cub.2004.08.038.

Small, I., Peeters, N., Legeai, F., and Lurin, C. (2004). Predotar: A tool for rapidly screening proteomes for N-terminal targeting sequences. *PROTEOMICS* 4, 1581–1590. doi: 10.1002/pmic.200300776.

Snyder, A. M., Clark, B. M., Robert, B., Ruban, A. V., and Bungard, R. A. (2004). Carotenoid specificity of light-harvesting complex II binding sites. Occurrence of 9-cis-violaxanthin in the neoxanthin-binding site in the parasitic angiosperm *Cuscuta reflexa*. *Journal of Biological Chemistry* 279 (7), 5162-5168. doi: 10.1074/jbc.M309676200.

Sobotka, R., Esson, H.J., Koník, P. Trsková, E., Moravcová, L., Horák, A., Dufková, P., and Oborník, M. (2017). Extensive gain and loss of photosystem I subunits in chromerid algae, photosynthetic relatives of apicomplexans. *Sci Rep* 7 (1), 13214. doi: 10.1038/s41598-017-13575-x.

Sobotka, R., Tichy, M., Wilde, A., and Neil Hunter, C. (2011). Functional assignments for the carboxyl-terminal domains of the ferrochelatase from *Synechocystis PCC 6803*: The CAB domain plays a regulatory role, and region ii is essential for catalysis. *Plant Physiology* 155, 1735–1747. doi: 10.1104/pp.110.167528.

Soldati, D., Foth, B. J., and Cowman, A. F. (2004). Molecular and functional aspects of parasite invasion. *Trends in Parasitology* 20 (12), 567-574. doi: 10.1016/j.pt.2004.09.009.

Sommer, M. S., Gould, S. B., Lehmann, P., Gruber, A., Przyborski, J. M., and Maier, U.G. (2007). Der1-mediated preprotein import into the periplastid compartment of chromalveolates? *Molecular biology and evolution* 24, 918–928. doi: 10.1093/molbev/msm008.

Srere, P. A., and Sumegi, B. (1994). Processivity and fatty acid oxidation. *Biochemical Society transactions* 22, 446–450. doi: 10.1042/bst0220446.

Stork, S., Lau, J., Moog, D., and Maier, U. G. (2013). Three old and one new: Protein import into red algal-derived plastids surrounded by four membranes. *Protoplasma* 250, 1013–1023. doi: 10.1007/s00709-013-0498-7.

Stroupe, M. E., and Getzoff, E. D. (2009). "The role of siroheme in sulfite and nitrite reductases," in *Tetrapyrroles: Birth, Life and Death*, eds. M. J. Warren and A. G. Smith (New York, NY: Springer New York), 375–389. doi: 10.1007/978-0-387-78518-9_24.

Su, H. J., Barkman, T. J., Hao, W., Jones, S. S., Naumann, J., Skippington, E., Wafula, E. K., Hu, J. M., Palmer, J. D., and DePamphilis, C. W. (2019). Novel genetic code and record-setting AT-richness in the highly reduced plastid genome of the holoparasitic plant *Balanophora*. *Proceedings of the National Academy of Sciences of the United States of America* 116 (3), 934-943. doi: 10.1073/pnas.1816822116.

Suplick, K., Akella, R., Saul, A., and Vaidya, A. B. (1988). Molecular cloning and partial sequence of a 5.8 kilobase pair repetitive DNA from *Plasmodium falciparum*. *Molecular and Biochemical Parasitology* 30, 289–290. doi: 10.1016/0166-6851(88)90098-9.

Sutak, R., Slapeta, J., San Roman, M., Camadro, J.-M., and Lesuisse, E. (2010). Nonreductive iron uptake mechanism in the marine alveolate *Chromera velia*. *Plant physiology* 154, 991–1000. doi: 10.1104/pp.110.159947.

Swenson, S. A., Moore, C. M., Marcero, J. R., Medlock, A. E., Reddi, A. R., and Khalimonchuk, O. (2020). From synthesis to utilization: The ins and outs of mitochondrial heme. *Cells* 9, 579-undefined. doi: 10.3390/cells9030579.

Tanaka, R., Kobayashi, K., and Masuda, T. (2011). Tetrapyrrole metabolism in *Arabidopsis thaliana*. *The Arabidopsis Book* 9, e0145-undefined. doi: 10.1199/tab.0145.

Tanaka, R., and Tanaka, A. (2007). Tetrapyrrole biosynthesis in higher plants. *Annual Review of Plant Biology* 58, 321–346. doi: 10.1146/annurev.arplant.57.032905.105448.

Tielens, A. G. M., and van Hellemond, J. J. (2009). Surprising variety in energy metabolism within Trypanosomatidae. *Trends in Parasitology* 25, 482–490. doi: 10.1016/j.pt.2009.07.007.

Tomčala, A., Kyselová, V., Schneedorferová, I., Opekarová, I., Moos, M., Urajová, P., Kručinská, J., and Oborník, M. (2017). Separation and identification of lipids in the photosynthetic cousins of Apicomplexa *Chromera velia* and *Vitrella brassicaformis*. *Journal of Separation Science* 40, 3402–3413. doi: 10.1002/jssc.201700171.

Tomčala, A., Michálek, J., Schneedorferová, I., Füssy, Z., Gruber, A., Vancová, M., and Oborník, M. (2020). Fatty acid biosynthesis in chromerids. *Biomolecules* 10 (8), 1102. doi: 10.3390/biom10081102.

Tonkin, C. J., Kalanon, M., and McFadden, G. I. (2008). Protein targeting to the malaria parasite plastid. *Traffic* 9 (1), 166-175. doi: 10.1111/j.1600-0854.2007.00660.x.

Toso, M. A., and Omoto, C. K. (2007). Gregarina niphandrodes may lack both a plastid genome and organelle. *Journal of Eukaryotic Microbiology* 54 (1), 66-72. doi: 10.1111/j.1550-7408.2006.00229.x.

Turner, D. R., and Hunter, K. A. (2001). *The Biogeochemistry of Iron in Seawater*. John Wiley & Sons, Ltd. ISBN: 978-0-471-49068-5.

Vaidya, A. B., Akella, R., and Suplick, K. (1989). Sequences similar to genes for two mitochondrial proteins and portions of ribosomal RNA in tandemly arrayed 6-kilobase-pair DNA of a malarial parasite. *Molecular and Biochemical Parasitology* 35, 97–107. doi: 10.1016/0166-6851(89)90112-6.

Vavilin, D. v., and Vermaas, W. F. J. (2002). Regulation of the tetrapyrrole biosynthetic pathway leading to heme and chlorophyll in plants and cyanobacteria. *Physiologia Plantarum* 115 (1), 9-24. doi: 10.1034/j.1399-3054.2002.1150102.x.

Vazač, J., Füssy, Z., Hladová, I., Killi, S., and Oborník, M. (2018). Ploidy and number of chromosomes in the alveolate alga *Chromera velia*. *Protist* 169 (1), 53-63. doi: 10.1016/j.protis.2017.12.001.

von Heijne, G. (1983). Patterns of amino acids near signal-sequence cleavage sites. *European Journal of Biochemistry* 133, 17–21. doi: 10.1111/j.1432-1033.1983.tb07424.x.

von Heijne, G. (1984). Analysis of the distribution of charged residues in the N-terminal region of signal sequences: implications for protein export in prokaryotic and eukaryotic cells. *The EMBO journal* 3, 2315–2318. doi: 10.1002/j.1460-2075.1984.tb02132.x.

von Heijne, G., and Abrahmsèn, L. (1989). Species-specific variation in signal peptide design implications for protein secretion in foreign hosts. *FEBS Letters* 244, 439–446. doi: 10.1016/0014-5793(89)80579-4.

von Heijne, G., Steppuhn, J., and Herrmann, R. G. (1989). Domain structure of mitochondrial and chloroplast targeting peptides. *European Journal of Biochemistry* 180, 535–545. doi: 10.1111/j.1432-1033.1989.tb14679.x.

Votýpka, J., Modrý, D., Oborník, M., Šlapeta, J., and Lukeš, J. (2017). "Apicomplexa," in *Handbook of the Protists*, eds. J. M. Archibald, A. G. B. Simpson, and C. H. Slamovits (Cham: Springer International Publishing), 567–624. doi: 10.1007/978-3-319-28149-0_20.

Wachowska, M., Muchowicz, A., Firczuk, M., Gabrysiak, M., Winiarska, M., Wańczyk, M., Bojarczuk, K., and Golab, J. (2011). Aminolevulinic acid (ALA) as a prodrug in photodynamic therapy of cancer. *Molecules* 16, 4140–4164. doi: 10.3390/molecules16054140.

Waller, R. F., and McFadden, G. I. (2005). The apicoplast: A review of the derived plastid of apicomplexan parasites. *Current Issues in Molecular Biology* 7, 57–80. doi: 10.21775/cimb.007.057.

Walter, P., and Blobel, G. (1980). Purification of a membrane-associated protein complex required for protein translocation across the endoplasmic reticulum. *Biochemistry* 77 (12), 7112-7116. doi: 10.1073/pnas.77.12.7112.

Weatherby, K., Murray, S., Carter, D., and Šlapeta, J. (2011). Surface and flagella morphology of the motile form of *Chromera velia* revealed by field-emission scanning electron microscopy. *Protist* 162 (1), 142-513. doi: 10.1016/j.protis.2010.02.003.

Wiedemann, N., and Pfanner, N. (2017). Mitochondrial machineries for protein import and assembly. *Annual Review of Biochemistry* 86, 685–714. doi: 10.1146/annurev-biochem-060815-014352.

Williamson, D. H., Gardner, M. J., Preiser, P., Moore, D. J., Rangachari, K., and Wilson, R. J. M. (1994). The evolutionary origin of the 35 kb circular DNA of *Plasmodium falciparum*: new evidence supports a possible rhodophyte ancestry. *Molecular and General Genetics MGG* 243, 249–252. doi: 10.1007/BF00280323.

Williamson, D. H., Wilson, R. J. M., Bates, P. A., McCready, S., Perler, F., and Qiang, B.-U. (1985). Nuclear and mitochondrial DNA of the primate malarial parasite *Plasmodium knowlesi*. *Molecular and Biochemical Parasitology* 14, 199–209. doi: 10.1016/0166-6851(85)90038-6.

Wilson, R. J. M. (Iain), Denny, P. W., Preiser, P. R., Rangachari, K., Roberts, K., Roy, A., Whyte, A., Strath, M., Moore, D. J., Moore, P. W., and Williamson, D. H. (1996). Complete gene map of the plastid-like DNA of the malaria parasite *Plasmodium falciparum*. *Journal of Molecular Biology* 261 (2), 155-172. doi: 10.1006/jmbi.1996.0449.

Wunder, T., Martin, R., Löffelhardt, W., Schleiff, E., and Steiner, J. M. (2007). The invariant phenylalanine of precursor proteins discloses the importance of Omp85 for protein translocation into cyanelles. *BMC evolutionary biology* 7, 236. doi: 10.1186/1471-2148-7-236.

York Jr., R.H., (1986). Isolation and culture of symbiotic algae. In: *Jokiel, P.L., Richmond, R.H., Rogers, R.A. (Eds.), Coral Reef Population Biology.* Hawaii University, Sea Grant College Program, Honolulu, HI, pp. 486–487. doi: not available.

Zhang, J., Kang, Z., Chen, J., and Du, G. (2015). Optimization of the heme biosynthesis pathway for the production of 5-aminolevulinic acid in *Escherichia coli*. *Scientific Reports* 5, 8584. doi: 10.1038/srep08584.

Zhang, Z., Green, B. R., and Cavalier-Smith, T. (1999). Single gene circles in dinoflagellate chloroplast genomes. *Nature* 400 (6740), 155-159. doi: 10.1038/22099.

Zhao, M., and Qu, H. (2010). PathLocdb: a comprehensive database for the subcellular localization of metabolic pathways and its application to multiple localization analysis. *BMC Genomics* 11, Suppl 4: S13. doi: 10.1186/1471-2164-11-S4-S13.

Zhu, G., Marchewka, M. J., and Keithly, J. S. (2000). *Cryptosporidium parvum* appears to lack a plastid genome. *Microbiology* 146 (2), 315-321. doi: 10.1099/00221287-146-2-315.

Paper I

USING DIATOM AND APICOMPLEXAN MODELS TO STUDY THE HEME PATHWAY OF CHROMERA VELIA

Richtová, J.; Sheiner, L.; Gruber, A.; Yang, S.; Kořený, L.; Striepen, B.; and Oborník, M.

Using Diatom and Apicomplexan Models to Study the Heme Pathway of *Chromera velia*

Jitka Richtová [1,2], Lilach Sheiner [3], Ansgar Gruber [1], Shun-Min Yang [1,2], Luděk Kořený [4], Boris Striepen [5] and Miroslav Oborník [1,2,*]

1   Biology Centre CAS, Laboratory of Evolutionary Protistology, Institute of Parasitology, 370 05 České Budějovice, Czech Republic; jitka.richtova@paru.cas.cz (J.R.); ansgar.gruber@paru.cas.cz (A.G.); shun-min.yang@paru.cas.cz (S.-M.Y.)
2   Faculty of Science, University of South Bohemia, 370 05 České Budějovice, Czech Republic
3   Welcome Centre for Integrative Parasitology, College of Medical, Veterinary and Life Sciences, Institute of Infection, Immunity and Inflammation, University of Glasgow, Glasgow G12 8QQ, UK; lilach.sheiner@glasgow.ac.uk
4   Department of Biochemistry, University of Cambridge, Cambridge CB2 1TN, UK; lk360@cam.ac.uk
5   Department of Pathobiology, School of Veterinary Medicine, University of Pennsylvania, Philadelphia, PA 19104, USA; striepen@vet.upenn.edu
*   Correspondence: obornik@paru.cas.cz; Tel.: +420-387-775-464

Abstract: Heme biosynthesis is essential for almost all living organisms. Despite its conserved function, the pathway's enzymes can be located in a remarkable diversity of cellular compartments in different organisms. This location does not always reflect their evolutionary origins, as might be expected from the history of their acquisition through endosymbiosis. Instead, the final subcellular localization of the enzyme reflects multiple factors, including evolutionary origin, demand for the product, availability of the substrate, and mechanism of pathway regulation. The biosynthesis of heme in the apicomonad *Chromera velia* follows a chimeric pathway combining heme elements from the ancient algal symbiont and the host. Computational analyses using different algorithms predict complex targeting patterns, placing enzymes in the mitochondrion, plastid, endoplasmic reticulum, or the cytoplasm. We employed heterologous reporter gene expression in the apicomplexan parasite *Toxoplasma gondii* and the diatom *Phaeodactylum tricornutum* to experimentally test these predictions. 5-aminolevulinate synthase was located in the mitochondria in both transfection systems. In *T. gondii*, the two 5-aminolevulinate dehydratases were located in the cytosol, uroporphyrinogen synthase in the mitochondrion, and the two ferrochelatases in the plastid. In *P. tricornutum*, all remaining enzymes, from ALA-dehydratase to ferrochelatase, were placed either in the endoplasmic reticulum or in the periplastidial space.

Keywords: tetrapyrrole biosynthesis; heterologous expression; *Chromera velia*; predictions

1. Introduction

Life as we know it, would not be possible without tetrapyrroles, namely chlorophyll and heme. While chlorophyll is used exclusively in photosynthesis, heme can be involved in various electron transport chains and redox reactions [1]. Heme appears to be essential for almost all life on Earth, with only a few exceptions among pathogenic and anaerobic bacteria, and a single exception in aerobic eukaryotes, the kinetoplastid *Phytomonas serpens* [2]. All other organisms either synthesize their own heme or obtain it from external sources [2]. Both heme and chlorophyll share a common synthetic pathway (up to protoporphyrinogen IX), which is well conserved among all three domains of life [3] (outlined in Figure 1). The first precursor of this pathway, 5-aminolevulinic acid (ALA), can be synthesized in two fundamentally different ways: primary heterotrophic eukaryotes and Alphaproteobacteria use the C4 (or Shemin) pathway, the condensation of succinyl-CoA and glycine, while Eubacteria, Archaea, and eukaryotic phototrophs form ALA from glutamate via a set of

reactions termed the C5 pathway [4]. Eight molecules of ALA are assembled in three consecutive steps to uroporphyrinogen III, the first macrocyclic tetrapyrrole, which can convert to siroheme, or, alternatively, the next three steps of the synthesis lead to protoporphyrinogen IX. In the chlorophyll synthesis branch, magnesium-chelatase inserts an Mg^{2+} ion into the center of the porphyrin ring. In the heme synthesis branch, insertion of a Fe^{2+} ion into the ring by ferrochelatase (FECH) finally completes the heme [1].
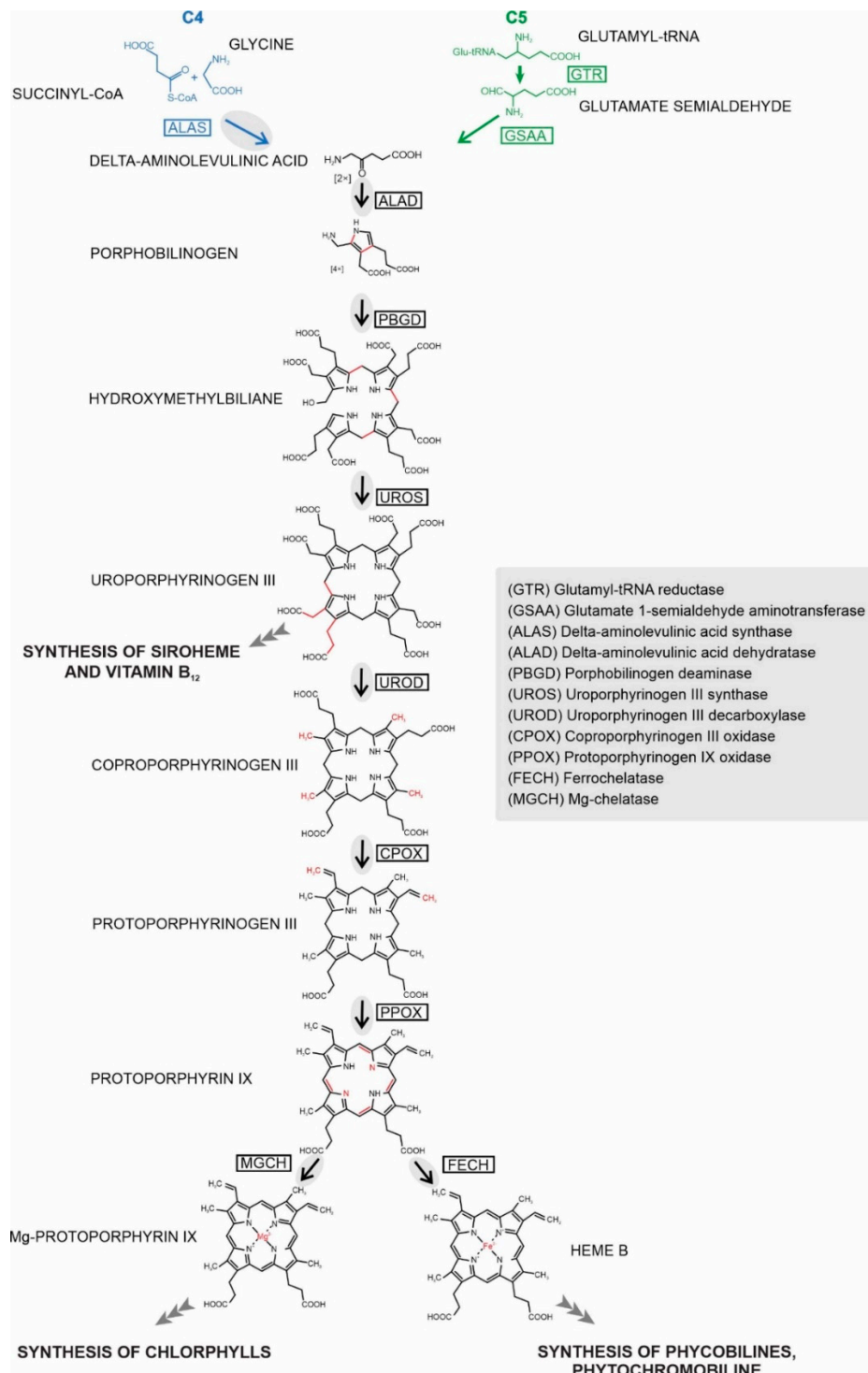

Figure 1. Tetrapyrrole synthesis. Enzymes working in particular steps of the synthesis are denoted by acronyms in boxes with their full names explained in the grey panel. Enzymatic steps (arrows) present in *C. velia* are in the grey oval. Changes in product structure are highlighted in red.

Tetrapyrrole biosynthesis in eukaryotes is largely influenced by past endosymbiotic events, in which mitochondria and plastids were acquired. This is reflected in the phylogenetic affinities of the associated genes, that often demonstrate similarity to homologous genes in Alphaproteobacteria or cyanobacteria, for mitochondrial or a plastid origin, respectively [4,5]. While the tetrapyrrole pathway is almost universally present, the subcellular distribution of the enzymes differs widely across the eukaryotic biodiversity. Location corresponds to the trophic strategy of the organism, cellular demand for the final products of the pathway, the evolutionary origin of the enzyme, and the need for tight regulation of the pathway [6–10].

In primary eukaryotic heterotrophs, both the initial and terminal steps of the synthesis take place in the mitochondria, which is not surprising considering the availability of the precursor, succinyl-CoA, and the demand for heme in the cytochromes of the respiratory chain [4,5,11]. The common location for the start and completion of heme synthesis is also important for the regulation of the pathway, which is mainly achieved by the heme-mediated inhibition of ALA formation [6–10]. The middle part of the pathway in heterotrophs takes place in the cytosol, which necessitates the transport of ALA and a porphyrin intermediate across the mitochondrial membranes [12,13]. Most phototrophs use the C5 pathway to begin the tetrapyrrole synthesis, and the whole process is located inside the plastid, the place with the highest demand for the final products, chlorophyll, and heme [14]. The euglenid alga *Euglena gracilis* [15] and the chlorarachniophyte *Bigelowiella natans* [16] possess both the plastid located (C5 based) pathway, and the mitochondrially-cytosolic (C4 based) pathway. Apicomplexan parasites [17] such as *Plasmodium* or *Toxoplasma* harbor a non-photosynthetic relic plastid (the apicoplast) and possess a rather peculiar heme synthesis. The pathway starts via the C4 route in the mitochondrion, the next four steps are apicoplast localized, consecutively, coproporphyrinogen oxidase (CPOX) is active in the cytosol, and the synthesis is completed by protoporphyrinogen oxidase (PPOX) and FECH in the mitochondrion again [5,11,18–21]. Such complicated intracellular distribution of heme pathway enzymes most likely arose because of the transition from a photosynthetic to a parasitic lifestyle [5,11,20].

All tetrapyrrole pathway enzymes from the organisms mentioned above are encoded in the nucleus and hence must be targeted to a relevant compartment, after translation in the cytosol. For that purpose, cells evolved various targeting signals that can be N-terminal or C-terminal extensions, or lie internally within the protein [22]. For the transport through the ER, proteins are equipped with an N-terminal "signal peptide" (SP). Proteins targeted to plastids of primary phototrophs bear a "transit peptide" (TP) that is identified by translocons of outer and inner chloroplast membrane (TOC and TIC), respectively [23,24]. Complex plastids are coated with additional membranes; to pass them, proteins need a "bipartite targeting sequence" (BTS) consisting of a SP, that is cleaved immediately after crossing the outermost membrane, and a TP that escorts the protein to plastid stroma, where the TP is also excised to expose the mature protein [22–26].

Chromera velia is an alveolate alga, belonging to the group Apicomonada [27], isolated from stony corals from Sydney Harbor in Australia [28]. Together with *Vitrella brassicaformis*, it represents the closest known phototrophic relative to apicomplexan parasites [29]. Similar to other Apicomplexa and algae with complex plastids, both chromerids host rhodophyte-derived plastids surrounded by four membranes [28–34]. Although *C. velia* is a phototroph, it uses mitochondrially-located ALA synthase (ALAS) for the synthesis of ALA in the C4 route. All the C5 pathway enzymes found in other phototrophs are missing from chromerids [11]. The remaining enzymes of the pathway (from ALA to heme) display mosaic evolutionary origins (cyanobacterial, eukaryotic, and proteobacterial). Most of the enzymes involved in the pathway possess predicted bipartite targeting sequences (BTS) known to mediate import of nuclear-encoded proteins into complex plastids [11,35,36].

To see how the pathway is organized in the photosynthetic chromerids and to better understand what evolutionary forces shaped the unusual pathway in Apicomplexa, we experimentally tested the locations of heme pathway enzymes in the *C. velia*. As there is no transfection system for *C. velia* yet, we decided to use the heterologous expression in a photosynthetic diatom and in an apicomplexan parasite. This also allowed insight into the compatibility of targeting mechanisms between diatoms and apicomplexans, including chromerids. The best-established transfection systems in organisms related to *C. velia* are those for the apicomplexans *Toxoplasma gondii* and *Plasmodium falciparum*, and for the diatoms *Thalassiosira pseudonana* and *Phaeodactylum tricornutum* [37–41]. Both groups of organisms, apicomplexans, and diatoms contain secondary plastids surrounded by four membranes, and their plastid targeting mechanisms have been extensively studied [23,42–48]. The apicomplexan parasites are more closely related to *C. velia*; however, the plastids in *C. velia* were hypothesized to originate from a tertiary endosymbiotic event with a stramenopile [29,33,34,49,50]. Moreover, diatoms and *C. velia* share a phototrophic lifestyle, which requires more complex regulation of the tetrapyrrole synthesis due to the presence of the chlorophyll branch [5,15,16]. In this study, we localized six heme pathway enzymes from *C. velia* in the apicomplexan parasite *T. gondii* and in the diatom *P. tricornutum*: ALAS, two ALA dehydratases (ALAD1, ALAD2), uroporphyrinogen synthase (UROS) and two ferrochelatases (FECH1, FECH2). We also used specific antibodies generated against *C. velia* ALAS to localize this enzyme directly in *C. velia* cells by immunogold labeling and transmission electron microscopy.

2. Results

2.1. Prediction of Localization of Heme Synthesis Enzymes in C. velia

Various bioinformatics tools can be used to predict N-terminal targeting presequences typically associated with targeting to specific subcellular compartments. We analyzed the predicted targeting of the *C. velia* heme pathway enzymes using the following algorithms: SignalP 4.1 [51] in combination with TargetP 1.1 [52], to determine the presence of bipartite targeting sequences (BTS). As *C. velia* hosts complex plastid surrounded by four membranes [28,31], we also took advantage of the ASAFind predictor, designed to predict protein targeting to rhodophyte-derived complex plastids [53]. We ran ASAFind combined with different versions of SignalP and also used the C. velia optimized predictor ASAFind+ [54] in conjunction with SignalP 4.1. For mitochondrial transit peptides, we also used the prediction method MitoFates [55]. All results are summarized in the Supplementary File S1.

According to SignalP 4.1 and TargetP 1.1, ALAS has no detectable ER signal peptide (ER-SP) or TP. This also applies to ALAD2 and UROS. Complete BTSs composed of SPs and TPs were found in ALAD1, porphobilinogen deaminase (PBGD), uroporphyrinogen decarboxylase 1 (UROD1), UROD2, both coproporphyrinogen oxidases (CPOX1, CPOX2), protoporphyrinogen oxidase 1 (PPOX1) and FECH1. ER-SPs without subsequent TP were found in UROD3 and FECH2. Mitochondrial TPs were detected in ALAD3 and PPOX2 by TargetP, while MitoFates predicted mitochondrial TPs for UROD1 and PPOX2 (all other enzymes were negative, results were identical regardless of the choice of organism group, Supplementary File S1). Due to the good prediction performance of SignalP- and TargetP- based methods in diatoms [53,56] and *C. velia* [54], we decided to weight the results of SignalP/TargetP in conjunction with ASAFind or ASAFind+ higher than the MitoFates results.

All ASAFind predictions consistently suggested plastid localization for ALAD1, PBGD, UROD1, UROD2, UROD3, CPOX1, CPOX2, PPOX1, and FECH1. The remaining enzymes of the pathway appear to lack the ER-SP. The output of ASAFind and ASAFind+ combined with TargetP 2.0 agreed with the results mentioned above, except for FECH2, which according to TargetP 2.0, also has an ER-SP but no predicted plastid targeting by either ASAFind or ASAFind+. All above-mentioned predictors agreed on ALAS, ALAD2 and UROS lacking N-terminal targeting signal (Figure 2, Supplementary Table S1).
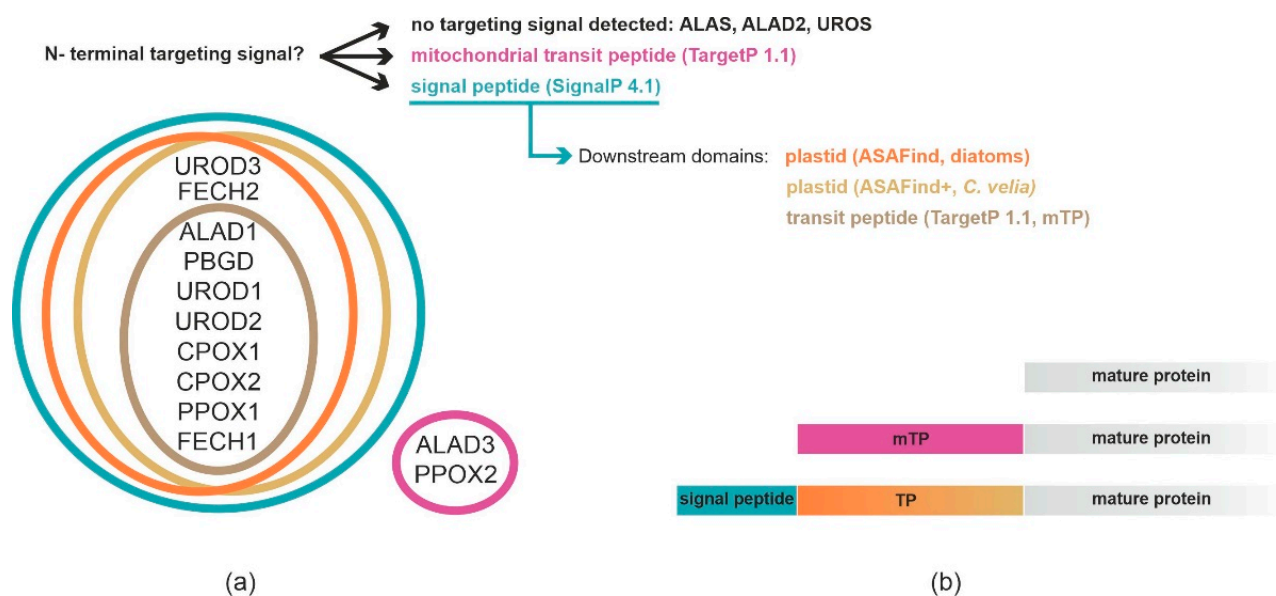

Figure 2. In silico targeting predictions for heme biosynthesis pathway enzymes in *C. velia*. (**a**) Euler diagram displays interpretation of targeting signals by various predictors. (**b**) Scheme showing different possibilities of N-terminal targeting signals.

We interpret the results as follows: ALAS, ALAD2 and UROS have no detectable targeting signal. ALAD3 and PPOX2 have TP (detected by TargetP 1.1). The remaining enzymes (ALAD1, PBGD, UROD1, UROD2, UROD3, CPOX1, CPOX2, PPOX1, and FECH1) were predicted to be plastid-targeted proteins by most of the used predictors.

2.2. Analyses of C. velia Heme Pathway Enzymes N-termini Sequence

We analyzed the N-terminus sequence of *C. velia* heme pathway enzymes with predicted BTS. We compared the aa distribution and overall net charge of these proteins with works already published on the set of plastid targeted proteins from diatoms [53] and *C. velia* [54]. We found that *C. velia* has about 50% lower frequency of serine, and an overall higher proportion of positively charged residues within the first 20 aa of the TPs than diatoms (Figure 3). Seven of the nine predicted BTS of the *C. velia* enzymes of interest contain negatively charged residues that are almost absent in diatoms [53].
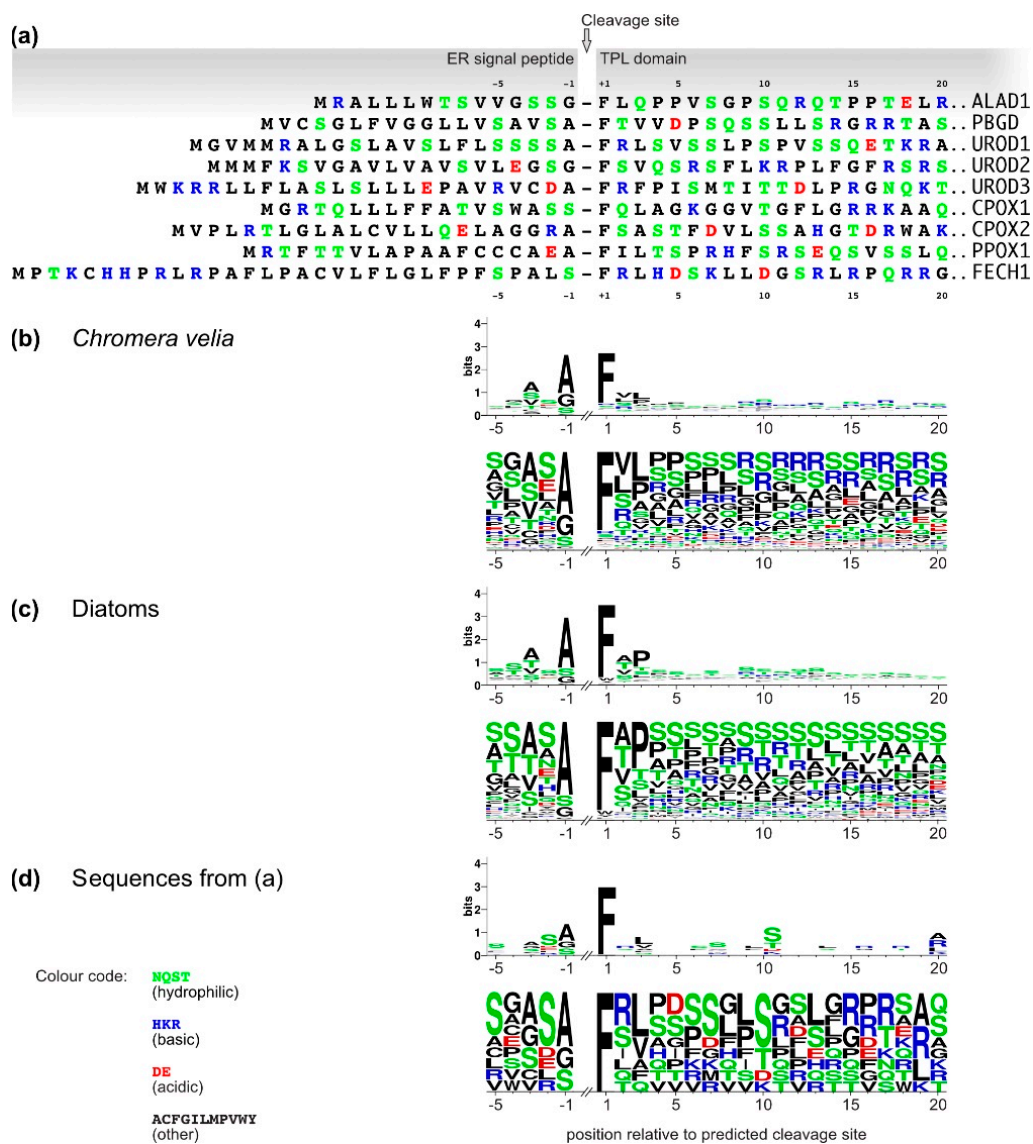
Figure 3. (**a**) ER-SP and TP domains of *C. velia* heme pathway enzymes. Coordinates are relative to the predicted SP cleavage site (arrow). Only enzymes that were positive for BTS are shown, amino acids in one letter code, color code is identical for all panels. (**b**–**d**) Sequence logos (upper panels) and frequency plots (lower panels) of plastid targeting BTS cleavage site motifs and TPs from (**b**) *C. velia* (*n* = 146 data from [5]), (**c**) diatoms (*n* = 166, reproduced from [53]), and (**d**) the *C. velia* heme pathway enzymes shown in A (*n* = 9).

2.3. Localization of C. velia Heme Synthesis Enzymes via Heterologous Expression

For the heterologous reporter gene expression experiments, we selected six different genes from *C. velia*, which encode enzymes for four steps of the synthesis: ALAS synthesizes the first precursor of the pathway (ALA); ALAD catalyzes the condensation of two ALA molecules to the monopyrrole porphobilinogen; UROS represents the middle step of the pathway and forms the first macrocyclic tetrapyrrole—uroporphyrinogen III; FECH terminates the pathway by chelating the protoporphyrin IX with Fe^{2+} thus generating heme. Our attempts to heterologously express full-length *C. velia* genes showed toxicity for *P. tricornutum* (data not shown). Therefore, we used truncated genes to express only the N-terminal regions of the enzymes that included the targeting signals (if predicted), and some additional amino acids of the mature protein to end up with maximally 121 aa long sequence fused to an eYFP reporter gene (Figure 4).

ALAS (Cvel_28814.t1):

```
01        10        20        30        40        50        60
MFSSGTARSFLTFASQEVKKLCPFVGKMGEMSRGKDLSKMAEMCPVASKMDKPIVIVDGDDAK
64    70        80        90        100       110       121
ASPAAHGRHYHTSAASSSSEKIGHHDSTPLYGHHHHQGNLVTHGRKSKPQVYLEHFDG:eYFP
```

ALAD1 (Cvel_108.t1):

```
01        10        20        30        40        50        60
MRALLLWTSVVGSSGFLQPPVSGPSQRQTPPTELRGLPQSSPFKGVPDSETPGALREELQPLV
64    70        80        90  92
DLATRPRRNRRNQVFRSLMQETVVRPSNL:eYFP
```

ALAD2 (Cvel_13826.t1):

```
01        10        20        30        40        50        60
MWSNASSDSSTCGAPVKRTEEGRSVCSTHDDPKRSRGSGDLSVERGPLQIPSRHRLQAGFSGS
64    68
LLRSW:eYFP
```

UROS (Cvel_15018.t1):

```
01        10        20        30        40        50        60
MNFSCFTFLLNCRPSTPSKELRADRVEEVHFCTPTGGDASPETDLLTHSLYLQSAGVMVSVIP
64    70        80        90    98
WLAFLCPSSSGHSLLGKRAARRACALMTESSQPSP:eYFP
```

FECH1 (Cvel_18167.t1):

```
01        10        20        30        40        50        60
MPTKCHHPRLRPAFLPACVLFLGLFPFSPALSFRLHDSKLLDGSRLRPQRRGVRGVRGVEAPE
64    70        80      89
LTALSSEVSPSSRCTSSGVRSPPLSE:eYFP
```

FECH2 (Cvel_26873.t1):

```
01        10        20        30        40        50        60
MSRRVQGRRPRGCTPLLWLGLFVLSLSVRFAVGIGSSSVSVQEPFLKVPPFLSEARFTFKTIN
64    70        80        90        100  103
ARLKEKFHEEMDNIYHRFSSSLKQYGAGRKNRVGVLLVNL:eYFP
```

Figure 4. Constructs for heterologous expression of *P. tricornutum* and *T. gondii* with truncated *C. velia* proteins. Numbers above the aa sequence correspond to amino acid position in the protein. Presequences are marked in grey, predicted SPs are underlined. Enhanced yellow fluorescent protein used to tag the construct is displayed as acronym (eYFP) in a black box. CryptoDB accession numbers of proteins are given in parenthesis behind the protein name.

2.3.1. Localization in Phaeodactylum tricornutum

To express selected *C. velia* enzymes in *P. tricornutum*, we used two vectors, one bearing the gene of interest fused to the eYFP reporter and the other encoding the antibiotic resistance cassette, and co-transformed the diatom cells via micro-particle bombardment with a mixture of both vectors. Transformed genes are thought to be randomly integrated and stably maintained in the diatom genome [37]. After the antibiotic selection, we looked for eYFP positive cells using the fluorescence microscope and inspected them in detail via confocal microscopy. The signal from CvALAS- eYFP spanned through the diatom cell in the way typical for *P. tricornutum* mitochondria [57,58] and colocalized with the MitoTracker signal (Figure 5). The remaining enzymes, CvALAD1, CvALAD2, CvUROS, CvFECH1, and CvFECH2, consistently showed the so-called "blob-like" structures (Figure 5), a dense signal in close proximity to the plastid [35,59], with the same signal found even in the cases of CvALAD2, CvUROS, and CvFECH2, that lack SPs. The "blob-like" structure indicates targeting to the periplastidial space, between the two outermost and the two innermost membranes of the diatom complex plastid [60]. While the "blob-like" structure pattern was observed in the majority (88.9%) of cells in culture, 11.1% of cells showed co-localization of eYFP signals with ER-Tracker, indicating the presence of the enzyme in the ER (Supplementary Figure S3). These results suggest that all tested enzymes, except for the mitochondria located CvALAS, are trapped either in the ER or in the periplastidial compartment of the diatom plastid, thus not entering the plastid stroma.
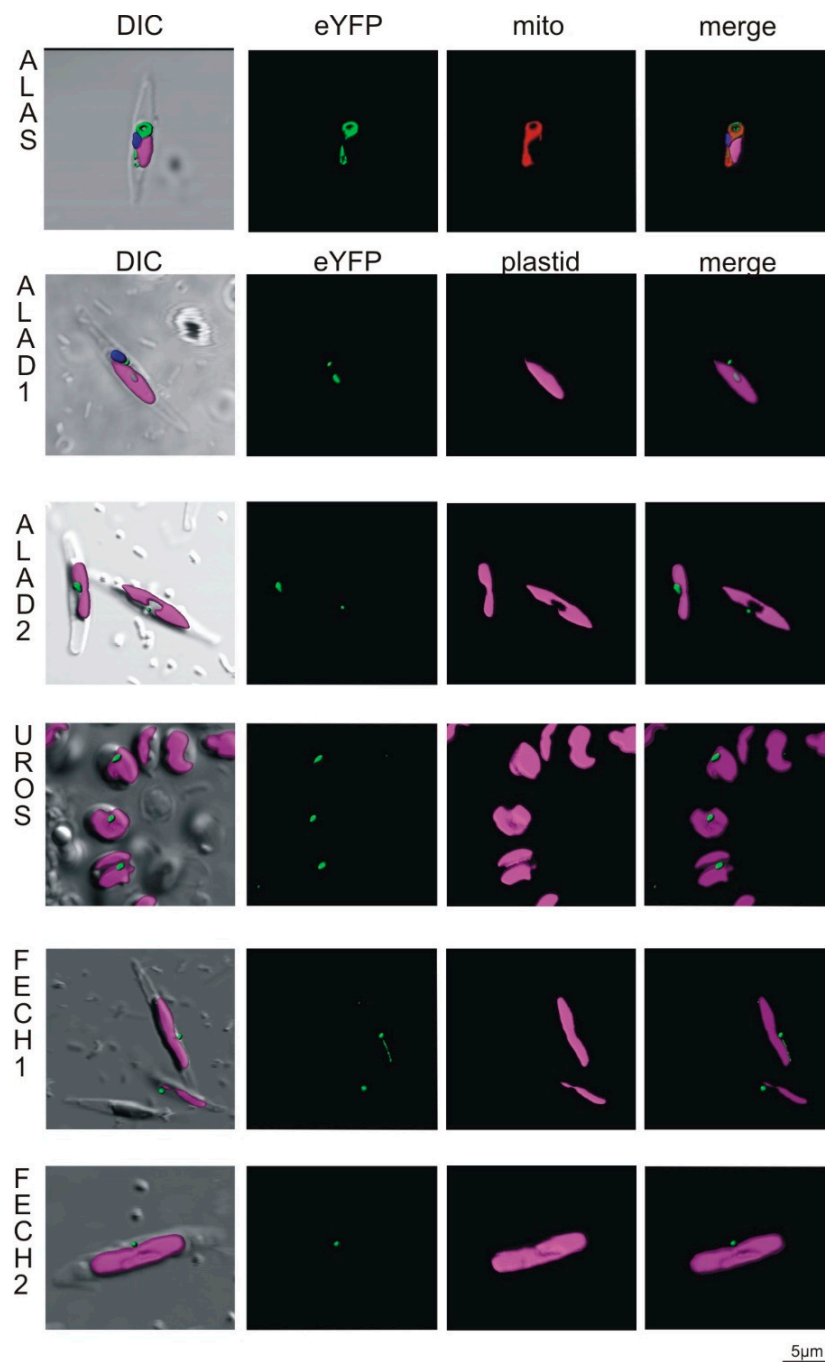
Figure 5. Heterologous expression of *Phaeodactylum tricornutum* with genes from *Chromera velia* heme pathway enzymes. Selected enzymes were tagged on their C-terminus by eYFP (green), magenta indicates plastid autofluorescence, MitoTracker® Orange CM-H2TMRos (ALAS, red) indicates mitochondrion. Green eYFP signal of *C. velia* ALA synthase colocalizes with red signal of *P. tricornutum* mitochondrion (row ALAS). Typical "blob-like" structures are found in heterologous expression of ALA dehydratases (ALAD1, ALAD2), uroporphyrinogen synthase (UROS) and both ferrochelatases (FECH1, FECH2).

2.3.2. Localization in *Toxoplasma gondii*

Toxoplasma gondii cells were transfected via electroporation with a vector bearing both, the chloramphenicol resistance cassette, and the *C. velia* heme pathway truncated gene, enabling fast selection of transfectants. In agreement with the *P. tricornutum* heterologous system, we also localized CvALAS in mitochondria of *T. gondii* (Figure 6) with the signal

overlapping with the mitochondrial marker TgMys [47,61]. However, localization of CvALAD1, CvALAD2, and CvUROS in *T. gondii* conflicted with that found in *P. tricornutum*. Both CvALAD1 and CvALAD2 displayed cytosolic distribution in the apicomplexan model, while CvUROS was targeted to the mitochondrion. In agreement with the predictions, CvFECH1 localized to the apicoplast of *T. gondii*, but so did the CvFECH2, which has no predicted targeting signal (Figure 2).
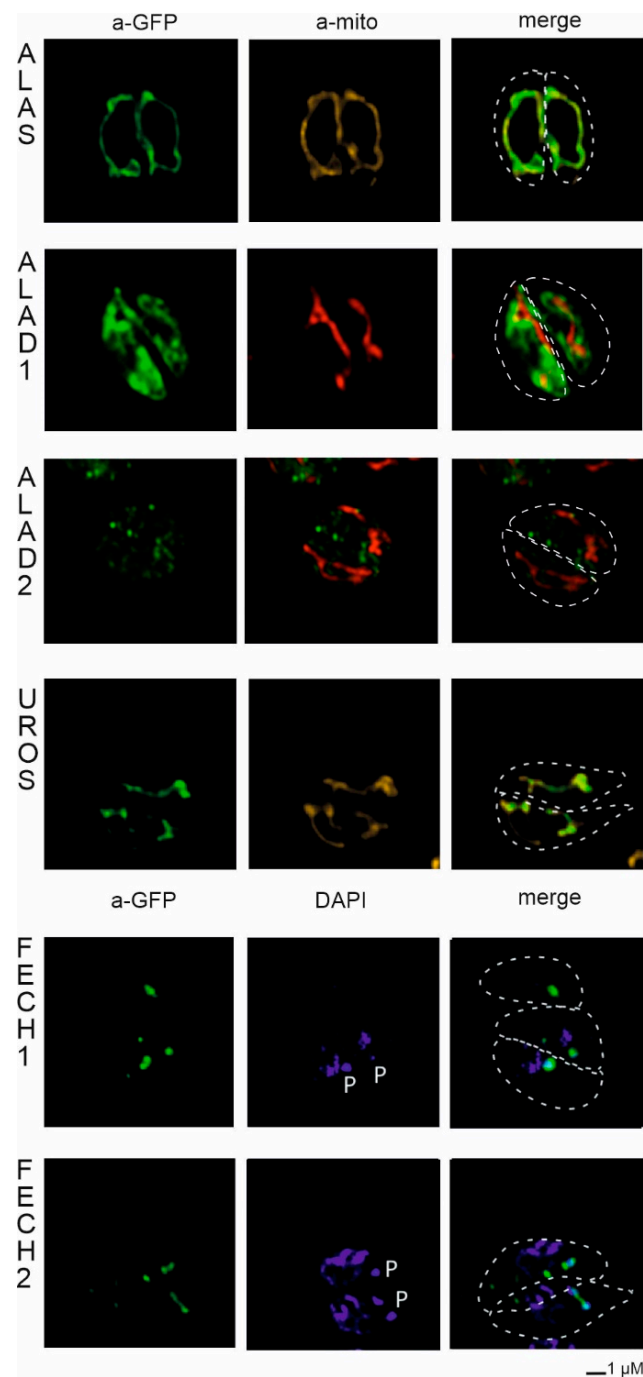

Figure 6. Heterologous expression of *Toxoplasma gondii* with genes from *Chromera velia* heme pathway enzymes. Immunofluorescence assays of transfected *T. gondii*, anti-GFP antibody were used to detect eYFP tagged *C. velia* enzymes. Anti-GFP (green) colocalized with mitochondrial anti-TgMys (a-mito, red and yellow) signal in case of ALAS and UROS. ALAD1 and ALAD2 signal were detected in the cytosol. FECH1 and FECH2 signal was found to overlap with DAPI (blue) signal at the area of parasite apicoplast. Apicoplast is denoted by "P". Dashed line indicates *T. gondii* cell border.

2.4. Direct ALAS Localization via Immune Gold Labeling of C. velia Cells

We used a custom-made polyclonal rabbit antibody designed to detect *C. velia* ALAS (described in detail in materials and methods), to localize the enzyme on cell sections via immunogold labeling. As a control we used anti-βATPase [62]. Western blots on total protein extract from *C. velia* were performed prior to in vivo experiments to verify specificity of antibodies. The size of the mature ALAS protein of *C. velia* was estimated to be ~48 kDa (Protein Calculator v3.4; protcalc.sourceforge.net), our Western blot data showed a single band of approximately 42 kDa (Figure 7a). Anti-βATPase antibody was also tested on Western blot where we detected a signal of ~53 kDa (Figure 7d). Gold particles conjugated to secondary antibodies marking anti-CvALAS were in the majority (77%) of inspected *C. velia* sections detected in light-grey compartments of the cell (Figure 7b). Anti-βATP was in 61% detected in the same compartments as anti-CvALAS, beside it was also in 16% detected in plastids (Figure 7e). This finding was consistent in the majority of inspected *C. velia* sections (Figure 7c,f).
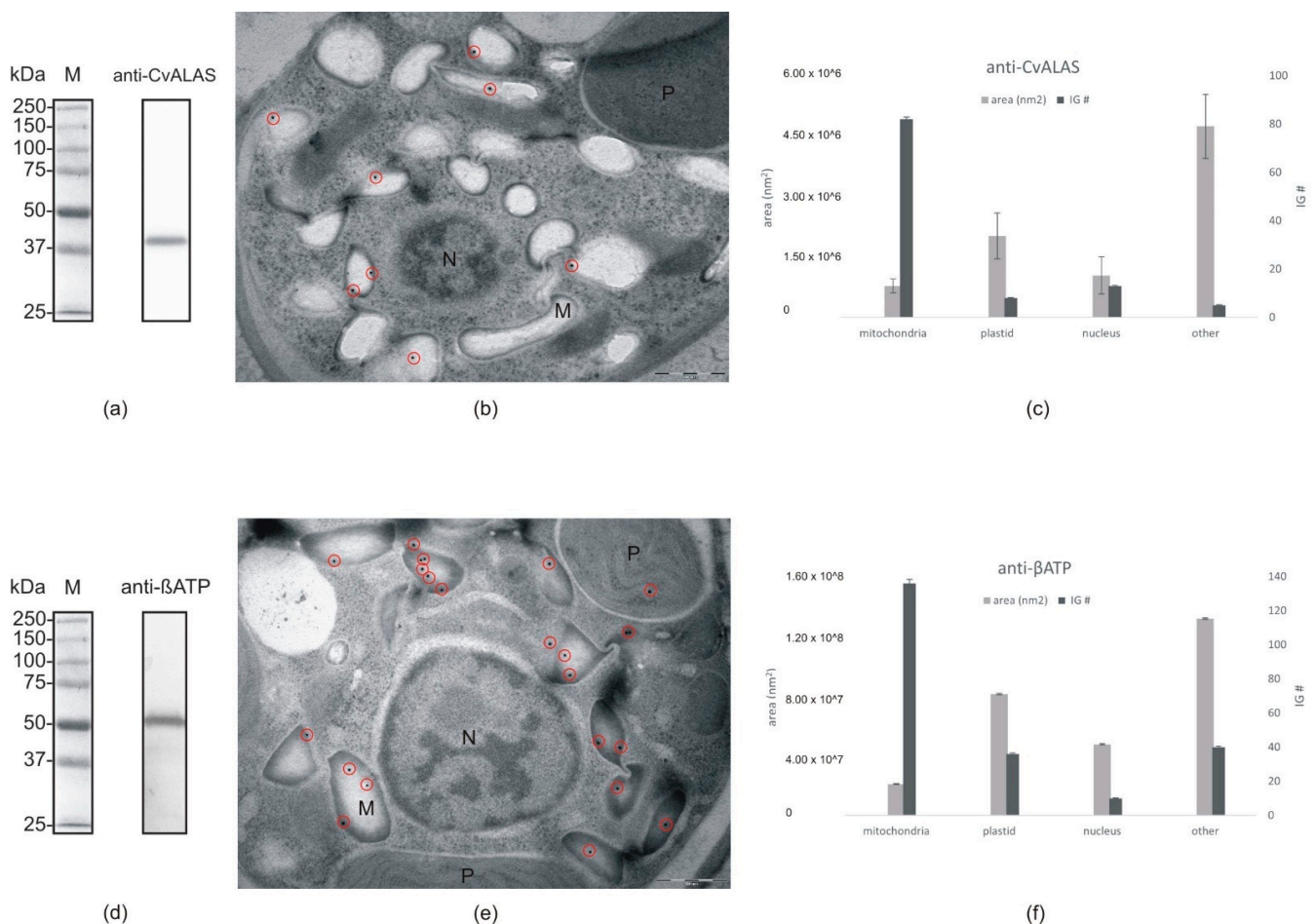

Figure 7. Immunogold labeling: (**a**) Western blot with anti-CvALAS on total protein extract from *C. velia* (**b**) Micrograph of *C. velia* ultrathin section after immunogold labeling with specific anti-CvALAS as a primary antibody. The majority of gold particles (encircled) were detected in the mitochondria. (**c**) Distribution of secondary IG particles (detecting anti-CvALAS) among cell compartments counted from all 35 micrographs. (**d**) Western blot with anti-βATP on total protein extract from *C. velia* (**e**) Micrograph of *C. velia* ultrathin section after immunogold labeling with specific anti-βATP as a primary antibody. The majority of gold particles (encircled) were detected in *C. velia* mitochondria. (**f**) Distribution of secondary IG particles (detecting anti-βATP) among cell compartments counted from all 35 micrographs. N = nucleus, M = mitochondria, P = plastid.

3. Discussion

To synthesize heme is crucial to the survival and growth of almost all living organisms. Two variants of heme biosynthesis pathways are known, the C4 pathway (in Alphaproteobacteria and most heterotrophic eukaryotes), and the C5 pathway (in Archaea, Eubacteria other than Alphaproteobacteria, and most phototrophic eukaryotes) [2]. Over the course of evolution, the specific localization of a particular enzyme is the result of multiple factors, including its evolutionary and endosymbiotic origin, which compartment has a major need of the resulting product and can also reflect pathway regulation, and/or the substrate availability [16,63,64]. *Chromera velia*, the closest known phototrophic relative to apicomplexan parasites, possesses a unique heme pathway, in which 5-aminolevulinic acid (ALA) is synthesized by the heterotrophic C4 pathway in mitochondria, like in apicomplexans parasites and primary heterotrophic eukaryotes. The downstream steps of the pathway were predicted to take place in the plastid [11]. We applied a combination of experimental and computational approaches to get a better insight into the heme biosynthesis in *C. velia* (Figure 8). Since a heterologous expression system of *C. velia* is not yet available, we decided to transfect more or less closely related well-established models, particularly the pennate diatom *P. tricornutum* [37,65,66] and the coccidian *T. gondii* [40,67] with the genes (or gene fragments) from *C. velia*.
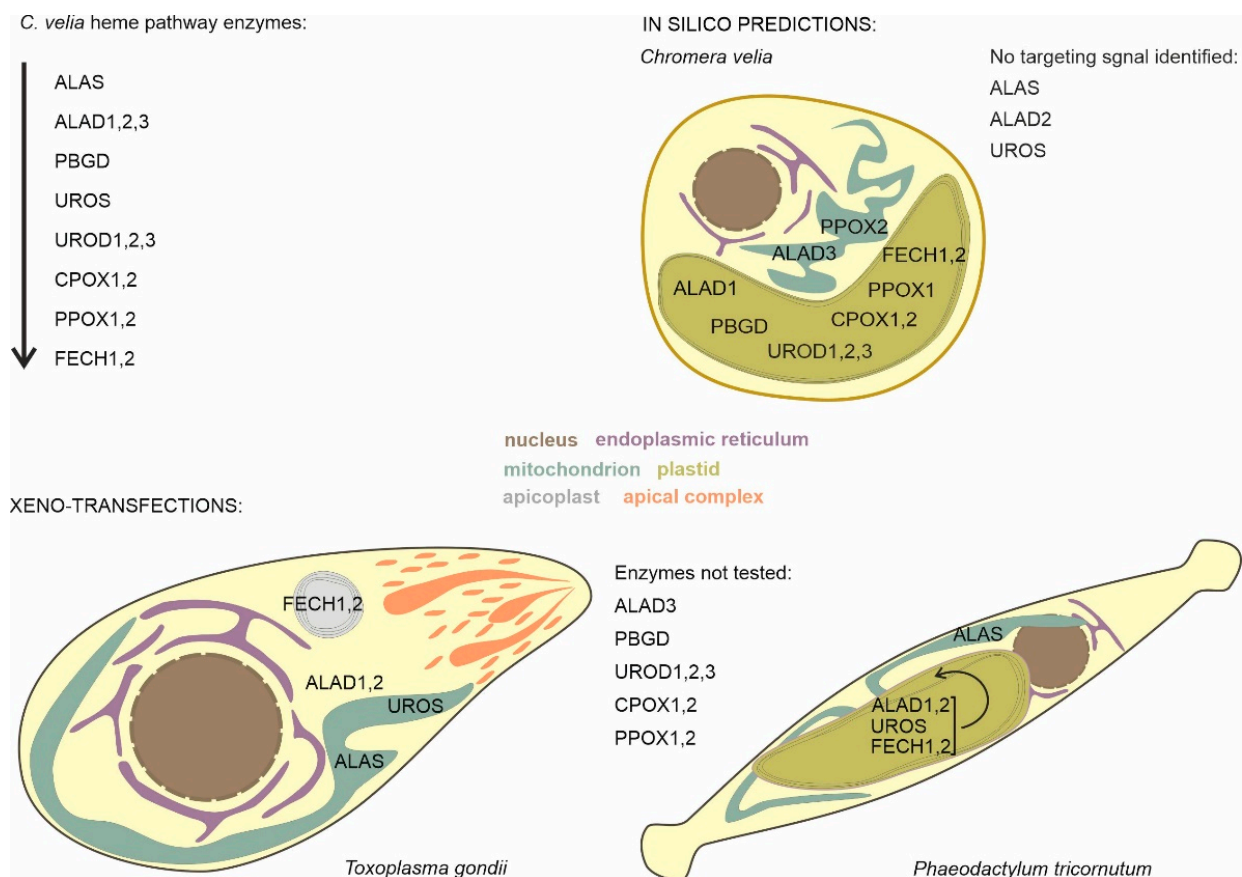

Figure 8. Intracellular distribution of heme biosynthesis in *Chromera velia*, inferred from predictions, and heterologous reporter gene expression in *Toxoplasma gondii* and *Phaeodactylum tricornutum*.

Our results from both approaches (protein targeting predictions and heterologous transfections) were multivalent with a single exception for ALAS that constantly displayed mitochondrial localization. We also tested anti-CvALAS directly on *C. velia* section where the antibody was predominantly found in compartments that we assume to be mitochondria as the anti-βATP [62] localized to the same compartment. The anti-βATP that we used is regularly used as a mitochondrial marker in *Trypanosoma brucei* [62]. The ATP synthase is known to work in plastids of photosynthetic organism as well [68]; therefore, we detected a minor number of IG particles (16%) also in *C. velia* plastids (Figure 7). Mitochondrial localization of ALAS likely reflects the use of succinyl-CoA, the product of mitochondrial TCA cycle, as one of the substrates [11]. Although predictors failed to detect a mitochondrial TP in ALAS, the enzyme contains a presequence at the N-terminus when compared to the Alphaproteobacterial counterparts, showing some characters of mitochondrial TPs. Moreover, the pre-sequence contains two conserved heme-binding CP motifs that are shared with the ALAS sequences of animals and fungi, where the excess of heme blocks the ALAS import into the mitochondrion and thus inhibits the synthesis of ALA and heme [11]. ALA dehydratase (syn. porphobilinogen synthase) catalyzes condensation of two ALA molecules to constitute porphobilinogen [69]. Three ALAD pseudoparalogs were found in the *C. velia* genome [70] after the gradual refinements of gene models (CryptoDB database; http://cryptodb.org/cryptodb/app). Each pseudoparalog displays a different targeting pattern (Figure 2). The plastid localization of ALAD1 in *C. velia* was consistently suggested by all the predictors, reflecting its evolutionary origin in cyanobacteria [11]. ALAD2 seems to originate from the primary host nucleus (the nucleus of engulfed alga) [16]; however, we detected no targeting presequences here. The ALAD3, that was suspected to originate from the secondary host nucleus [16], lacks any ER-SP but contains a putative chloroplast TP. All predictors agreed in the plastid localization of PBGD while the following enzyme, UROS, has no detectable targeting signal. However, transfection in the diatom shows periplastid localization of UROS. UROS is always localized together with its accompanying enzymes: PBGD and UROD [5,15,16,64]. Such arrangement enables fast processing of hydroxymethylbiliane to uroporphyrinogen III. It was shown that if there is no UROS present during or immediately after the PBGD forms hydroxymethylbiliane, the biologically inactive isomer, uroporphyrinogen I (which is not a precursor of heme), forms spontaneously [71,72]. All three pseudoparalogs of UROD are putatively plastid targeted (Figure 2), despite their diverse evolutionary origin: UROD1 in cyanobacteria, UROD2 in the endosymbiont (primary host) nucleus, and UROD3 in the secondary host (exosymbiont) nucleus [11]. Although all three pseudoparalogs were predicted by ASAF and ASAFind+ prediction tools to be plastid targeted, SignalP 4.1 combined with TargetP 1.1 showed only low confidence for SP and no TP in UROD3 (Figure 2, Supplementary Table S1). Therefore, it is possible that at least two UROD (1, 2) enzymes are plastid located. There are two pseudoparalogs of CPOX found in *C. velia*. Again, all the predictions placed both CPOX to the plastid (Figure 2). PPOX and FECH were found to form a complex allowing efficient channeling of metabolites through the thylakoid membranes, which protects the highly reactive protoporphyrinogen IX [73,74]. Therefore, these enzymes should share the same compartment. Almost all the predictors coupled PPOX1 and FECH1 as plastid-targeted enzymes and PPOX2 with FECH2 as situated out of the plastid. SignalP 4.1+TargetP 1.1 suggests only PPOX1 as a plastid-targeted protein. The prediction algorithm did not find ER-SP in PPOX2, FECH2 was found to be SP positive; however, TP was not detected (Figure 2, Supplementary Table S1).

Transfections of *P. tricornutum* and *T. gondii* with selected *C. velia* heme pathway enzymes showed inconsistent results except for the mitochondrially located CvALAS. The mitochondrial TP was not found by any predictor in *C. velia* ALAS; however, the enzyme possesses N-terminal extension in its sequence [11] that directed the protein to mitochondria of both transfected organisms (Figures 5 and 6). This finding suggests high versatility of the mitochondrial import machinery.

Transfections of *P. tricornutum* localized CvALAD1, CvALAD2, CvUROS, CvFECH1, and CvFECH2 outside the stroma of the diatom plastid, in the periplastidial space or the ER. These results may suggest that the diatom protein import machinery failed to recognize the TP domain in the *C. velia* enzyme or passed over the cleavage site between the ER-SP and the TP. The "blob-like" structure pattern of our constructs may, in some cases, phenotypically resemble peroxisome targeting [75]; however, peroxisome targeting in *P. tricornutum* relies on extreme C-terminal signal used by PTS1 import pathway, and the N-terminal depending import mechanism (PTS2) is not present at all [75]. In our work we used constructs formed predominantly by the N- terminus of *C. velia* heme pathway enzyme directly connected to eYFP (Figure 4). Therefore, we assume that the targeting into the peroxisome is not possible. The observed phenotype known as "blob-like" structure [35], has been explained as a block within the multistep plastid protein import pathway consisting of independent steps: Sec61 in cER, ERAD/SELMA in PPM and TOC and TIC in the outer and inner plastid envelope [26,76]. Plastid import in our constructs most probably stops before reaching the TOC complex of the second innermost membrane due to insufficient targeting signal within the sequence of *C. velia* heme enzyme constructs. This corresponds to the presence of the reporter protein in the periplastidial compartment (PPC), the space between the second and third plastid membranes. The reason for that could lie in the sequence of SP/TP motif of *C. velia* enzymes. SP leads the targeted protein through Sec61complex of the diatom chloroplast-ER membrane. Inside the lumen, the SP is cleaved off, and the TP is exposed to the translocon, which directs the protein across the second outermost membrane via the SELMA complex and through the TOC and TIC machinery of two innermost plastid membranes, respectively [26,76]. Kilian et al. [35] showed that possession of phenylalanine in position +1 of the TP is crucial for targeting the diatom plastid stroma. This specific phenylalanine requirement later broadened to required presence of F, Y, W and L [53,77,78]. Patron et al. [36] showed that this motif is well conserved among diatoms and brown algae. They also suggested that the ASA-F motif might be common for organisms with the rhodophyte-derived complex plastids. However, our analyses of *C. velia* heme pathway enzymes with predicted BTS have shown that the typical ASA-F motif is absent, and that negatively charged residues, which are almost absent in diatoms [53], are present in some *C. velia* heme pathway enzymes (Figure 3). It should be noted that the "blob-like" phenotype of the GFP accumulation in the diatom periplastidial compartment was first described as miss-targeting of plastid proteins with mutated BTS [35]. Later it was found that even a single amino acid substitution can change the targeting from the plastid to the periplastidial compartment [59,60]. This might explain the "blob-like" phenotype observed in our experiments because the BTSs of *C. velia* (Figure 3), in fact, resemble some of the mutated *P. tricornutum* BTSs, particularly in the case of changes in the TP net charges [78].

All investigated enzymes, except for ALAS, entered the periplastidial space of the diatom plastid or were captured in the ER just before crossing the second outermost plastid membrane. In other words, the transfected polypeptide successfully delivered eYFP over one (ER membrane) or two (periplastid membrane) outermost diatom plastid membranes but did not enter the plastid stroma. The SELMA translocon machinery, found in all rhodophyte-derived complex plastids with four membraned envelopes, is responsible for transporting protein across the second outermost membrane and mediates contact between the protein and TOC and TIC system of the two innermost plastid membranes [76]. We can speculate that if the proteins from *C. velia* contained a "proper" diatom ASA-F cleavage site, they would all end up in the stroma of the diatom plastid, in agreement with in silico predictions. On the other hand, ALAD2, UROS, and FECH2 show the same periplastid location in the diatom, even in the absence of a predictable BTS signal. As mentioned above, a minor fraction of the diatom transformants showed localization of proteins in the ER. As the ER is continuous with the outermost membrane of the diatom plastid, the observed pattern documents a failure to pass the second outermost membrane. That the enzymes reached the periplastidial space supports the presence of a functional ER-SP.

Our results indicate the presence of a strict control mechanism controlling plastid protein import machinery of *P. tricornutum*.

In *T. gondii*, the cleavage site motif is less conserved than in algae [36]. Experimental localization of *C. velia* enzymes in *T. gondii* showed a more complex pattern (Figure 6). Both ALAD enzymes were located in the *T. gondii* cytosol with the signal of CvALAD2 displaying punctuated pattern distributed throughout the whole cell in a similar way as already described in [79,80]. The cytosolic localization suggests the inability of *T. gondii* translocon machinery to recognize the chromerid ER-SP, which is not surprising for CvALAD2 lacking a targeting presequence. On the other hand, even this enzyme was targeted to the diatom periplastidial compartment. However, without biochemical work that separates soluble and membrane fraction we cannot be 100% certain that both ALAD enzymes are localized only within *T. gondii* cytosol. The outermost membrane of the *T. gondii* apicoplast lacks, contrary to diatom plastid, a direct connection to ER [81]. Although the SP is also recognized by Sec61 translocon in the ER membrane, proteins are then transported via the ER and Golgi apparatus that directs protein-containing vesicles through the cytoplasm to the apicoplast [82]. After crossing the first membrane barrier, the remaining three membranes are equipped with a similar translocon system: periplastid membrane utilizes translocation ERAD/SELMA machinery [26,48,83–86], and both apicomplexans and diatoms employ homologous TOC and TIC plastid import machinery to transfer proteins over the outer and inner plastid membrane, respectively [48,87,88].

The mitochondrial targeting system seems to be more versatile. About 60% of mitochondrial proteins need to have positively charged amphipathic alpha-helical N-terminal presequence that is necessary for translocation through TOM and TIM mitochondrial membrane complexes. The remaining proteins do not carry cleavable presequence and rely on various internal targeting signal [89,90]. CvUROS was in *T. gondii* localized in mitochondria, contrary to its periplastidial localization in *P. tricornutum*. Despite the absence of any detectable targeting presequence *C. velia* UROS contains prolongation at the N-terminus when aligned with bacterial homologs (data not shown). Mitochondrial location of CvUROS in *T. gondii* demonstrates that the N-terminal presequence interpreted by the translocon machinery as mitochondrial TP is not always recognized by bioinformatic predictors. Both, *C. velia* FECHs were experimentally localized in the apicoplast of *T. gondii*. As mentioned above, the apicoplast is a minute organelle of approximately 0.15–1.5 μm in diameter [91]. Therefore, using confocal microscope, we are not able to distinguish whether the transfected CvFECHs arrived into the apicoplast stroma or remain trapped in any of the intermembrane spaces (similar to what we have seen in the diatom transfections) in immunofluorescence data. We hypothesize that *T. gondii* localizations of the *C. velia* enzymes are less likely to reflect real intracellular localizations in *C. velia,* due to the transport of intermediates over a high number of membranes (outlined in Figure 8).

The intracellular arrangement of the heme pathway in chromerids is non-canonical. Moreover, it seems to continue and terminate outside mitochondria [11]. Primary eukaryotic heterotrophs and some complex eukaryotic phototrophs are known to operate the tetrapyrrole pathway in different cell compartments. However, the first and terminal steps of the pathway usually locate in the same organelle, thus enabling easy pathway regulation [6,63]. There are two genes encoding terminal enzymes (FECHs) of the pathway in the genome of *C. velia*. One originates from a cyanobacterium, while the second is proteobacterial [11]. The corresponding proteobacterial FECH is in apicomplexan parasites mitochondrially targeted, while the cyanobacterial gene was lost during evolution. Multicellular plants also have two paralogue ferrochelatases originating in the gene duplication event. The first enzyme contains a C-terminal chlorophyll-binding domain and functions in the photosynthetic tissues. The second, which lacks the C-terminal domain, is utilized in the non-photosynthetic tissues such as roots [92,93]. However, the latter is also induced in photosynthetic tissues under various stress conditions [94,95]. We searched for a C-terminal chlorophyll-binding domain in both *C. velia* FECHs [96,97], but were not able to identify one. The reason for *C. velia* having two ferrochelatases in the plastid is therefore unknown.

There are various mechanisms of tetrapyrrole synthesis regulation that work on different levels of the synthesis and together form a strong and sensitive network [95]. Among them, the heme-mediated feedback inhibition of ALA synthesis, which is conserved through different domains of life, plays a major role [10,61,98,99]. In various heterotrophs, ALAS, PPOX and FECH constitute the "heme metabolome complex". The complex facilitates substrate channeling and coordinates tetrapyrrole metabolism [13,100]. However, the existence of a similar complex has not yet been proven in phototrophs; placement of these steps in different cellular compartments would require ambitious regulation and transport systems. Kořený et al. [11] found heme regulatory motifs in the sequence of *C. velia* ALAS, which indicates the presence of heme-mediated regulation of ALA synthesis. Therefore, we originally expected the location of proteobacterial FECH in the mitochondrion of *C. velia* (together with ALAS) as an intermediate state in the path to apicomplexan parasites, but the data do not support this hypothesis. All predictors agreed that FECH1 (the plastid originating pseudoparalog) possesses features typical for a plastid targeted protein, while the FECH2 should locate and outwith the plastid, but likely not in the mitochondrion. However, experimental localization showed both FECHs either in the diatom periplastidial compartment or the apicoplast. Therefore, we speculate that the possible role of the two ferrochelatases in a single cell could be protection of the cell under stress conditions.

While the tetrapyrrole pathway starts with the ALAS in the mitochondrion in chromerids, the remaining steps likely take place in the plastid. This model is further supported by the phylogenetic relationships among the individual enzymes of the pathway [11]. We summarized our findings in Table 1. The heterologous expression of *C. velia* ALAD1 and ALAD2 gave the same inconsistent results, placing the protein in the cytosol of *T. gondii* and PPC/ER in *P. tricornutum.* Despite that, we assume that ALAD1 is more likely a plastid-targeted protein, because our experimental results in *P. tricornutum* showed that the construct was transferred at least through the two outermost membranes of the diatom plastid. This, together with the combination of its cyanobacterial evolutionary origin, leads us to the conclusion that plastid localization is more plausible. The same cogitation was applied for FECH1 where the corresponding enzyme is also of cyanobacterial origin, and when heterologously expressed, it localized to PPC/ER of *P. tricornutum* and also to the apicoplast of *T. gondii*. We decided to conclude with an "uncertain localization" statement for ALAD3 and PPOX2 due to the absence of the experimental evidence and predictable ER signal peptides (see Supplementary Table S1 for details), and their proteobacterial and eukaryotic origin, respectively. Both enzymes possess predicted mitochondrial transit peptides; however, particularly in PPOX, which makes a complex with FECH, its placement in the mitochondrion without FECH is unlikely. The localization of ALAD3 in the mitochondrion and a formation of porphobilinogen in this organelle would require additional transport of porphobilinogen to the plastid over its four membranes envelopes. The remaining enzymes (PBGD, UROD1, UROD2, UROD3, CPOX1, CPOX2, and PPOX1) were concluded as "plastid" localized due to the congruency of the prediction result. However, spatial separation of the beginning and the end of the pathway is unprecedented, and it would require regulatory mechanisms that are not yet known. Therefore, we cannot rule out the possibility of recent reassignments of intracellular locations or dual targeting of the enzymes. Our work on localization of *C. velia* heme pathway enzymes shows that the subcellular localization of biosynthetic pathway within any organism is a concert of multiple factors rather than a solo for one major element.

Table 1. Table showing results described in this manuscript. Enzymes are listed according to their order during the synthesis of heme. Evolutionary origins of each of the enzymes are based on phylogenetic analyses from the work of [11,16]. The last column of the table contains our hypothetical conclusions about the *C. velia* enzyme localization based on our findings.

Enzyme	Accession (CryptoDB)	Evolutionary Origin	Targeting Prediction	Localization *T. gondii*	Localization *P. tricornutum*	Conclusion
ALAS	Cvel_28814.t1	Alphaproteobacteria	No targeting signal identified	Mitochondria	Mitochondria	Mitochondria
ALAD1	Cvel_108.t1	Cyanobacteria	Plastid	Cytosol	PPC/ER	Plastid
ALAD2	Cvel_13826.t1	Primary alga	No targeting signal identified	Cytosol	PPC/ER	Uncertain location
ALAD3	Cvel_36189.t1	Proteobacterial	Mitochondria	Not tested	Not tested	Uncertain location
PBGD	Cvel_26028.t1	Alphaproteobacteria	Plastid	Not tested	Not tested	Plastid
UROS	Cvel_15018.t1	Uncertain origin in primary alga	No targeting signal identified	Mitochondria	PPC/ER	Uncertain location
UROD1	Cvel_14720.t1	Cyanobacteria	Plastid	Not tested	Not tested	Plastid
UROD2	Cvel_5098.t1	Endosymbiont nucleus	Plastid	Not tested	Not tested	Plastid
UROD3	Cvel_31936.t1	Secondary host nucleus	Plastid	Not tested	Not tested	Plastid
CPOX1	Cvel_21486.t1	Secondary host nucleus	Plastid	Not tested	Not tested	Plastid
CPOX2	Cvel_2641.t1	Uncertain origin in primary alga	Plastid	Not tested	Not tested	Plastid
PPOX1	Cvel_13840.t1	Cyanobacteria	Plastid	Not tested	Not tested	Plastid
PPOX2	Cvel_18037.t1	Eukaryotic origin	Mitochondria	Not tested	Not tested	Uncertain location
FECH1	Cvel_18167.t1	Cyanobacteria	Plastid	Apicoplast	PPC/ER	Plastid
FECH2	Cvel_26873.t1	Alphaproteobacteria	Signal peptide positive	Apicoplast	PPC/ER	Uncertain location

4. Conclusions

C. velia is a coral-associated alga bearing complex rhodophyte-derived plastid with a peculiar tetrapyrrole pathway. It synthesizes ALA using heterotrophic C4 path, however, which additionally supplies chlorophyll for photosystems. Using a combination of bioinformatics and experimental approaches we investigated the localizations of heme pathway enzymes in *C. velia*. Our data show that the pathway very likely starts in the mitochondrion with the remaining enzymes located to the plastid. We demonstrate that the proteins are targeted to various cellular compartments by stringent translocon mechanisms that are not universal even for evolutionary related organisms.

5. Materials and Methods

Targeting predictions and sequence analyses: Protein sequences of *C. velia* heme pathway enzymes as available at CryptoDB were used as input for all predictors used in this work. Prediction results of SignalP [101] and TargetP [102] were received from a web server (http://www.cbs.dtu.dk/services/), with SignalP 4.1 in "sensitive" mode. The ASAFind was used according to [53,103] and ASAFind+ was applied by modifying

the original ASAFind code from Gruber et al. [53], according to the method described by Füssy et al. [54]. MitoFates [55] results were obtained from the MitoFates web service (http://mitf.cbrc.jp/MitoFates/cgi-bin/top.cgi). Sequence logos [103] and frequency plots were prepared using the WebLogo (http://weblogo.berkeley.edu/ [104]).

Cultivation conditions: *C. velia* (CCMP 2878) and *P. tricornutum* (CCMP 632) were grown in Guillard's (f/2) medium (Sigma-Aldrich, St. Louis, MI, USA) in seawater and kept stationary in a 12/12 light/dark cycle regime at 26 °C and 18 °C, respectively [28,37]. Illumination during the light cycle was 100 µE m-2s-1. *Toxoplasma gondii* was grown in primary human foreskin fibroblasts (HFF) and treated as described in [46].

cDNA preparation and cloning: *C. velia* culture was harvested by centrifugation at 3000 rpm/10 min at 10 °C. The cell pellet was homogenized in TRI Reagent (Sigma-Aldrich, St. Louis, MI, USA) and total RNA was isolated following manufacturer's instructions. cDNA was amplified from RNA with Superscript II reverse Transcriptase (Invitrogen, Thermo Fisher Scientific Inc, Waltham, MA, USA). Genes of the *C. velia* heme pathway were amplified from cDNA using specific primers designed for the Gateway cloning system (Invitrogen, Waltham, CA, USA). The amplified regions included the start codon and 201–360 bp downstream of the gene. Amplified genes were cloned into pENTR vectors (Invitrogen, Waltham, CA, USA) and verified by sequencing. pENTR vectors were subsequently recombined with pDEST-eYFP vectors by LR recombination reactions (Invitrogen, Waltham, CA, USA). Resulting pDEST-eYFP vectors contained the gene of interest followed by the sequence of the eYFP tag and were expressed under the fcp*b* promotor for *P. tricornutum* or under the tub promotor for *T. gondii* heterologous expression, respectively.

Phaeodactylum tricornutum heterologous expression: *P. tricornutum* cells were co-transfected with pDEST vector (fcp*b* promotor, *C. velia* heme pathway gene, eYFP tag) and pFCPFp-Sh ble vector (phleomycin resistance cassette). 1 µg/µL of vectors were mixed in a 1:1 ratio, mounted on tungsten (M-17) particles and introduced to the *P. tricornutum* nucleus by microparticle bombardment using the Biolistic PDS-1000/He Particle Delivery System (Bio-Rad, Hercules, Hercules, CA, USA). Cells were selected on 1% f/2 agar plates supplemented with 100 µg/mL phleomycin for 3–4 weeks in standard cultivation conditions. Phleomycin resistant colonies were subsequently transformed into liquid f/2 media and cultures of OD_{600} 0.2 were examined by fluorescent microscopy.

Phaeodactylum tricornutum fluorescent labelling of living cells: For mitochondria staining, 2 mL of *P. tricornutum* culture (OD_{600} 0.2) were incubated with 100 nM MitoTracker™ Orange CM-H2TMRos in standard cultivation conditions overnight. ER staining was done with ER-Tracker™ Red (BODIPY® TR Glibenclamide) according to manufacturer's instructions. A total of 0.1 µg/mL DAPI was used to incubate with cells for 15 min in dark. All chemicals used for staining were from: Thermo Fisher Scientific Inc, Waltham, MA, USA. Prior to confocal microscopy, 1ml of cells were harvested by centrifugation (6000 rcf/10 min/room temperature), washed, and resuspended in 100 µL of PHEM buffer.

Toxoplasma gondii transient transfection: *T. gondii* RH strain tachyzoites were purified from suspension using 3-µm-pore size polycarbonate filters, spun down by centrifugation (15,000 rcf/20 min/11 °C) and resuspended in electroporation buffer [105–107]. A total of 300 µL of parasites (appx. 10^7) and 20 µL of plasmid DNA (4.5 ng/µL) were transferred to a sterile electroporation cuvette and electroporated (1500 V, 25 Ω). The whole volume of the cuvette was poured into a well containing coverslips with confluent monolayer of HFF cells. Parasites were fixed and examined by immunofluorescence assay after 3 days of cultivation.

Toxoplasma gondii immunofluorescence assay: HFF-covered 12 mm round coverslips were inoculated with transfected *T. gondii* and grown for 24–72 h in standard growing conditions. Growing media was replaced with 4% paraformaldehyde in PBS and incubated for 20 min to fix parasites at RT. Permeabilization was done in 0.25% Triton X-100 in PBS for 20 min at RT. Coverslips were blocked in 1% BSA in PBS for 20 min before incubation in primary antibody (anti-TgMys 1:1000, anti-GFP 1:200, anti ROM 4 1:1000; all in 1% BSA/1xPBS) for 1 h at RT. Coverslips were washed in 1% BSA in Triton X-100 in PBS three

times and incubated with secondary antibody for 30 min at RT. A final wash in 1% BSA in Triton X-100 in PBS three times was conducted, and coverslips were mounted.

Microscopy: Cellular localizations were analyzed in both transfection systems and *C. velia* with the Fluo View™ 1000 confocal system configured with an inverted mobile IX81 microscope (Olympus, Tokyo, Japan). A scanning laser with wavelength 515 nm was used for excitation of chlorophyll and eYFP. The emission spectra were detected using the following bandwidths: DAPI 345–455 nm, eYFP 525–571 nm, chlorophyll 620–710 nm, and MitoTracker® Orange CM-H$_2$TMRos 554–576 nm, ER-Tracker™ Red (BODIPY® TR Glibenclamide) 590–640 nm. All chemicals used for staining were from: Thermo Fisher Scientific Inc., Waltham, MA, USA. Images were processed using Olympus FV10-ASW software and Imaris (Olympus, Tokyo, Japan).

Oligopeptide selection for antibodies production: Antibodies for direct localization *C. velia* ALAS were generated by Clonestar s.r.o. (Brno, Czech Republic) using synthetic oligopeptide conjugated to KHL/BSA. The oligopeptide sequence was chosen according to sequence analysis with Dnastar Lasergene Protean software suite version 7.1 (Madison, WI, USA), followed by analysis of conserved motives in Geneious (Biomatters Ltd., Auckland, New Zealand). Candidate oligopeptides were mapped to known tertiary structures on the NCBI server. Oligopeptide sequence (14 aa) with the most plausible epitope and surface probability, conservation in sequences alignment and surface mapping on tertiary structure was chosen.

SDS-PAGE and Western blotting: For SDS-PAGE and Western blotting we used the Bio-Rad Mini-Protean tetra cell system according to manufacturer's instructions. A total of 2–8 μL of *C. velia* protein lysate was loaded on 5/12% SDS-PAGE gel and then transferred to a PVDF membrane (GE Healthcare Life Sciences, Chicago, IL, USA). The membrane was then blocked with 5% nonfat dry milk in TBS and incubated for 1 h with the primary antibody (1:5000) in blocking solution containing 0.2% Tween 20 (TTBS). The membrane was washed three times with TTBS and incubated for 1 h with Anti-Rabbit Immunoglobulins/HRP (Dako, Glostrup, Denmark) (dilution 1:1300). Chemiluminescence reactions were performed using Clarity Western ECL Substrate (Bio-Rad). The expected size of enzyme was determined based on the protein sequence using online software Protein Calculator v3.4 (protcalc.sourceforge.net).

Immuno-gold labelling and Transmission electron microscopy: For antibody labelling, samples were blocked by placing the nickel grids with ultra-thin sections of *C. velia* on a drop (30 μL) of blocking/wash buffer (3% BSA, 0.1 M HEPES pH 7.4, 0.05% Tween-20) for one hour. The grids were moved to a drop of blocking/wash buffer containing Rabbit IgG anti-ALAS antibody (1:40), or anti-βATP (1:40) for 15 min and washed with a drop of blocking/wash buffer six times for 15 min each. Secondary immunolabelling was done with protein A conjugated to 15 nm gold, diluted 1:50 in blocking/wash buffer, for one hour. Labelling was followed by six washing steps with a drop of blocking/wash buffer, each 15 min, and finally grids were rinsed two times rinse with a drop of deionized H$_2$O and dried on paper. Post-contrasting was done in a drop of saturated Uranyl-Acetate/ethanol for 12 min. The grids were washed with 30% ethanol 3 times each for 90 s and finally dried on paper. All preceding steps were completed at room temperature. Images were obtained with a transmission electron microscope (JEM 1010, JEOL Ltd., Tokyo, Japan) at an acceleration voltage of 80 kV.

Quantification of immune-gold labeling distribution: Immuno-gold (IG) labeling of *C. velia* was quantified according to the method described in [108,109]. IG particles from a set of 35 micrographs of both IG labeling (anti-CvALAS, anti-βATP) of the same magnitude (40,000×) was quantified using the ImageJ software (https://imagej.nih.gov/) using a grid with cross distance 280 nm. Number of IG particles was counted (for each compartment) as follows:

$$\text{IG number} = \sum \text{gold particles} \tag{1}$$

Total area of each compartment: mitochondria, plastid, nucleus and other (=remaining organelles, vacuoles and cytoplasm) was estimated as follows:

$$\text{area nm}^2 = \sum P \times d \times d \tag{2}$$

where "P" means points (crosses) hits and "d" means the distance between crosses in the grid used in ImageJ software.

References

1. Tanaka, R.; Tanaka, A. Tetrapyrrole biosynthesis in higher plants. *Annu. Rev. Plant Biol.* **2007**, *58*, 321–346. [CrossRef]
2. Koreny, L.; Sobotka, R.; Kovarova, J.; Gnipova, A.; Flegontov, P.; Horvath, A.; Obornik, M.; Ayala, F.J.; Lukes, J. Aerobic kinetoplastid flagellate *Phytomonas* does not require heme for viability. *Proc. Natl. Acad. Sci. USA* **2012**, *109*, 3808–3813. [CrossRef] [PubMed]
3. Jordan, P.M. Highlights in haem biosynthesis. *Curr. Opin. Struct. Biol.* **1994**, *4*, 902–911. [CrossRef]
4. Oborník, M.; Green, B.R. Mosaic origin of the heme biosynthesis pathway in photosynthetic eukaryotes. *Mol. Biol. Evol.* **2005**, *22*, 2343–2353. [CrossRef] [PubMed]
5. Kořený, L.; Oborník, M.; Lukeš, J. Make it, take it, or leave it: Heme metabolism of parasites. *PLoS Pathog.* **2013**, *9*, e1003088. [CrossRef]
6. Masuda, T.; Fujita, Y. Regulation and evolution of chlorophyll metabolism. *Photochem. Photobiol. Sci.* **2008**, *7*, 1131–1149. [CrossRef] [PubMed]
7. Czarnecki, O.; Grimm, B. Post-translational control of tetrapyrrole biosynthesis in plants, algae, and cyanobacteria. *J. Exp. Bot.* **2012**, *63*, 1675–1687. [CrossRef]
8. Ikushiro, H.; Nagami, A.; Takai, T.; Sawai, T.; Shimeno, Y.; Hori, H.; Miyahara, I.; Kamiya, N.; Yano, T. heme-dependent inactivation of 5-aminolevulinate synthase from *Caulobacter crescentus*. *Sci. Rep.* **2018**, *8*, 1–13. [CrossRef]
9. Wißbrock, A.; George, A.A.P.; Brewitz, H.H.; Kühl, T.; Imhof, D. The molecular basis of transient heme-protein interactions: Analysis, concept and implementation. *Biosci. Rep.* **2019**, *39*. [CrossRef]
10. Kloehn, J.; Harding, C.R.; Soldati-Favre, D. Supply and demand—Heme synthesis, salvage and utilization by Apicomplexa. *FEBS J.* **2021**, *288*, 382–404. [CrossRef]
11. Kořený, L.; Sobotka, R.; Janouškovec, J.; Keeling, P.J.; Oborník, M. Tetrapyrrole synthesis of photosynthetic chromerids is likely homologous to the unusual pathway of apicomplexan parasites. *Plant Cell* **2011**, *23*, 3454–3462. [CrossRef]
12. Hamza, I. Intracellular trafficking of porphyrins. *ACS Chem. Biol.* **2006**, *1*, 627–629. [CrossRef]
13. Swenson, S.A.; Moore, C.M.; Marcero, J.R.; Medlock, A.E.; Reddi, A.R.; Khalimonchuk, O. From synthesis to utilization: The ins and outs of mitochondrial heme. *Cells* **2020**, *9*, 579. [CrossRef]

14. Mochizuki, N.; Tanaka, R.; Grimm, B.; Masuda, T.; Moulin, M.; Smith, A.G.; Tanaka, A.; Terry, M.J. The cell biology of tetrapyrroles: A life and death struggle. *Trends Plant Sci.* **2010**, *15*, 488–498. [CrossRef]

15. Kořený, L.; Oborník, M. Sequence evidence for the presence of two tetrapyrrole pathways in *Euglena gracilis. Genome Biol. Evol.* **2011**, *3*, 359–364. [CrossRef] [PubMed]

16. Cihlář, J.; Füssy, Z.; Horak, A.; Oborník, M. Evolution of the tetrapyrrole biosynthetic pathway in secondary algae: Conservation, redundancy and replacement. *PLoS ONE* **2016**, *11*, e0166338. [CrossRef] [PubMed]

17. Votýpka, J.; Modrý, D.; Oborník, M.; Šlapeta, J.; Lukeš, J. Apicomplexa. In *Handbook of the Protists*; Archibald, J.M., Simpson, A.G.B., Slamovits, C.H., Eds.; Springer International Publishing: Cham, Switzerland, 2017; pp. 567–624. [CrossRef]

18. Ralph, S.A.; Van Dooren, G.G.; Waller, R.; Crawford, M.J.; Fraunholz, M.; Foth, B.J.; Tonkin, C.J.; Roos, D.; McFadden, G.I. Metabolic maps and functions of the Plasmodium falciparum apicoplast. *Nat. Rev. Microbiol.* **2004**, *2*, 203–216. [CrossRef]

19. Seeber, F.; Limenitakis, J.; Soldati-Favre, D. Apicomplexan mitochondrial metabolism: A story of gains, losses and retentions. *Trends Parasitol.* **2008**, *24*, 468–478. [CrossRef]

20. Van Dooren, G.G.; Kennedy, A.T.; McFadden, G.I. The use and abuse of heme in apicomplexan parasites. *Antioxid. Redox Signal.* **2012**, *17*, 634–656. [CrossRef] [PubMed]

21. Tjhin, E.T.; Hayward, J.A.; McFadden, G.I.; van Dooren, G.G. Characterization of the apicoplast-localized enzyme TgUroD in *Toxoplasma gondii* reveals a key role of the apicoplast in heme biosynthesis. *J. Biol. Chem.* **2020**, *295*, 1539–1550. [CrossRef]

22. Dalbey, R.; von Heijne, G. *Protein Targeting, Transport, and Translocation*, 1st ed.; Academic Press: Cambridge, MA, USA, 2002; 336p.

23. Kroth, P.G. Protein transport into secondary plastids and the evolution of primary and secondary plastids. *Int. Rev. Cytol.* **2002**, *221*, 191–255. [CrossRef] [PubMed]

24. Gould, S.B.; Waller, R.; McFadden, G.I. Plastid evolution. *Annu. Rev. Plant Biol.* **2008**, *59*, 491–517. [CrossRef]

25. Bolte, K.; Bullmann, L.; Hempel, F.; Bozarth, A.; Zauner, S.; Maier, U.G. Protein targeting into secondary plastids. *J. Eukaryot. Microbiol.* **2009**, *56*, 9–15. [CrossRef] [PubMed]

26. Maier, U.G.; Zauner, S.; Hempel, F. Protein import into complex plastids: Cellular organization of higher complexity. *Eur. J. Cell Biol.* **2015**, *94*, 340–348. [CrossRef] [PubMed]

27. Cavalier-Smith, T. Kingdom Chromista and its eight phyla: A new synthesis emphasising periplastid protein targeting, cytoskeletal and periplastid evolution, and ancient divergences. *Protoplasma* **2018**, *255*, 297–357. [CrossRef]

28. Moore, R.B.; Oborník, M.; Janouškovec, J.; Chrudimský, T.; Vancová, M.; Green, D.H.; Wright, S.W.; Davies, N.W.; Bolch, C.J.S.; Heimann, K.; et al. A photosynthetic alveolate closely related to apicomplexan parasites. *Nature* **2008**, *451*, 959–963. [CrossRef] [PubMed]

29. Oborník, M.; Modrý, D.; Lukeš, M.; Černotíková-Stříbrná, E.; Cihlář, J.; Tesařová, M.; Kotabová, E.; Vancová, M.; Prasil, O.; Lukeš, J. Morphology, ultrastructure and life cycle of *Vitrella brassicaformis* n. sp., n. gen., a novel chromerid from the Great Barrier Reef. *Protist* **2012**, *163*, 306–323. [CrossRef]

30. Janouškovec, J.; Tikhonenkov, D.; Burki, F.; Howe, A.T.; Kolísko, M.; Mylnikov, A.P.; Keeling, P.J. Factors mediating plastid dependency and the origins of parasitism in apicomplexans and their close relatives. *Proc. Natl. Acad. Sci. USA* **2015**, *112*, 10200–10207. [CrossRef]

31. Oborník, M.; Kručinská, J.; Esson, H. Life cycles of chromerids resemble those of colpodellids and apicomplexan parasites. *Perspect. Phycol.* **2016**, *3*, 21–27. [CrossRef]

32. Füssy, Z.; Masařová, P.; Kručinská, J.; Esson, H.J.; Oborník, M. Budding of the alveolate alga *Vitrella brassicaformis* resembles sexual and asexual processes in apicomplexan parasites. *Protist* **2017**, *168*, 80–91. [CrossRef]

33. Oborník, M. Endosymbiotic evolution of algae, secondary heterotrophy and parasitism. *Biomolecules* **2019**, *9*, 266. [CrossRef]

34. Oborník, M. Photoparasitism as an intermediate state in the evolution of apicomplexan parasites. *Trends Parasitol.* **2020**, *36*, 727–734. [CrossRef]

35. Kilian, O.; Kroth, P.G. Identification and characterization of a new conserved motif within the presequence of proteins targeted into complex diatom plastids. *Plant J.* **2005**, *41*, 175–183. [CrossRef]

36. Patron, N.J.; Waller, R. Transit peptide diversity and divergence: A global analysis of plastid targeting signals. *BioEssays* **2007**, *29*, 1048–1058. [CrossRef] [PubMed]

37. Apt, K.E.; Grossman, A.R.; Kroth-Pancic, P.G. Stable nuclear transformation of the diatom *Phaeodactylum tricornutum. Mol. Gen. Genet. MGG* **1996**, *252*, 572–579. [CrossRef] [PubMed]

38. Striepen, B.; He, C.Y.; Matrajt, M.; Soldati-Favre, D.; Roos, D. Expression, selection, and organellar targeting of the green fluorescent protein in *Toxoplasma gondii. Mol. Biochem. Parasitol.* **1998**, *92*, 325–338. [CrossRef]

39. Poulsen, N.; Chesley, P.M.; Kröger, N. MOLECULAR genetic manipulation of the diatom *Thalassiosira pseudonana* (bacillariophyceae). *J. Phycol.* **2006**, *42*, 1059–1065. [CrossRef]

40. Striepen, B.; Soldati, D. Genetic manipulation of *Toxoplasma gondii*. In *Toxoplasma Gondii*; Academic Press: Cambridge, MA, USA, 2007; pp. 391–418. [CrossRef]

41. Zhang, C.; Hu, H. High-efficiency nuclear transformation of the diatom *Phaeodactylum tricornutum* by electroporation. *Mar. Genom.* **2014**, *16*, 63–66. [CrossRef]

42. McFadden, G.I. Plastids and protein targeting. *J. Eukaryot. Microbiol.* **1999**, *46*, 339–346. [CrossRef] [PubMed]

43. Roos, D.S.; Crawford, M.J.; Donald, R.G.; Kissinger, J.; Klimczak, L.J.; Striepen, B. Origin, targeting, and function of the apicomplexan plastid. *Curr. Opin. Microbiol.* **1999**, *2*, 426–432. [CrossRef]

44. DeRocher, A.; Hagen, C.B.; Froehlich, J.E.; Feagin, J.E.; Parsons, M. Analysis of targeting sequences demonstrates that trafficking to the Toxoplasma gondii plastid branches off the secretory system. *J. Cell Sci.* **2000**, *113*, 3969–3977. [CrossRef]

45. Waller, R.F.; Reed, M.B.; Cowman, A.F.; McFadden, G.I. Protein trafficking to the plastid of *Plasmodium falciparum* is via the secretory pathway. *EMBO J.* **2000**, *19*, 1794–1802. [CrossRef]

46. Apt, K.E.; Zaslavkaia, L.; Lippmeier, J.C.; Lang, M.; Kilian, O.; Wetherbee, R.; Grossman, A.R.; Kroth, P.G. In vivo characterization of diatom multipartite plastid targeting signals. *J. Cell Sci.* **2002**, *115*, 4061–4069. [CrossRef]

47. Sheiner, L.; Demerly, J.L.; Poulsen, N.; Beatty, W.L.; Lucas, O.; Behnke, M.; White, M.W.; Striepen, B. A systematic screen to discover and analyze apicoplast proteins identifies a conserved and essential protein import factor. *PLOS Pathog.* **2011**, *7*, e1002392. [CrossRef]

48. Huesgen, P.F.; Alami, M.; Lange, P.F.; Foster, L.J.; Schröder, W.P.; Overall, C.M.; Green, B.R. Proteomic amino-termini profiling reveals targeting information for protein import into complex plastids. *PLoS ONE* **2013**, *8*, e74483. [CrossRef] [PubMed]

49. Füssy, Z.; Oborník, M. Chromerids and their plastids. In *Advances in Botanical Research*; Elsevier: Amsterdam, The Netherlands, 2017; Volume 84, pp. 187–218. [CrossRef]

50. Oborník, M.; Lukeš, J. Cell biology of chromerids. In *International Review of Cell and Molecular Biology*; Academic Press: Cambridge, MA, USA, 2013; Volume 306, pp. 333–369. [CrossRef]

51. Nielsen, H. Predicting secretory proteins with SignalP. In *Protein Function Prediction*; Kihara, D., Ed.; Humana Press: New York, NY, USA, 2017; pp. 59–73. [CrossRef]

52. Emanuelsson, O.; Brunak, S.; Von Heijne, G.; Nielsen, H.A. Locating proteins in the cell using TargetP, SignalP and related tools. *Nat. Protoc.* **2007**, *2*, 953–971. [CrossRef] [PubMed]

53. Gruber, A.; Rocap, G.; Kroth, P.G.; Armbrust, E.V.; Mock, T. Plastid proteome prediction for diatoms and other algae with secondary plastids of the red lineage. *Plant J.* **2015**, *81*, 519–528. [CrossRef]

54. Füssy, Z.; Faitová, T.; Oborník, M. subcellular compartments interplay for carbon and nitrogen allocation in *Chromera velia* and *Vitrella brassicaformis*. *Genome Biol. Evol.* **2019**, *11*, 1765–1779. [CrossRef] [PubMed]

55. Fukasawa, Y.; Tsuji, J.; Fu, S.-C.; Tomii, K.; Horton, P.; Imai, K. MitoFates: Improved prediction of mitochondrial targeting sequences and their cleavage sites. *Mol. Cell. Proteom.* **2015**, *14*, 1113–1126. [CrossRef]

56. Gruber, A.; McKay, C.; Kroth, P.G.; Armbrust, E.V.; Mock, T. Comparison of different versions of SignalP and TargetP for diatom plastid protein predictions with ASAFind. *Matters* **2020**, *81*, 519–528. [CrossRef]

57. Bártulos, C.R.; Rogers, M.B.; Williams, T.; Gentekaki, E.; Brinkmann, H.; Cerff, R.; Liaud, M.-F.; Hehl, A.; Yarlett, N.R.; Gruber, A.; et al. Mitochondrial glycolysis in a major lineage of eukaryotes. *Genome Biol. Evol.* **2018**, *10*, 2310–2325. [CrossRef] [PubMed]

58. Tanaka, A.; De Martino, A.; Amato, A.; Montsant, A.; Mathieu, B.; Rostaing, P.; Tirichine, L.; Bowler, C. ultrastructure and membrane traffic during cell division in the marine pennate diatom *Phaeodactylum tricornutum*. *Protist* **2015**, *166*, 506–521. [CrossRef] [PubMed]

59. Gould, S.B.; Sommer, M.S.; Hadfi, K.; Zauner, S.; Kroth, P.G.; Maier, U.G. Protein targeting into the complex plastid of cryptophytes. *J. Mol. Evol.* **2006**, *62*, 674–681. [CrossRef] [PubMed]

60. Gould, S.B.; Sommer, M.S.; Kroth, P.G.; Gile, G.H.; Keeling, P.J.; Maier, U.G. Nucleus-to-nucleus gene transfer and protein retargeting into a remnant cytoplasm of cryptophytes and diatoms. *Mol. Biol. Evol.* **2006**, *23*, 2413–2422. [CrossRef] [PubMed]

61. Ovciarikova, J.; Lemgruber, L.; Stilger, K.L.; Sullivan, W.J.; Sheiner, L. Mitochondrial behaviour throughout the lytic cycle of Toxoplasma gondii. *Sci. Rep.* **2017**, *7*, 42746. [CrossRef]

62. Šubrtová, K.; Panicucci, B.; Zíková, A. ATPaseTb2, a unique membrane-bound FoF1-ATPase component, is essential in blood-stream and dyskinetoplastic trypanosomes. *PLOS Pathog.* **2015**, *11*, e1004660. [CrossRef]

63. Brzezowski, P.; Richter, A.S.; Grimm, B. Regulation and function of tetrapyrrole biosynthesis in plants and algae. *Biochim. Biophys. Acta Bioenerg.* **2015**, *1847*, 968–985. [CrossRef]

64. Cihlář, J.; Füssy, Z.; Oborník, M. Evolution of tetrapyrrole pathway in eukaryotic phototrophs. In *Advances in Botanical Research*; Academic Press: Cambridge, MA, USA, 2019; Volume 90, pp. 273–309. [CrossRef]

65. Zaslavskaia, L.A.; Lippmeier, J.C.; Grossman, A.R.; Kroth, P.G.; Apt, K.E. Transformation of the diatom *Phaeodactylum tricornutum* (Bacillariophyceae) with a variety of selectable marker and reporter genes. *J. Phycol.* **2000**, *36*, 379–386. [CrossRef]

66. Niu, Y.-F.; Yang, Z.; Zhang, M.-H.; Zhu, C.-C.; Yang, W.-D.; Liu, J.-S.; Li, H.-Y. Transformation of *diatom Phaeodactylum tricornutum* by electroporation and establishment of inducible selection marker. *Biotechniques* **2012**, *52*. [CrossRef]

67. Weiss, L.M.; Kim, K. *Toxoplasma Gondii: The Model Apicomplexan—Perspectives and Methods*, 2nd ed.; Elsevier: Amsterdam, The Netherlands, 2013; 1085p. [CrossRef]

68. Igamberdiev, A.U.; Kleczkowski, L.A. Optimization of ATP synthase function in mitochondria and chloroplasts via the adenylate kinase equilibrium. *Front. Plant Sci.* **2015**, *6*. [CrossRef]

69. Warren, M.J.; Smith, A.G.; Schubert, H.L.; Erskine, P.T.; Cooper, J.B. 5-Aminolaevulinic acid dehydratase, porphobilinogen deaminase and uroporphyrinogen III synthase. In *Tetrapyrroles*; Springer: New York, NY, USA, 2009; pp. 43–73. [CrossRef]

70. Woo, Y.H.; Ansari, H.; Otto, T.; Klinger, C.M.; Kolisko, M.; Michálek, J.; Saxena, A.; Shanmugam, D.; Tayyrov, A.; Veluchamy, A.; et al. Chromerid genomes reveal the evolutionary path from photosynthetic algae to obligate intracellular parasites. *eLife* **2015**, *4*, e06974. [CrossRef]

71. Shepherd, M.; Medlock, A.; Dailey, H. Porphyrin metabolism. In *Encyclopedia of Biological Chemistry*, 2nd ed.; Elsevier: Amsterdam, The Netherlands, 2013; pp. 544–549. [CrossRef]

72. Bhagavan, N.; Ha, C.-E. Metabolism of iron and heme. In *Essentials of Medical Biochemistry*; Academic Press: Cambridge, MA, USA, 2015; pp. 511–529. [CrossRef]

73. Masoumi, A.; Heinemann, I.U.; Rohde, M.; Koch, M.; Jahn, M.; Jahn, D. Complex formation between protoporphyrinogen IX oxidase and ferrochelatase during haem biosynthesis in *Thermosynechococcus elongatus*. *Microbiology* **2009**, *154*, 3707–3714. [CrossRef] [PubMed]

74. Herbst, J.; Hey, D.; Grimm, B. Posttranslational control of tetrapyrrole biosynthesis: Interacting proteins, chaperones, auxiliary factors. In *Advances in Botanical Research*; Elsevier: Amsterdam, The Netherlands, 2019; pp. 163–194. [CrossRef]

75. Gonzalez, N.H.; Felsner, G.; Schramm, F.D.; Klingl, A.; Maier, U.-G.; Bolte, K. A single peroxisomal targeting signal mediates matrix protein import in diatoms. *PLoS ONE* **2011**, *6*, e25316. [CrossRef] [PubMed]

76. Stork, S.; Lau, J.; Moog, D.; Maier, U.-G. Three old and one new: Protein import into red algal-derived plastids surrounded by four membranes. *Protoplasma* **2013**, *250*, 1013–1023. [CrossRef]

77. Gruber, A.; Vugrinec, S.; Hempel, F.; Gould, S.B.; Maier, U.-G.; Kroth, P.G. Protein targeting into complex diatom plastids: Functional characterisation of a specific targeting motif. *Plant Mol. Biol.* **2007**, *64*, 519–530. [CrossRef] [PubMed]

78. Felsner, G.; Sommer, M.S.; Maier, U.G. The physical and functional borders of transit peptide-like sequences in secondary endosymbionts. *BMC Plant Biol.* **2010**, *10*, 223. [CrossRef]

79. Blume, M.; Nitzsche, R.; Sternberg, U.; Gerlic, M.; Masters, S.L.; Gupta, N.; McConville, M.J. A *Toxoplasma gondii* gluconeogenic enzyme contributes to robust central carbon metabolism and is essential for replication and virulence. *Cell Host Microbe* **2015**, *18*, 210–220. [CrossRef]

80. Brown, K.M.; Long, S.; Sibley, L.D. Plasma membrane association by N-Acylation governs PKG function in *Toxoplasma gondii*. *mBio* **2017**, *8*, e00375-17. [CrossRef]

81. Sheiner, L.; Striepen, B. Protein sorting in complex plastids. *Biochim. Biophys. Acta Mol. Cell Res.* **2013**, *1833*, 352–359. [CrossRef]

82. Boucher, M.J.; Yeh, E. Plastid–endomembrane connections in apicomplexan parasites. *PLoS Pathog.* **2019**, *15*, e1007661. [CrossRef]

83. Agrawal, S.; van Dooren, G.G.; Beatty, W.L.; Striepen, B. Genetic evidence that an endosymbiont-derived endoplasmic reticulum-associated protein degradation (ERAD) system functions in import of apicoplast proteins. *J. Biol. Chem.* **2009**, *284*, 33683–33691. [CrossRef] [PubMed]

84. Hempel, F.; Bullmann, L.; Lau, J.; Zauner, S.; Maier, U.G. ERAD-derived preprotein transport across the second outermost plastid membrane of diatoms. *Mol. Biol. Evol.* **2009**, *26*, 1781–1790. [CrossRef] [PubMed]

85. Hempel, F.; Bolte, K.; Klingl, A.; Zauner, S.; Maier, U.-G. Protein transport into plastids of secondarily evolved organisms. In *Plastid Biology*; Springer: New York, NY, USA, 2014; pp. 291–303.

86. Bullmann, L.; Haarmann, R.; Mirus, O.; Bredemeier, R.; Hempel, F.; Maier, U.G.; Schleiff, E. Filling the gap, evolutionarily conserved Omp85 in plastids of chromalveolates. *J. Biol. Chem.* **2010**, *285*, 6848–6856. [CrossRef]

87. Glaser, S.; van Dooren, G.G.; Agrawal, S.; Brooks, C.F.; McFadden, G.I.; Striepen, B.; Higgins, M.K. Tic22 is an essential chaperone required for protein import into the apicoplast. *J. Biol. Chem.* **2012**, *287*, 39505–39512. [CrossRef] [PubMed]

88. Sheiner, L.; Fellows, J.D.; Ovciarikova, J.; Brooks, C.F.; Agrawal, S.; Holmes, Z.C.; Bietz, I.; Flinner, N.; Heiny, S.; Mirus, O.; et al. *Toxoplasma gondii* Toc75 functions in import of stromal but not peripheral apicoplast proteins. *Traffic* **2015**, *16*, 1254–1269. [CrossRef]

89. Roger, A.J.; Muñoz-Gómez, S.A.; Kamikawa, R. The origin and diversification of mitochondria. *Curr. Biol.* **2017**, *27*, R1177–R1192. [CrossRef]

90. Wiedemann, N.; Pfanner, N. Mitochondrial machineries for protein import and assembly. *Annu. Rev. Biochem.* **2017**, *86*, 685–714. [CrossRef] [PubMed]

91. Maréchal, E.; Cesbron-Delauw, M.-F. The apicoplast: A new member of the plastid family. *Trends Plant. Sci.* **2001**, *6*, 200–205. [CrossRef]

92. Smith, A.; Santana, M.; Wallace-Cook, A.; Roper, J.; Labbe-Bois, R. Isolation of a cDNA encoding chloroplast ferrochelatase from *Arabidopsis thaliana* by functional complementation of a yeast mutant. *J. Biol. Chem.* **1994**, *269*, 13405–13413. [CrossRef]

93. Tanaka, R.; Kobayashi, K.; Masuda, T. Tetrapyrrole metabolism in *Arabidopsis thaliana*. *Arab. Book* **2011**, *9*, e0145. [CrossRef]

94. Nagai, S.; Koide, M.; Takahashi, S.; Kikuta, A.; Aono, M.; Sasaki-Sekimoto, Y.; Ohta, H.; Takamiya, K.-I.; Masuda, T. Induction of isoforms of tetrapyrrole biosynthetic enzymes, AtHEMA2 and AtFC1, under stress conditions and their physiological functions in arabidopsis. *Plant Physiol.* **2007**, *144*, 1039–1051. [CrossRef]

95. Kobayashi, K.; Masuda, T. Transcriptional regulation of tetrapyrrole biosynthesis in *Arabidopsis thaliana*. *Front. Plant Sci.* **2016**, *7*. [CrossRef]

96. Sobotka, R.; Tichy, M.; Wilde, A.; Hunter, C.N. Functional assignments for the carboxyl-terminal domains of the ferrochelatase from synechocystis PCC 6803: The CAB domain plays a regulatory role, and region II is essential for catalysis. *Plant Physiol.* **2011**, *155*, 1735–1747. [CrossRef]

97. Pazderník, M.; Mareš, J.; Pilný, J.; Sobotka, R. The antenna-like domain of the cyanobacterial ferrochelatase can bind chlorophyll and carotenoids in an energy-dissipative configuration. *J. Biol. Chem.* **2019**, *294*, 11131–11143. [CrossRef] [PubMed]

98. Franken, A.C.W.; Lokman, B.C.; Ram, A.F.J.; Punt, P.J.; van den Hondel, C.A.M.J.J.; de Weert, S. Heme biosynthesis and its regulation: Towards understanding and improvement of heme biosynthesis in filamentous fungi. *Appl. Microbiol. Biotechnol.* **2011**, *91*, 447–460. [CrossRef] [PubMed]

99. Zhang, J.; Kang, Z.; Chen, J.; Du, G. Optimization of the heme biosynthesis pathway for the production of 5-aminolevulinic acid in *Escherichia coli*. *Sci. Rep.* **2015**, *5*, 8584. [CrossRef] [PubMed]

100. Medlock, A.E.; Shiferaw, M.T.; Marcero, J.R.; Vashisht, A.A.; Wohlschlegel, J.A.; Phillips, J.D.; Dailey, H.A. Identification of the mitochondrial heme metabolism complex. *PLoS ONE* **2015**, *10*, e0135896. [CrossRef]

101. Petersen, T.N.; Brunak, S.; Von Heijne, G.; Nielsen, H. SignalP 4.0: Discriminating signal peptides from transmembrane regions. *Nat. Methods* **2011**, *8*, 785–786. [CrossRef]

102. Emanuelsson, O.; Nielsen, H.; Brunak, S.; von Heijne, G. Predicting subcellular localization of proteins based on their N-terminal amino acid sequence. *J. Mol. Biol.* **2000**, *300*, 1005–1016. [CrossRef]

103. Schneider, T.D.; Stephens, R.M. Sequence logos: A new way to display consensus sequences. *Nucleic Acids Res.* **1990**, *18*, 6097–6100. [CrossRef]

104. Crooks, G.E.; Hon, G.; Chandonia, J.-M.; Brenner, S.E. WebLogo: A sequence logo generator. *Genome Res.* **2004**, *14*, 1188–1190. [CrossRef] [PubMed]

105. Roos, D.; Donald, R.G.K.; Morrissette, N.S.; Moulton, A.L.C. Molecular tools for genetic dissection of the protozoan parasite *Toxoplasma gondii*. In *Methods in Cell Biology*; Elsevier: Amsterdam, The Netherlands, 1995; Volume 45, pp. 27–63. [CrossRef]

106. Donald, R.G.; Roos, D. Stable molecular transformation of *Toxoplasma gondii*: A selectable dihydrofolate reductase-thymidylate synthase marker based on drug-resistance mutations in malaria. *Proc. Natl. Acad. Sci. USA* **1993**, *90*, 11703–11707. [CrossRef] [PubMed]

107. Jacot, D.; Meissner, M.; Sheiner, L.; Soldati-Favre, D.; Striepen, B. Genetic manipulation of *Toxoplasma gondii*. In *Toxoplasma Gondii, The Model Apicomplexan—Perspectives and Methods*, 2nd ed.; Elevier: Amsterdam, The Netherlands, 2014; pp. 577–611. [CrossRef]

108. Lucocq, J.M.; Habermann, A.; Watt, S.; Backer, J.M.; Mayhew, T.M.; Griffiths, G. A rapid method for assessing the distribution of gold labeling on thin sections. *J. Histochem. Cytochem.* **2004**, *52*, 991–1000. [CrossRef]

109. Lucocq, J.M.; Gawden-Bone, C. Quantitative assessment of specificity in immunoelectron microscopy. *J. Histochem. Cytochem.* **2010**, *58*, 917–927. [CrossRef] [PubMed]

Paper II

ISOLATION OF PLASTIDS AND MITOCHONDRIA FROM CHROMERA VELIA

Sharaf, A.; Füssy, Z.; Tomčala, A.; Richtová, J.; and Oborník, M.

ORIGINAL ARTICLE

Isolation of plastids and mitochondria from *Chromera velia*

Abdoallah Sharaf[1,2] · Zoltán Füssy[1] · Aleš Tomčala[1] · Jitka Richtová[1,3] · Miroslav Oborník[1,3]

Abstract

Main conclusion We present an easy and effective procedure to purify plastids and mitochondria from *Chromera velia*. Our method enables downstream analyses of protein and metabolite content of the organelles.

Abstract Chromerids are alveolate algae that are the closest known phototrophic relatives to apicomplexan parasites such as *Plasmodium* or *Toxoplasma*. While genomic and transcriptomic resources for chromerids are in place, tools and experimental conditions for proteomic studies have not been developed yet. Here we describe a rapid and efficient protocol for simultaneous isolation of plastids and mitochondria from the chromerid alga *Chromera velia*. This procedure involves enzymatic treatment and breakage of cells, followed by differential centrifugation. While plastids sediment in the first centrifugation step, mitochondria remain in the supernatant. Subsequently, plastids can be purified from the crude pellet by centrifugation on a discontinuous 60%/70% sucrose density gradient, while mitochondria can be obtained by centrifugation on a discontinuous 33%/80% Percoll density gradient. Isolated plastids are autofluorescent, and their multi-membrane structure was confirmed by transmission electron microscopy. Fluorescent optical microscopy was used to identify isolated mitochondria stained with MitoTracker[TM] green, while their intactness and membrane potential were confirmed by staining with MitoTracker[TM] orange CMTMRos. Total proteins were extracted from isolated organellar fractions, and the purity of isolated organelles was confirmed using immunoblotting. Antibodies against the beta subunit of the mitochondrial ATP synthase and the plastid protochlorophyllide oxidoreductase did not cross-react on immunoblots, suggesting that each organellar fraction is free of the residues of the other. The presented protocol represents an essential step for further proteomic, organellar, and cell biological studies of *C. velia* and can be employed, with minor optimizations, in other thick-walled unicellular algae.

Paper III

BUDDING OF THE ALVEOLATE ALGA VITRELLA BRASSICAFORMIS RESEMBLES SEXUAL AND ASEXUAL PROCESSES IN APICOMPLEXAN PARASITES

Füssy, Z.; Masařová, P.; Kručinská, J.; Esson, H.; and Oborník, M.

Protist

ORIGINAL PAPER

Budding of the Alveolate Alga *Vitrella brassicaformis* Resembles Sexual and Asexual Processes in Apicomplexan Parasites

CrossMark

Zoltán Füssy[a], Petra Masařová[a], Jitka Kručinská[a,b], Heather J. Esson[a], and Miroslav Oborník[a,b,c,1]

[a]Institute of Parasitology, Biology Centre, Czech Academy of Sciences, České Budějovice, Czechia
[b]Faculty of Science, University of South Bohemia, České Budějovice, Czechia
[c]Centre Algatech, Institute of Microbiology, Czech Academy of Sciences, Třeboň, Czechia

Ease of cultivation and availability of genomic data promoted intensive research of free-living phototrophic relatives of apicomplexans, i.e. *Chromera velia* and *Vitrella brassicaformis*. *Chromera* and *Vitrella* differ significantly in their physiology, morphology, phylogenetic position and genomic features, but *Vitrella* has not gained as much attention. Here we describe two types of *Vitrella* zoosporangia. One contains zoospores surrounded by roughly structured matter, with an intracytoplasmic axoneme predicted to develop into a mature flagellum upon spore release, similarly to *Plasmodium* microgametes; in the second type, cells concurrently bud off the center of the sporangium, surrounded by smooth matter, and flagella develop extracellularly. This process of budding is reminiscent of microsporogenesis as seen in *Toxoplasma*. We suggest one (or both) of these processes generates gamete-like flagellate progeny. Based on live staining, fusion of zoospores does occur in cultures of *V. brassicaformis*. We failed to find an apical structure similar to the pseudoconoid in any life stage. *V. brassicaformis* may therefore either represent an ancestral state lacking an apical complex or has lost the apical complex secondarily. We propose that the common ancestor of Apicomplexa and "chrompodellids" exhibited a complex life cycle, which was reduced in chromerids and colpodellids as dictated by their environment.
© 2016 Elsevier GmbH. All rights reserved.

Key words: *Vitrella brassicaformis*; life cycle; zoosporangium; zoospores; budding; ciliogenesis.

Paper IV

-104-

SEPARATION AND IDENTIFICATION OF LIPIDS IN THE PHOTOSYNTHETIC COUSINS OF APICOMPLEXA CHROMERA VELIA AND VITRELLA BRASSICAFORMIS

Tomčala, A.; Kyselová, V.; Schneedorferová, I.; Opekarová, I.; Moos, M.; Urajová, P.; Kručinská, J.; and Oborník, M.

RESEARCH ARTICLE

Separation and identification of lipids in the photosynthetic cousins of Apicomplexa *Chromera velia* and *Vitrella brassicaformis*

Aleš Tomčala[1] (iD) | **Veronika Kyselová[1,2]** | **Ivana Schneedorferová[1,2]** | **Iva Opekarová[3,4]** | **Martin Moos[3]** | **Petra Urajová[5]** | **Jitka Kručinská[1,2]** | **Miroslav Oborník[1,2,5]**

[1]Biology Centre CAS, v.v.i., Institute of Parasitology, Laboratory of Evolutionary Protistology, České Budějovice, Czech Republic

[2]Faculty of Science, University of South Bohemia, České Budějovice, Czech Republic

[3]Biology Centre CAS, v.v.i., Institute of Entomology, Laboratory of Analytical Biochemistry, České Budějovice, Czech Republic

[4]University of Chemistry and Technology, Faculty of Food and Biochemical Technology, Department of Chemistry of Natural Compounds, Prague, Czech Republic

[5]Institute of Microbiology CAS, Laboratory of Algal Biotechnology, Třeboň, Czech Republic

Correspondence
Dr. Aleš Tomčala, Biology Centre CAS, v.v.i., Institute of Parasitology, Laboratory of Evolutionary Protistology, Branišovská 31, 370 05 České Budějovice, Czech Republic.
Email: a.tomcala@centrum.cz

The alveolate algae *Chromera velia* and *Vitrella brassicaformis* (chromerids) are the closest known phototrophic relatives to apicomplexan parasites. Apicomplexans are responsible for fatal diseases of humans and animals and severe economic losses. Availability of the genome sequences of chromerids together with easy and rapid culturing of *C. velia* makes this alga a suitable model for investigating elementary biochemical principals potentially important for the apicomplexan pathogenicity. Such knowledge allows us to better understand processes during the evolutionary transition from a phototrophy to the parasitism in Apicomplexa. We explored lipidomes of both algae using high-performance liquid chromatography with mass spectrometry or gas chromatography with flame ionization detection. A single high-performance liquid chromatography with mass spectrometry analysis in both ionization modes was sufficient for the separation and semi-quantification of lipids in chromerid algae. We detected more than 250 analytes belonging to five structural lipid classes, two lipid classes of precursors and intermediates, and triacylglycerols as storage lipids. Identification of suggested structures was confirmed by high-resolution mass spectrometry with an Orbitrap mass analyzer. An outstandingly high accumulation of storage triacylglycerols was found in both species. All the investigated aspects make *C. velia* a prospective organism for further applications in biotechnology.

KEYWORDS
Chromera velia, glycerolipids, mass spectrometry, *Vitrella brassicaformis*

Paper V

-118-

LIFE CYCLES OF CHROMERIDS RESEMBLE THOSE OF COLPODELLIDS AND APICOMPLEXAN PARASITES

Oborník, M.; Kručinská, J.; and Esson, H.

Life cycles of chromerids resemble those of colpodellids and apicomplexan parasites

Miroslav Oborník[1,2,3*], Jitka Kručinská[1,2] & Heather Esson[1]

[1] Biology Centre CAS, Institute of Parasitology, Branišovská 31, České Budějovice, Czech Republic
[2] University of South Bohemia, Faculty of Science, Branišovská 31, České Budějovice, Czech Republic
[3] Institute of Microbiology CAS, Novohradská 237, Třeboň, Czech Republic
*Corresponding author: obornik@paru.cas.cz

With 5 figures

Abstract: Chromerids are alveolate algae with secondary plastids surrounded by four membranes, and with evolutionary positions close to the root of apicomplexan parasites. As both described chromerid species, *Chromera velia* and *Vitrella brassicaformis*, are, in spite of their phototrophy, distant relatives, there are some differences between their respective life cycles. Here, we summarize current knowledge of the life cycles of chromerid algae and the related colpodellids. We also describe zoosporangia formation and excystation in *C. velia*. We suggest that the formation of zoospores in *C. velia* is homologous to schizogony in apicomplexan parasites.

Keywords: *Chromera*, *Vitrella*, Chrompodelids, life cycle, schizogony, zoospore formation

Introduction

Alveolate algae with complex plastids, such as dinoflagellates, can form endosymbiotic relationships with corals (Harii et al. 2009; LaJeunesse 2001). In addition to the well-known symbiotic dinoflagellate genus *Symbiodinium*, members of a novel group of alveolate algae named chromerids have been isolated from Australian stony corals. The first species, *Chromera velia* (Fig. 1), was found in *Plesiastrea versipora* collected from Sydney Harbor and was formally described in 2008 (Moore et al. 2008). The second known chromerid species, *Vitrella brassicaformis* (Fig. 2), was isolated from *Leptastrea purpurea* from the Great Barrier Reef (Oborník et al. 2012). These algae are of particular interest due to their close phylogenetic relationship to apicomplexan parasites (Moore et al. 2008; Oborník et al. 2009; Janouškovec et al., 2010; Weatherby and Carter, 2013; Oborník & Lukeš 2013; Janouškovec et al. 2015). Apicomplexa belong to the SAR (Stramenopila + Aleveolata + Rhizaria) eukaryotic super group (Burki et al. 2007); they are known to cause many important human and veterinary diseases including malaria and toxoplasmosis. Apicomplexans typically possess an apical complex, a complex of membranous organelles used to penetrate host cells, and the apicoplast, a non-photosynthetic complex plastid (McFadden et al. 1996; Wilson et al. 1996; Köhler et al. 1997). This relic plastid contains a highly reduced genome consisting of a 35 kb circle and obviously originates from a secondary endosymbiotic event (Ralph et al. 2004; Oborník et al. 2009; Lim & McFadden 2010; McFadden 2011; Oborník & Lukeš 2013; Keeling 2014; Oborník & Lukeš 2015). The discovery of a plastid in the Apicomplexa suggested that the parasitic phylum was derived from a photosynthetic ancestor and instigated a search for photosynthetic relatives that could reveal the identity of this ancestor. The description of coral associated chromerid algae is therefore groundbreaking research: since they are related to the Apicomplexa and they contain regular photosynthetic plastids with genomes overlapping those of the apicoplast and dinoflagellate plastids, meaningful comparative studies can be carried out (Keeling 2008; Moore et al. 2008; Janouškovec et al. 2010). In addition to molecular phylogenies (Moore et al. 2008; Janouškovec et al. 2010; Janouškovec et al. 2015) the non-phylogenetic evidence for evolutionary relationship between chromerids and apicomplexans was also investigated. The presence of a non-canonical heme synthesis pathway in *C. velia*, which is partly homologous to that of apicomplexans (in the use of C4 pathway to synthesize aminolevulinate), provides a very strong argument for the common ancestry of *C. velia* and the Apicomplexa (Kořený et al. 2011). Furthermore, the structure of the plastid super operon suggests a common origin of apicomplexan, chromerid and heterokont plastids (Janouškovec et al. 2010). The use of non-canonical code for tryptophan (UGA) in some plastid encoded proteins has so
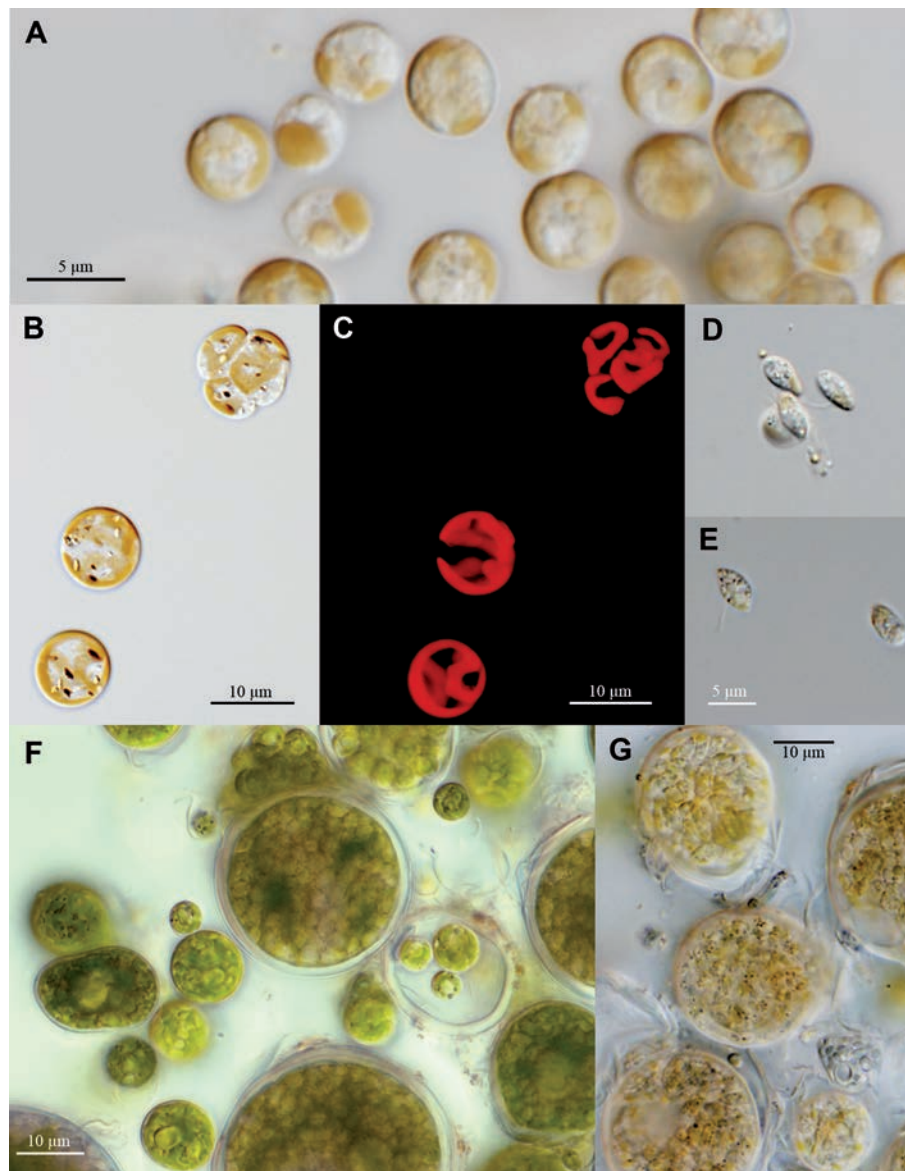
Fig. 1. Light microscopy of *Chromera velia* and *Vitrella brassicaformis*. (**A**) *C. velia* culture; (**B**) vegetative cell and autosporangium (top right) of *C. velia* with four autospores; (**C**) autofluorescence of plastid in *C. velia* vegetative cell and autosporangium; (**D**) zoospores of *C. velia*; (**E**) zoospores of *V. brassicaformis*; (**F**) vegetative cells and autosporangia of *V. brassicaformis*; (**G**) zoosporangia of *V. brassicaformis*.

far been reported exclusively in *C. velia* and coccidians – an advanced lineage of apicomplexan parasites. Analyses of transcriptomes from colpodellids (genera *Alphamonas*, *Colpodella* and *Voromonas*) and chromerids support the monophyly of "chrompodellids" (chromerids + colpodellids), with *V. brassicaformis* appearing at the root of the *Alphamonas* clade, while *C. velia* constitutes the earliest branch of the *Colpodella* + *Voromonas* clade (Janouškovec et al. 2015; Oborník & Lukeš 2015).

Chromerid ultrastructure, morphology and life cycles

Chromerids have been the subject of extensive ultrastructural studies, including descriptions of their vegetative life cycles (Wetherby et al. 2011; Oborník et al. 2011; Oborník et al. 2012; Portman et al. 2014). These studies revealed features typical of apicomplexan parasites – cortical alveoli subtended by a sheet of microtubules, micropores, a pseudoconoid and
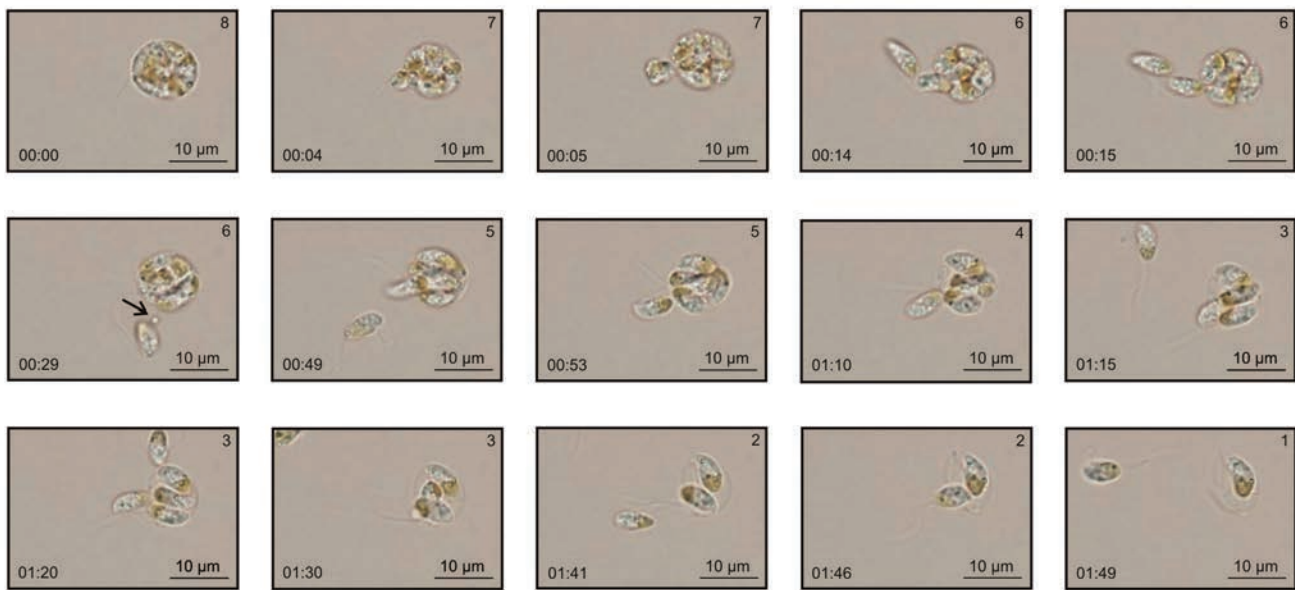
Fig. 2. Excystation of zoospores of *Chromera velia*. The entire process captured herein takes about two minutes. The zoospores starts to rotate within the zoosporangium that subsequently ruptures and spores are released one by one through a rupture in the wall. The release of the residual body is shown (6). Scale bar is 10 μm.

a four-membrane plastid envelope (Janouškovec et al. 2010; Oborník et al. 2011; Oborník et al. 2012; Oborník & Lukeš 2013). Three distinctive life stages have been documented so far in *C. velia* (Oborník et al. 2011). Vegetative coccoid cells (Fig. 1A, B) are the predominant life cycle stage in culture. They divide by binary division and form autosporangia (cysts) covered by an additional membrane (Fig. 1B) with 2–4 coccoid cells. Both immotile stages are protected by a thick and resistant cell wall. In addition to non-motile stages, zoospores (Fig. 1D) with thin cell walls and two heterodynamic flagella have been observed. They exhibit a typical finger-like projection on the shorter flagellum and their cell shape resembles that of colpodellid trophozoites. The appearance of zoospores in culture is induced by light (Oborník et al. 2011) and is also inferred to be influenced by salinity (Guo et al. 2010). However, zoosporangia were not initially observed in *C. velia* and zoospores were thought to develop directly from coccoid cells (Oborník et al. 2011). Later, the formation of two zoospores from a single maternal cell (zoosporangium) was described by Portman et al. (2014). Here we show the presence of large zoosporangia (up to 15 μm in diameter) observed in culture, which contain even numbers (2–10) of zoospores. The process of excystation starts with the movement of zoospores inside the zoosporangium, which ultimately leads to rupture of the zoosporangium wall. The speed of excystation depends on the rupture – the larger the tear, the faster the release of the zoospores. The excystation shown in Figure 2 (for the movie see the link at the end of this article) took about 2 minutes and zoospores were released

through a small rupture one by one. The release of a structure resembling the residual body in Apicomplexa was observed during the excystation of *C. velia* zoosporangia (Fig. 2 and the movie). However, we also observed much faster excystations where the zoosporangium wall ripped almost entirely around its circumference and zoospores were released simultaneously. Zoospores are highly abundant in culture between the 4th and 8th day after inoculation, when they can represent over 80% of the cells. Only asexual life stages have been observed in *C. velia*. Released autospores (immotile vegetative coccoid cells) divide forming autosporangia. In parallel, some vegetative cells develop to large zoosporangia with flagellated zoospores (Fig. 2). A zoospore can transform to a vegetative cell within 10 minutes and complete the life cycle (Oborník et al. 2011). The function of zoospores (Fig. 1D, E) is unknown; however, they may enable rapid dispersal and colonization of nearby areas. Furthermore, when the culture is exposed to concentrated high intensity light, all exposed cells disappear; it is possible that they form motile zoospores which subsequently escape from the exposed area. Since coral larvae infected by *C. velia* have been observed (Cumbo et al. 2013), it is tempting to speculate that zoospores function as an infective stage and invade corals (Fig. 3). At this point in time, however, nothing is known about *C. velia's* life cycle as a coral endosymbiont.

The ultrastructure of *Vitrella brassicaformis* is distinct from that of *Chromera velia*. The cell wall of vegetative cells and sporangia is laminated in *V. brassicaformis*, resulting in a cell shape resembling cabbage heads (Fig. 4A). We have
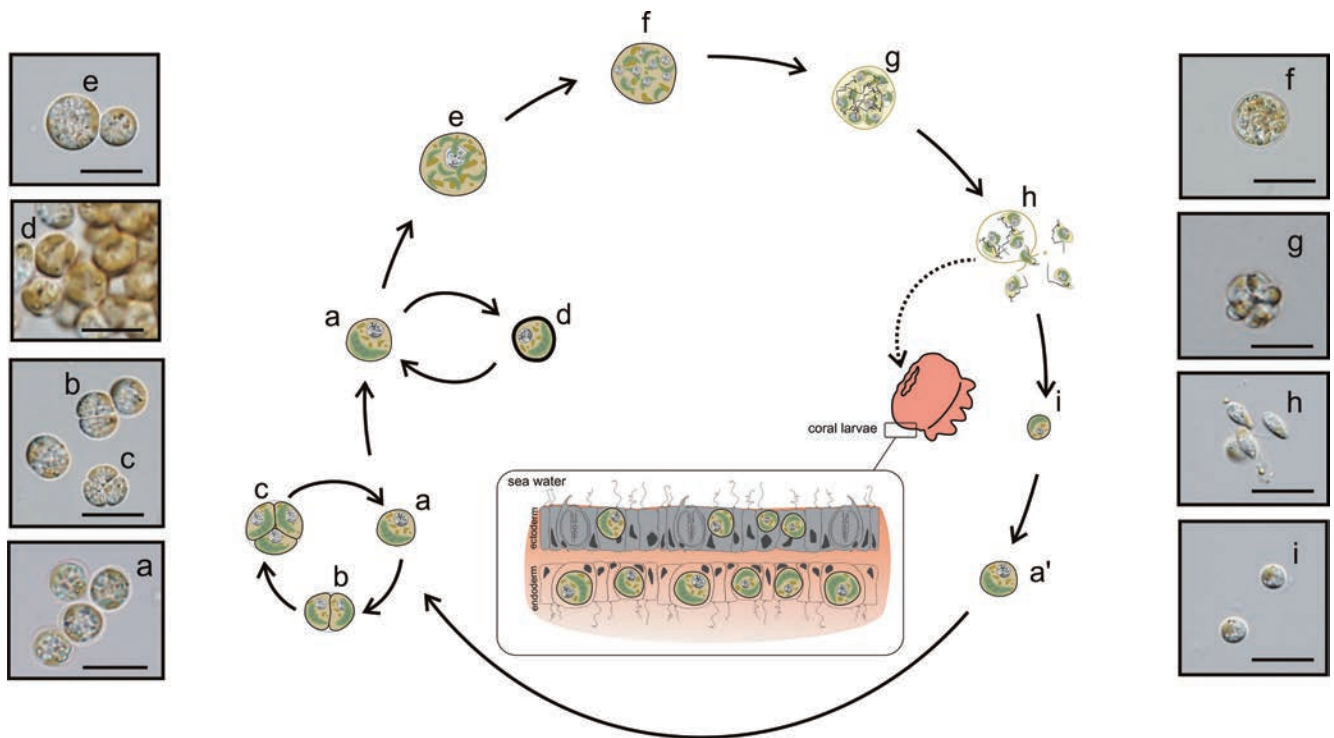
Fig. 3. Life cycle of *Chromera velia*: vegetative cell (**a, a'**) divides and form an autosporangium with dublets (**b**) to tetrades (**c**) of vegetative cells covered by additional membrane. The vegetative cell can develop to a zoosporangium (**g, h**) from which the zoospores are released through the rupture in the wall of sporangium. They are supposed to infect coral larvae or to encyst (**i**) and form a vegetative cell.

observed up to twelve cell wall layers. Although the cell wall is thick and multilayered, it is fully transparent, allowing for photosynthesis in all non-motile life stages. While vegetative cells of *C. velia* are all similar in size, ranging from 5–7 µm in diameter (Oborník et al. 2011), the size of vegetative cells in *V. brassicaformis* ranges from 3 µm (in released autospores) to 40 µm (in vegetative cells prior to sporangium formation) (Fig. 1F). Numbers of autospores and zoospores in sporangia are much higher in *V. brassicaformis* than in *C. velia*: they contain dozens of spores per sporangium (Oborník et al. 2012), in contrast to 4 autospores and 10 zoospores as maximum numbers for *C. velia* sporangia (Oborník et al. 2011; Oborník & Lukeš 2013). The zoosporangium of *V. brassicaformis* has a clearly visible operculum that readily serves as an exit point for the zoospores within (Oborník et al. 2012), in contrast to the unpredictable rupture of the zoosporangium wall in *C. velia*. Although *V. brassicaformis* seems like it should have, due to high numbers of spores in sporangia, higher reproductive rates, in culture it grows much more slowly than *C. velia* (Oborník et al. 2012; Flegontov et al. 2015). Zoospores of *V. brassicaformis* are also bi-flagellated, but the finger-like projection found in *C. velia* is not observed. Generally, the life cycle of *V. brassicaformis* is as follows: Autospores (immotile vegetative cells) are released and as vegetative

cells grow from an initial size of 3 µm up to 30–40 µm. They subsequently form one of two types of sporangia: autosporangia (green) are full of small autospores (Fig. 1F) and zoosporangia (gray) contain dozens of zoospores (Fig. 1G). They are both released through an operculum in the wall of the sporangium (Oborník et al. 2012; Oborník & Lukeš 2013). We should note that zoospores are rare in cultures of *V. brassicaformis*, and the life cycle together with the fate of zoospores is not as well-described as it is in *C. velia*. The slow growth of *V. brassicaformis* in culture also makes it less amenable to use as a model organism.

As previously mentioned, *C. velia* and *V. brassicaformis* are not closely related; they are recovered as isolated phototrophic lineages within the heterotrophic colpodellids (Gill & Slamovits 2014; Janouškovec et al. 2015; Oborník & Lukeš 2015). The two taxa combine to form a novel group, the "chrompodelids" (Janouškovec et al. 2015). In the life cycle of *Colpodella vorax* (Brugerolle 2002), trophozoites with two heterodynamic flagella encyst and divide into a four-celled cyst, similar to *C. velia*. New trophozoites are later released from the cyst. Trophozoites resemble chromerid zoospores and the cysts resemble the sporangia of *C. velia*, mainly due to the low and even number of trophozoites (spores) formed. In colpodellids conjugation between trophozoites has been reported (Simpson & Patterson 1996;
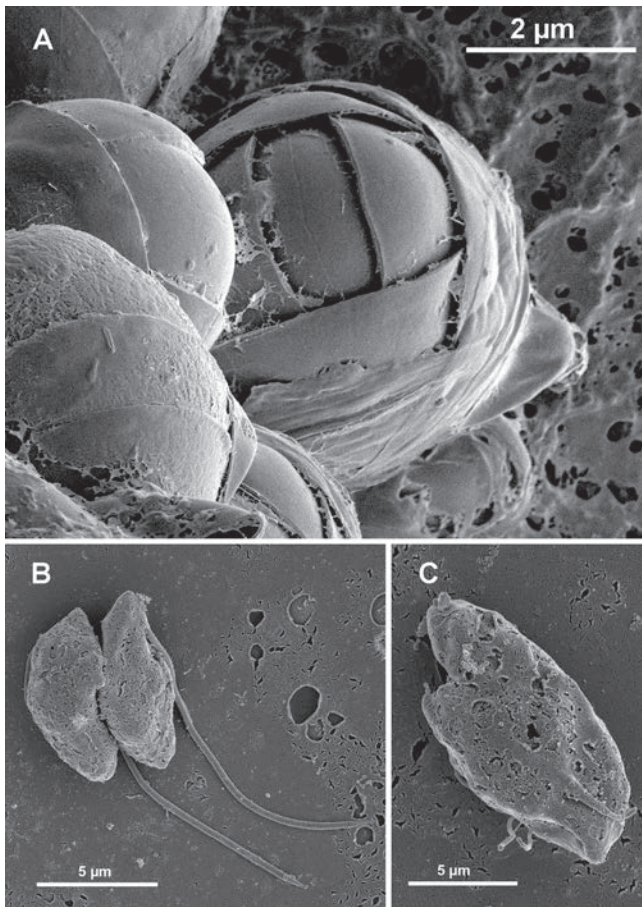
Fig. 4. (**A**) Scanning Electron Microscopy (SEM) picture of the vegetative cell of *Vitrella brassicaformis* resembles "cabbage head"; this shape gave together with full transparency of cell walls the alga name; (**B**) Possible fusion (or fission) of zoospores in chromerid alga *V. brassicaformis*. SEM picture was made using method described elsewhere (Moore et al. 2008).

Fig. 5. Transmission Electron Microscopy (TEM) picture shows formation of zoospores in the zoosporangium of *Chromera velia* that highly resembles schizogony in apicomplexan parasites. TEM picture was made using method described elsewhere (Moore et al. 2008).

Brugerolle 2002), suggesting a sexual phase in their life cycle; sexual stages have not been observed in *C. velia* (Oborník et al. 2011, 2012). Some electron micrographs of *V. brassicaformis* flagellates appear to depict cell fusion (Fig. 4); since we have only observed this behavior a few times out of hundreds of images, however, we believe that conjugation occurs rarely, if at all. Nevertheless, due to a possible homology with *Alphamonas edax*, we speculate that zoospores can fuse together; this suggests the occurrence of sexual reproduction in the *V. brassicaformis* clade (Fig. 4B, C).

The almost complete absence of synapomorphies in the life cycles of chromerids and apicomplexan parasites demonstrates the degree to which apicomplexan parasites are derived, because it is rather difficult to find any obvious developmental similarities between the two groups. *Chromera velia* contains a pseudoconoid, a primitive apical complex similar to that used for feeding by colpodellids and
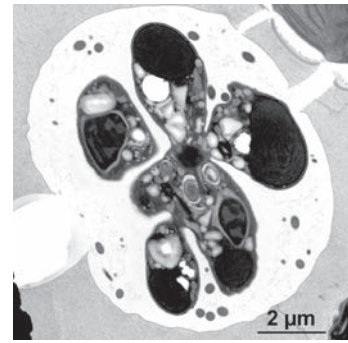
apicomplexans, which has not yet been found in *V. brassicaformis* (Oborník et al. 2011; Portman et al. 2014). When the zoosporangium of *C. velia* was investigated by transmission electron microscopy (TEM), zoospores appeared to be highly organized in the sporangium, forming a star-like structure similar to that observed during apicomplexan schizogony (Fig. 5), a stage in the asexual reproduction of apicomplexans involving multiple fission of the parasite nucleus followed by fragmentation of the cytoplasm. Similar arrangements of flagellated cells in a cyst were shown in *Colpodella tetrahymenae* intracyst division (Cavalier-Smith & Chao 2004), which is not, however, proposed to form multinuclear cells (Brugerolle 2002) as it is in the Apicomplexa. It is very likely that life cycles vary substantially between colpodellids, because they differ between chromerids and even in the genus *Colpodella*: resting cysts of *C. vorax* develop through two consequential mitotic divisions to the four-celled cyst, followed with formation and release of trophozoites (Brugerrole 2002), while *C. unguis* was documented to form trophozoites directly from the resting cyst, followed by feeding and fission of the trophozoites (Mylnikov 2009). The observation of dividing trophozoites in colpodellids opens the possibility that the inferred fusion of *V. brassicaformis* zoospores discussed above (Fig. 4B, C) could instead be fission.

Conclusions

Due to their high trophic diversity, we cannot at this time propose a general life cycle for chrompodellids; however, it almost certainly includes motile zoospores (trophozoites) as a predominant stage in the colpodellid cycles, and vegetative cells likely dominate chromerid life cycles. As colpodellids lost photosynthesis at some point in their evolutionary history; the predominance of trophozoites with an apical

complex-like feeding apparatus could reflect a reliance on predation for energy acquisition. Since photosynthesis seems to be optimized in chromerid vegetative cells, this may have resulted in their predominance within chromerid life cycles (Oborník et al. 2011). Zoospores of *C. velia* and trophozoites of colpodellids are formed in a process resembling schizogony in apicomplexan parasites; this represents the only known developmental synapomorphy between the Apicomplexa and their close relatives the chrompodelids.

This paper is accompanied by a youtube video showing excystation of the zoosporangium of *C. velia*: https://www.youtube.com/watch?v=o1NqX9BjCJY

References

Adl, S.M., Simpson, A.G.B., Lane, C.E., Lukeš, J., Bass, D., Bowser, S.S., Brown, M.W., Burki, F., Dunthorn, M., Hampl, V., Heiss, A., Hoppenrath, M., Lara, E., le Gall, L., Lynn, D.H., McManus, H., Mitchell, E.A.D., Mozley-Stanridge, S.E., Parfrey, L.W., Pawlowski, J., Rueckert, S., Shadwick, L., Schoch, C.L., Smirnov, A. & Spiegel, F.W. (2012): The Revised Classification of Eukaryotes. – J. Euk. Microbiol. 59: 429–493.

Burki, F., Shalchian-Tabrizi, K., Minge, M., Skjæveland, Å., Nikolajev, S.I., Jakobsen, K.S. & Pawlowski, J. (2007) Phylogenomics Reshuffles the Eukaryotic Supergroups. – PLoS ONE 2: e790.

Brugerolle, G. (2002): *Colpodella vorax*: Ultrastructure, Predation, Life-cycle, Mitosis, and Phylogenetic Relationships. – Eur. J. Protistol. 38: 113–125.

Cavalier-Smith, T. & Chao, E.E. (2004): Protalevolate Phylogeny and Systematics and the origins of Sporozoa and Dinoflagellates (phylum Myzozoa nom. nov.). – Eur. J. Protistol. 40: 185–212.

Cumbo, V.R., Baird, A.H., Moore, R.B., Negri, A.P., Salih, A., van Oppen, M.J., Wang, Y. & Marquis C.P. (2013): *Chromera velia* as Endosymbiotic in Larvae of the Reef Corals *Acropora digitifera* and *A. tenuis*. – Protist 164: 237–244.

Flegontov, P., Michálek, J., Janouškovec, J., Lai, H., Jirků, M., Hajdušková, E., Tomčala, A., Otto, T.D., Keeling, P.J., Pain, A., Oborník, M. & Lukeš, J. (2015): Divergent Mitochondrial Respiratory Chains in Phototrophic Relatives of Apicomplexan Parasites. – Mol. Biol. Evol. 32: 1115–1131.

Guo, J.T., Weatherby, K., Carter, D. & Šlapeta, J. (2010): Effect of Nutrient Concentration and Salinity on Immotile-Motile Transformation of *Chromera velia*. – J. Euk. Microbiol. 57: 444–446.

Harii, S., Yasuda, N., Rodriguez-Lanetty, M., Irie, T. & Hidaka, M. (2009): Onset of Symbiosis and Distribution Patterns of Symbiotic Dinoflagellates in the Larvae of Scleractinian Corals. – Mar. Biol. 156: 1203–1212.

Janouškovec, J., Horák, A., Oborník, M., Lukeš, J. & Keeling, P.J. (2010): A Common Red Algal Origin of the Apicomplexan, Dinoflagellate, and Heterokont Plastids. – Proc. Natl. Acad. Sci. USA 107: 10949–10954.

Janouškovec, J., Tikhonenkov, D.V., Burki, F., Howe, A.T., Kolísko, M., Mylnikov, A.P. & Keeling, P.J. (2015): Factors Mediating Plastid Dependency and the Origins of Parasitism in Apicomplexans and Their Close Relatives. – Proc. Natl. Acad. Sci. USA: doi/10.1073/pnas.1423790112

Keeling, P.J. (2008): Bridge Over Troublesome Plastids. – Nature 451: 896–897.

Keeling, P.J. (2014): The Number, Speed, and Impact of Plastid Endosymbioses in Eukaryotic Evolution. – Ann. Rev. Plant Biol. 64: 583–607.

Kohler, S., Delwiche, C.F., Denny, P.W., Tilney, L.G., Webster, P., Wilson, R.J.M., Palmer, J.D. & Roos, D.S. (1997): A Plastid of Probable Green Algal Origin in Apicomplexan Parasites. – Science 275: 1485–1489.

Kořený, L., Sobotka, R., Janouškovec, J., Keeling, P.J. & Oborník, M. (2011): Tetrapyrrole Synthesis of Photosynthetic Chromerids is Likely Homologous to the Unusual Pathway of Apicomplexan Parasites. – Plant Cell 23: 3454–3462.

LaJeunesse, T.C. (2001): Investigating the Biodiversity, Ecology, and Phylogeny of Endosymbiotic Dinoflagellates in the Genus *Symbiodinium* Using the ITS Region: In Search of a "Species" Level Marker. – J. Phycol. 37: 866–880.

Lim, L. & McFadden, G.I. (2010): The Evolution, Metabolism and Functions of the Apicoplast. – Phil. Trans. Royal Soc. B 365: 749–763.

McFadden, G.I. (2011): The Apicoplast. – Protoplasma 248: 641–650.

Moore, R.B., Oborník, M., Janouškovec, J., Chrudimský, T., Vancová, M., Green, D.H., Wright, S.W., Davies, N.W., Bolch, C.J.S., Heimann, K., Šlapeta, J., Hoegh-Guldberg, O., Logsdon, J.M. & Carter, D.A. (2008): A Photosynthetic Alveolate Closely Related to Apicomplexan Parasites. – Nature 451: 959–963.

Mylnikov, A.P. (2009): Ultrastructure and Phylogeny of Colpodellids (Colpodellida, Alveolata). – Biol. Bull. 36: 582–590.

Oborník, M. & Lukeš, J. (2013): Cell Biology of Chromerids, the Autotrophic Relatives to Apicomplexan Parasites. – Int. Rev. Cell Mol. Biol. 306: 333–369.

Oborník, M. & Lukeš, J. (2015): The Organellar Genomes of *Chromera* and *Vitrella*, the Phototrophic Relatives of Apicomplexan Parasites. – Ann. Rev. Microbiol. 69: 129–144.

Oborník, M., Vancová, M., Lai, D.H., Janouškovec, J., Keeling, J.P. & Lukeš J. (2011): Morphology and Ultrastructure of Multiple Life Cycle Stages of the Photosynthetic Relative of Apicomplexa, *Chromera velia*. – Protist 162: 115–130.

Oborník, M., Modrý, D., Lukeš, M., Černotíková-Stříbrná, E., Cihlář, J., Tesařová, M., Kotabová, E., Vancová, M., Prášil, O. & Lukeš J. (2012): Morphology, Ultrastructure and Life Cycle of *Vitrella brassicaformis* n. sp., n. gen., a Novel Chromerid from the Great Barrier Reef. – Protist 163: 306–323.

Oborník, M., Janouškovec, J., Chrudimský, T. & Lukeš, J. (2009): Evolution of the Apicoplast and Its Hosts: From Heterotrophy to Autotrophy and Back Again. – Int. J. Parasitol. 39: 1–12.

Portman, N., Foster, C., Walker, G. & Šlapeta, J. (2014): Evidence of Intraflagellar Transport and Apical Complex Formation in a Free-Living Relative of the Apicomplexa. – Euk. Cell 13: 10–20.

Ralph, S.A., van Dooren, G.G., Waller, R.F., Crawford, M.J., Fraunholz, M.J., Foth, B.J., Tonkin, C.J., Roos, D.S. & McFadden, G.I. (2004): Metabolic Maps and Functions of the

Plasmodium falciparum Apicoplast. – Nat. Rev. Microbiol. 2: 203–216.

Simpson, A.G.B. & Patterson, D.J. (1996): Ultrastructure and Identification of the Predatory Flagellate *Colpodella pugnax* Cienkowski (Apicomplexa) with a Description of *Colpodella turpis* n. sp. and Review of the Genus. – Syst. Parasitol. 33: 187–198.

Weatherby, K., Murray, S., Carter, D. & Šlapeta, J. (2011): Surface and Flagella Morphology of the Motile Form of *Chromera velia* Revealed by Field-Emission Scanning Electron Microscopy. – Protist 162: 142–153.

Weatherby, K. & Catrer, D. (2013): *Chromer velia:* The Missing Link in the Evolution of Parasitism. – Adv. Appl. Microbiol. 85: 119–144.

Wilson, R.J.M., Denny, P.W., Preiser, P.R., Rangachari, K., Roberts, K., Roy, A., Whyte, T., Strath, M., Moore, D.J., Moore, P.W. & Williamson, D.H. (1996): Complete map of the plastid-like DNA of the malaria parasite *Plasmodium falciparum*. – J. Mol. Biol. 261: 155–172.

CURRICULUM VITAE

Name:	Jitka Richtová
Nationality:	Czech
Date of birth:	8 August 1985
Home address:	Lomec 30, 374 01 Strážkovice

Education:

2009 - present   **Ph.D. student of Molecular and Cell Biology and Genetics**

Faculty of Science, University of South Bohemia, České Budějovice

Institute of Parasitology, Czech Academy of Sciences, Czech Republic

Thesis: "Localization of nuclear-encoded enzymes in *Chromera velia.*"

Supervisor: Prof. Miroslav Oborník, Institute of Parasitology, Biology Centre, ASCR, v.v.i, České Budějovice

2007 - 2009   **MSc. student of Experimental Biology**

Faculty of Science, University of South Bohemia, České Budějovice

Institute of Microbiology, ASCR, v.v.i, Třeboň, Czech Republic

Thesis: "Expression and purification of Synechocystis ferrochelatase from *Escherichia coli.*"

Supervisor: Dr. Roman Sobotka, Institute of Microbiology, ASCR, v.v.i, Třeboň

2004 - 2007   **BSc. student of Biology**

Faculty of Science, University of South Bohemia, České Budějovice

Institute of Microbiology, ASCR, v.v.i, Třeboň, Czech Republic

Thesis: "Construction of expression vector for cyanobacterium *Synechocystis sp. PCC 6803.*"

Supervisor: Dr. Roman Sobotka, Institute of Microbiology, ASCR, v.v.i, Třeboň

Employment:

2021- present   Research assistant

       Laboratory of Evolutionary Protistology, Institute of Parasitology,

       Biology Centre CAS, v.v.i.

2016 - 2020   maternity leave

2015 - 2016   Research assistant

       Laboratory of RNA Biology of Protists, Institute of Parasitology,

       Biology Centre CAS, v.v.i.

2009 - 2014   Graduate student

       Laboratory of Evolutionary Protistology, Institute of Parasitology,

       Biology Centre CAS, v.v.i.

Internship:

Aug 2011   **Short internship**

       The University of Sheffield (UK), Department of Chemistry, laboratory of Dr.
Jim Reid

       Purification of recombinant ferrochelatase, enzymatic measurements.

Sep-Oct 2010   **Internship**

       The University of Georgia (GA, USA), Center for Tropical and Emerging
Diseases, laboratory of Dr. Boris Striepen

       Localization of heme pathway enzymes from *C. velia* by xenotransfection in
Toxoplasma gondii

Jul-Sep 2007   **Erasmus internship**

       The University of Sheffield (UK), Department of Molecular Biology and
Biotechnology, laboratory of Dr. Christopher Neil Hunter

       Cloning of recombinant genes, overexpression, and purification of
recombinant enzymes from cyanobacterium *Synechocystis sp. PCC 6803*.

Teaching activities:

University of South Bohemia, Faculty of Science, České Budějovice

2011 – 2012   Supervisor – "High school scientific work"

2011   Instructor - Methods of molecular biology

2009   Instructor – Biochemistry

Conference contributions:

2015   45th International Meeting of Czech Society for Protozoology, Dubovice, Pelhřimov, Czech Republic

Presentation: Localization of *Chromera velia* heme pathway enzymes

2014   SMBE, Puerto Rico, USA

Poster presentation: Localization of *Chromera velia* heme pathway enzymes

44th International Meeting of Czech Society for Protozoology, Krásná, Czech Republic

Poster presentation: Characterization of the Chromerosome, a Mysterious Organelle in *Chromera velia*

2nd Chromera meeting, České Budějovice, Czech Republic

Presentation: Localization of *Chromera velia* heme pathway enzymes

Chantransia – student miniconference, Zlatá koruna, Czech Republic

presentation: *Chromera velia*

2013   ICOP XIV, Vancouver, Canada

Presentation: Localization of *Chromera velia* heme pathway enzymes

43rd International Meeting of Czech Society for Protozoology, Nový Dvůr u Týna and Vltavou, Czech Republic

Presentation: formation and exflagellation of zoosporangia of a coral reef alga *Chromera velia*

2012   Protist, Oslo, Norway

Poster presentation: Localization of *Chromera velia* heme pathway enzymes by xenotransfection.

42nd International Meeting of Czech Society for Protozoology, Kletečná u Humpolce, Czech Republic

Presentation: Heme pathway as the plastid evolution marker

2011   ICTPPO, Berlin, Germany

Poster presentation: Localization of *Chromera velia* heme pathway by xenotransfection in *Toxoplasma gondii* and *Phaeodactylum tricornutum*.
41st International Meeting of Czech Society for Protozoology, Kouty, Czech Republic
Presentation: Lokalizace enzymů hemové dráhy *Chromera velia* pomocí transfekce v Toxoplasma gondii

2006   12th International Symposium on Phototrophic Prokaryotes, Pau, France, 2006
passive

České Budějovice, 2021   Jitka Richtová

                                                      ……………………………………..

PUBLICATIONS:

Richtová J., Sheiner L., Gruber A., Yang S., Striepen B., Kořený L., Oborník M. (2021) **Using diatom and apicomplexan model to study the heme pathway of *Chromera velia*.** *International Journal of Molecular Sciences* 22: 6495. DOI: 10.3390/ijms221264950

Sharaf A., Füssy Z., Tomčala A., Richtová J., Oborník M. (2019) **Isolation of plastids and mitochondria from *Chromera velia*.** *Planta* 250: 1731–1741. DOI: 10.1007/s00425-019-03259-3

Jirsová D., Füssy Z., Richtová J., Gruber A., Oborník M. KMB 2019. **Morphology, ultrastructure, and mitochondrial genome of the marine non-photosynthetic bicosoecid *Cafileria marina* Gen. et sp. nov..** Microorganisms 7 (8), 240. doi: 10.3390/microorganisms7080240.

Füssy Z., Masařová P., Kručinská J., Esson H. J., Oborník M. (2017) **Budding of the alveolate alga *Vitrella brassicaformis* resembles sexual and asexual processes in apicomplexan parasites**. *Protist* 168: 80-91. DOI: 10.1016/j.protis.2016.12.001

Tomčala A., Kyselová V., Schneedorferová I., Opekarová I., Moos M., Urajová P., Kručinská J., Oborník M. (2017) **Separation and identification of lipids in the photosynthetic cousins of Apicomplexa *Chromera velia* and *Vitrella brassicaformis*.** *Journal of Separation Science* 40: 3402-3413. DOI: 10.1002/jssc.201700171

Oborník M., Kručinská J., Esson H. J. (2016) **Life cycles of chromerids resemble those of colpodellids and apicomplexan parasites.** *Perspectives in Phycology* 3: 21-27. DOI: 10.1127/pip/2016/0038